Satellite Remote Sensing of Volcanic Emissions

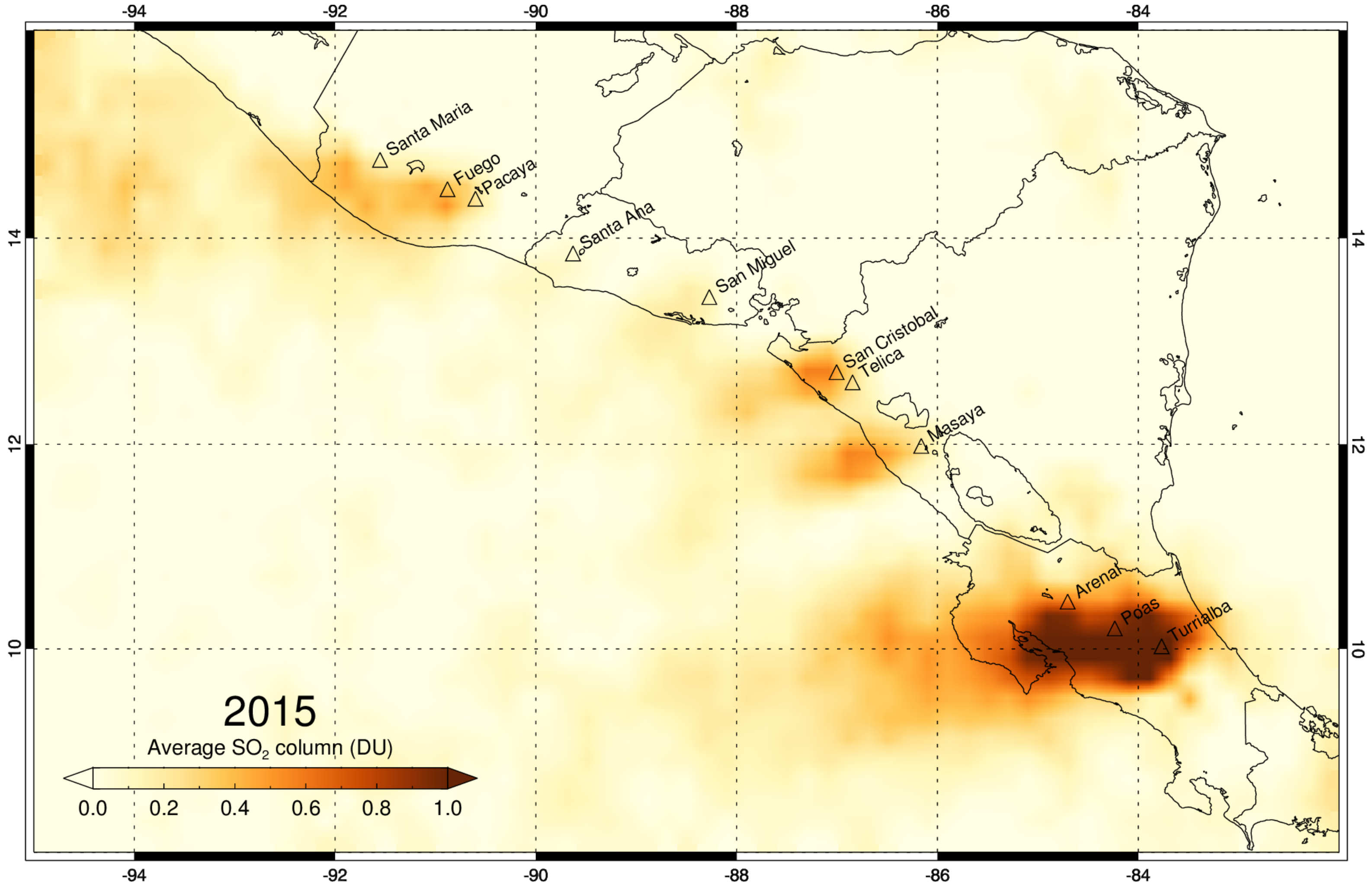

Michigan Technological University
1885

Simon Carn

@simoncarn

Goddard Space Flight Center

How big? How high? Climate impacts?

Pinatubo – June 12, 1991 *(Getty Images)*

Before the satellite era

Stratospheric particles sampled after the 1963 Agung eruption (*Mossop*, 1964)

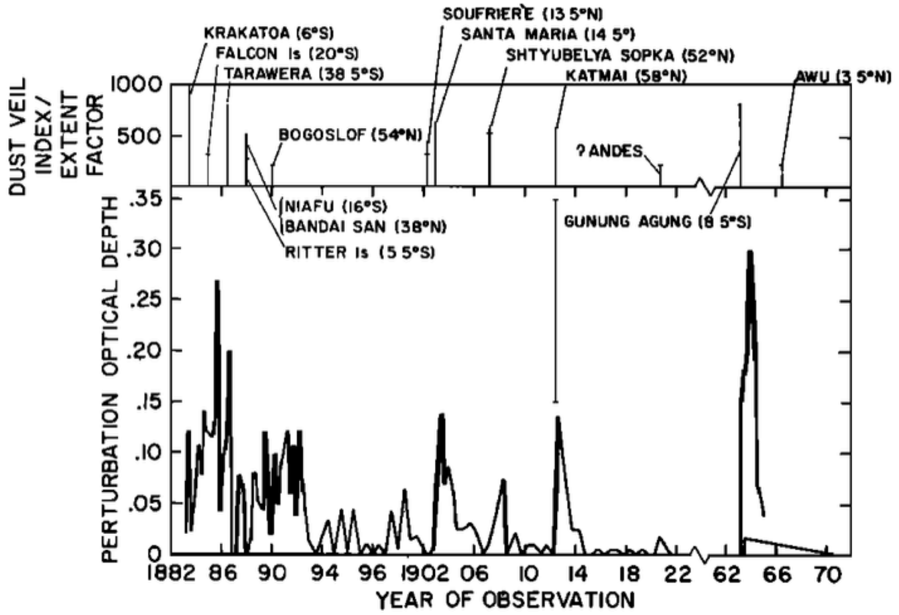

Fig. 10. Optical depth perturbation of the atmosphere as a function of time. Also shown are the times of volcanic explosions that had DVI values in excess of 170. The left side of the figure presents data for the time period from 1880 to 1925, while the right side presents corresponding information from 1962 to the present. There is a break in the time scale between these two sides. *Pollack et al.*, 1976

- Optical perturbations, direct sampling, ice cores

Lamb, 1970 (DVI); *Hammer*, 1977; *Hammer et al.*, 1980

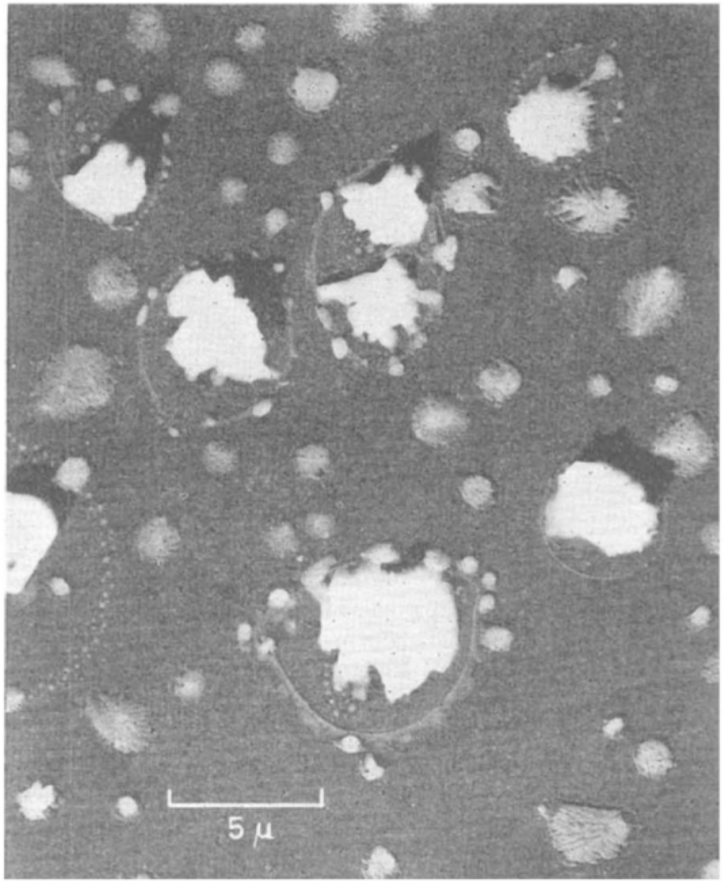

Fig. 1. Particles collected at 20 km between latitudes 44° and 40° S. on May 21, 1963, with metal shadowing. The large particles which cast an appreciable shadow are volcanic particles encased in soluble material, while the smaller flat 'rosettes' are typical of particles present at this level before the incursion of volcanic dust

'The material collected on the aircraft windshield is acid to litmus paper and painfully acid to the tongue.'

Detection of April 1982 El Chichon SO_2 cloud by the NASA Total Ozone Mapping Spectrometer (TOMS)

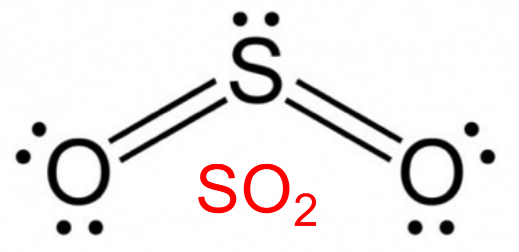

SO_2

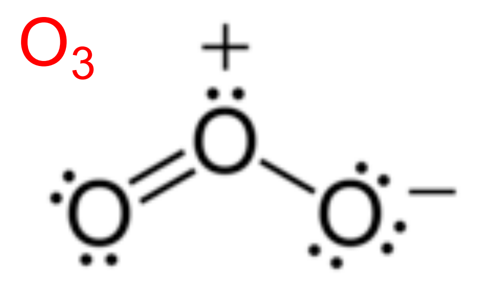

O_3

Krueger (1983)
Krueger et al. (2008)

24 JUNE 1983 · VOL. 220 · NO. 4604

$2.50

SCIENCE

AMERICAN ASSOCIATION FOR THE ADVANCEMENT OF SCIENCE

Volcanic SO_2 clouds measured by TOMS

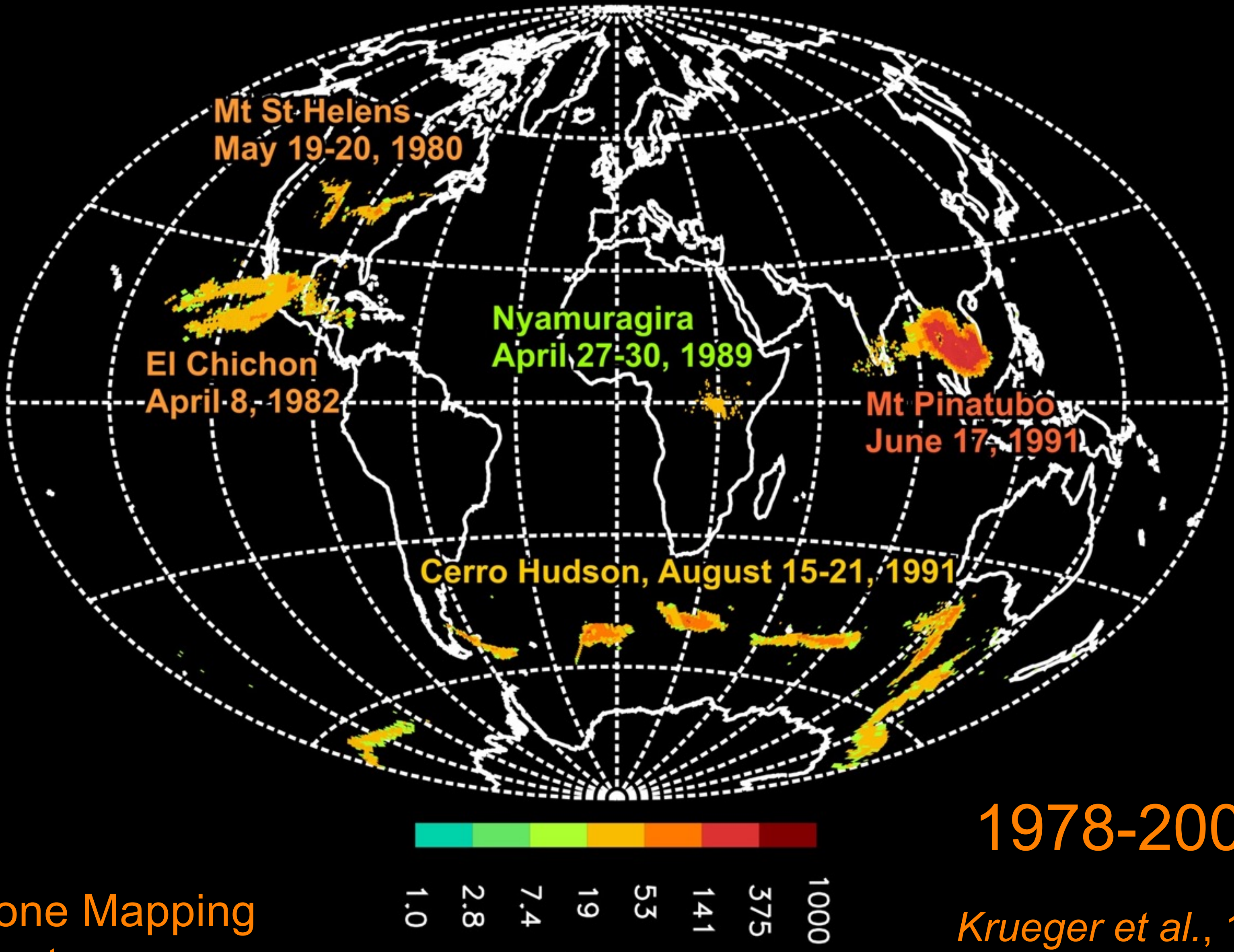

1978-2005

Total Ozone Mapping
Spectrometer

Krueger et al., 1995
Carn et al., 2003, 2016

UV satellite remote sensing of volcanic SO_2

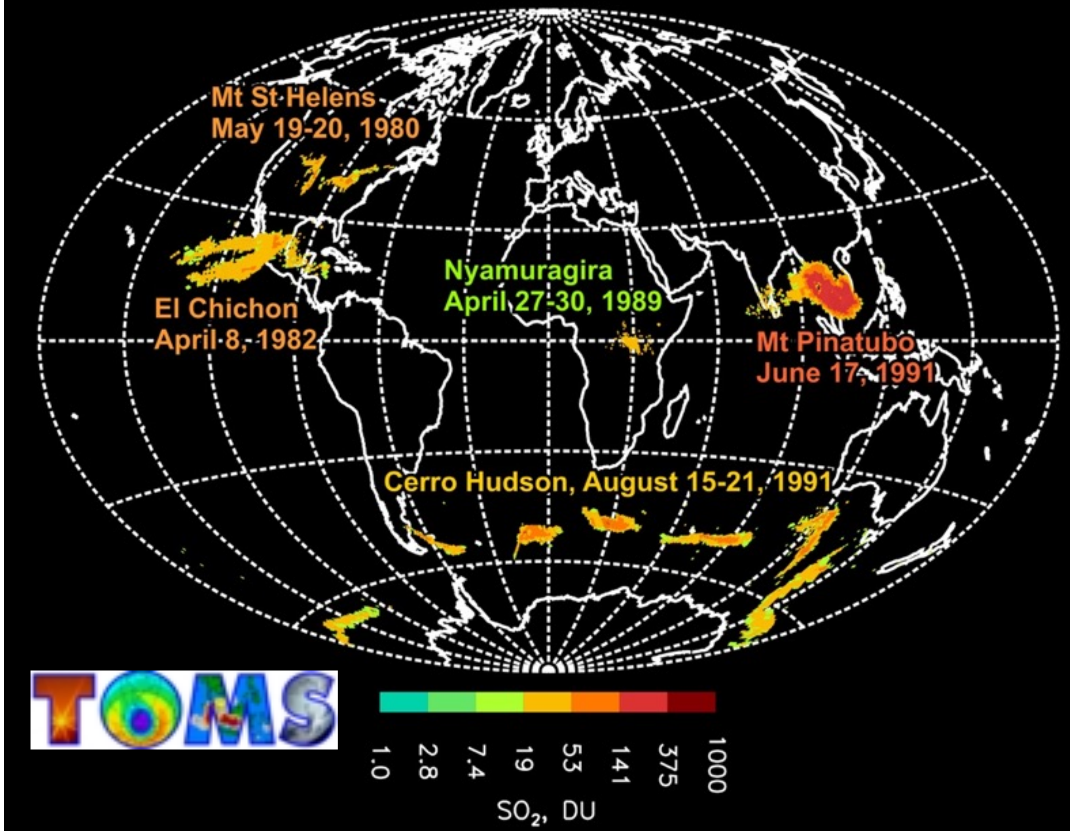

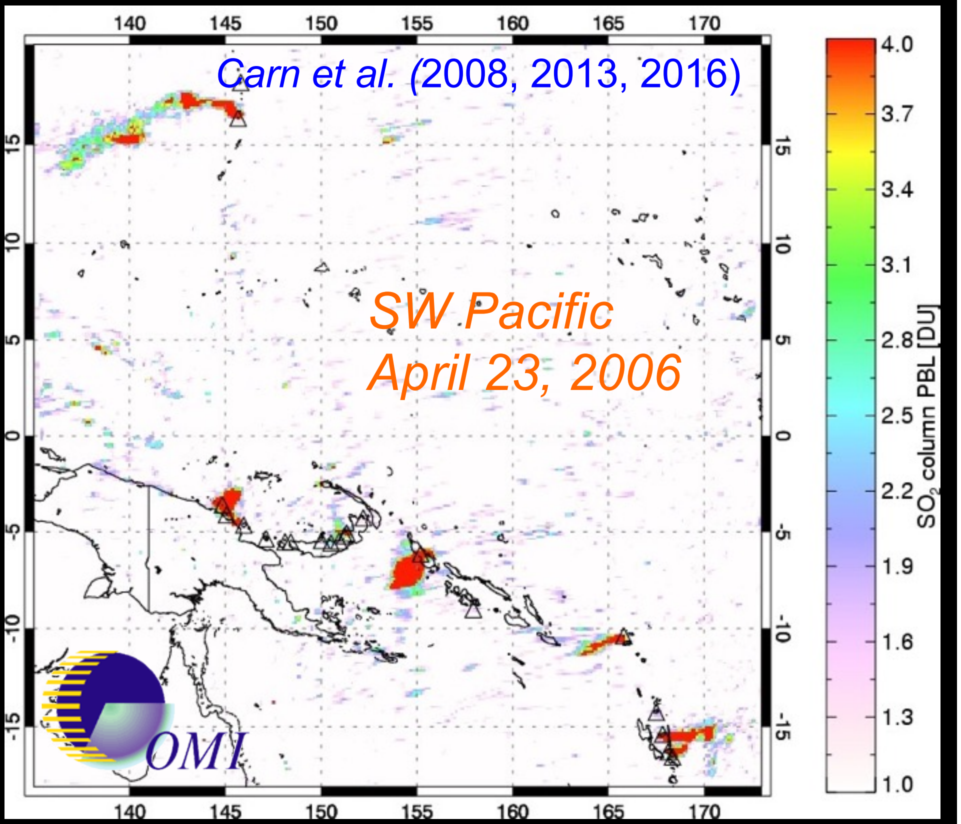

1978-2005
Total Ozone Mapping Spectrometer (TOMS)

1995-2003
Global Ozone Monitoring Experiment (GOME)

2004-
Ozone Monitoring Instrument (OMI)

2006-
GOME-2

2012- & 2017-
Ozone Mapping and Profiler Suite (OMPS)

2015-
DSCOVR/ EPIC

2018-
Sentinel 5P TROPOMI

Present: monitoring daily passive degassing from space

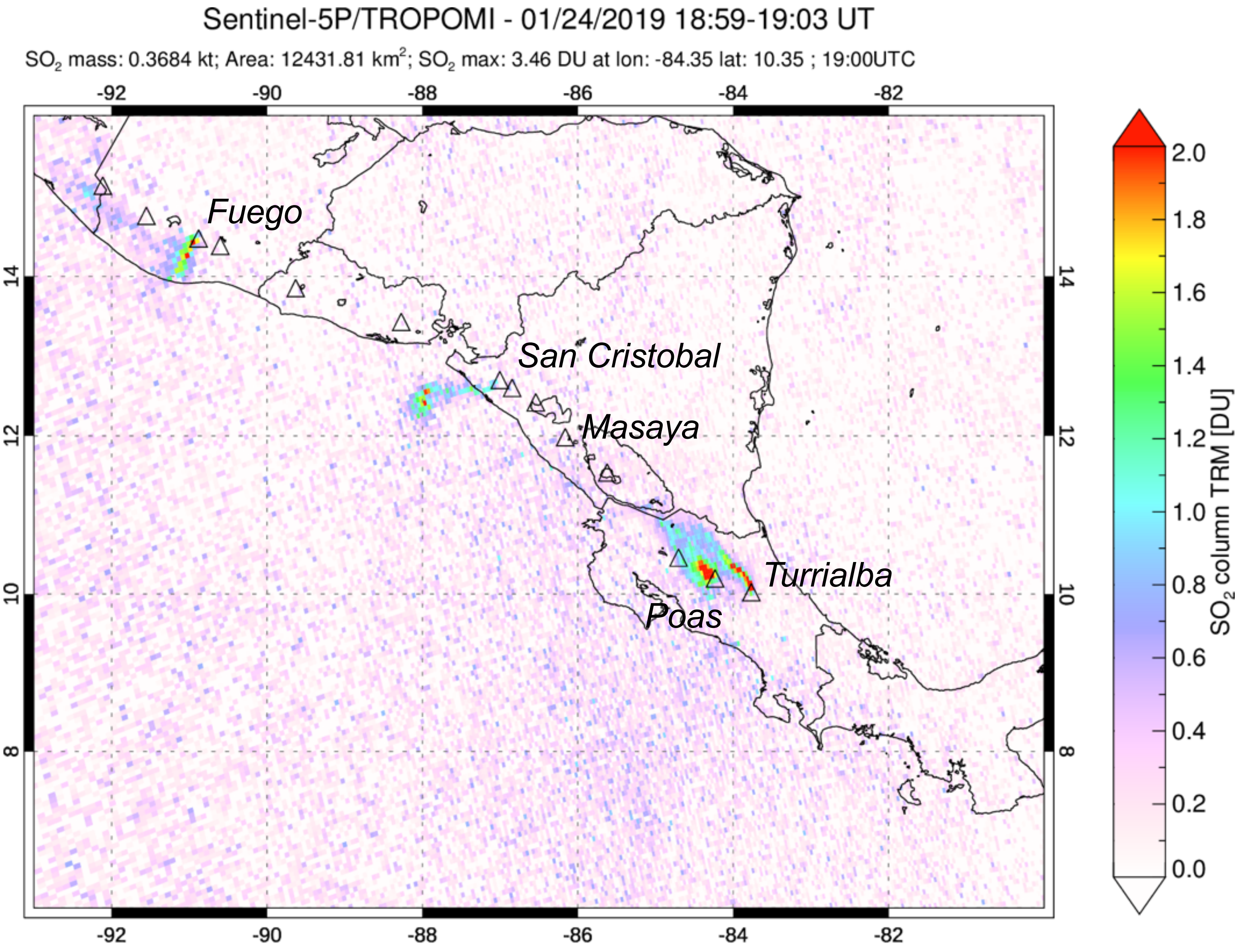

Data: BIRA-IASB/DLR/ESA/EU

Before satellites, records of volcanic activity were largely collated from ground-based and proxy observations, and hence were incomplete. Remote sensing now provides a less ‘biased’ view of global (subaerial) volcanism.

Aviation hazards from volcanic eruption clouds


Eyjafjallajökull (Iceland) 2010

- Near-catastrophic aviation encounters with volcanic ash in 1982 (Galunggung, Indonesia) and 1989 (Redoubt, AK, USA)
- Hazards include jet engine failure or damage, windshield abrasion, disruption of avionics
- Mitigation:
- – Immediate detection of fresh volcanic clouds
- – Tracking/forecast of cloud position and <u>altitude</u>

Casadevall (1994a, 1994b); *Prata and Tupper* (2009)

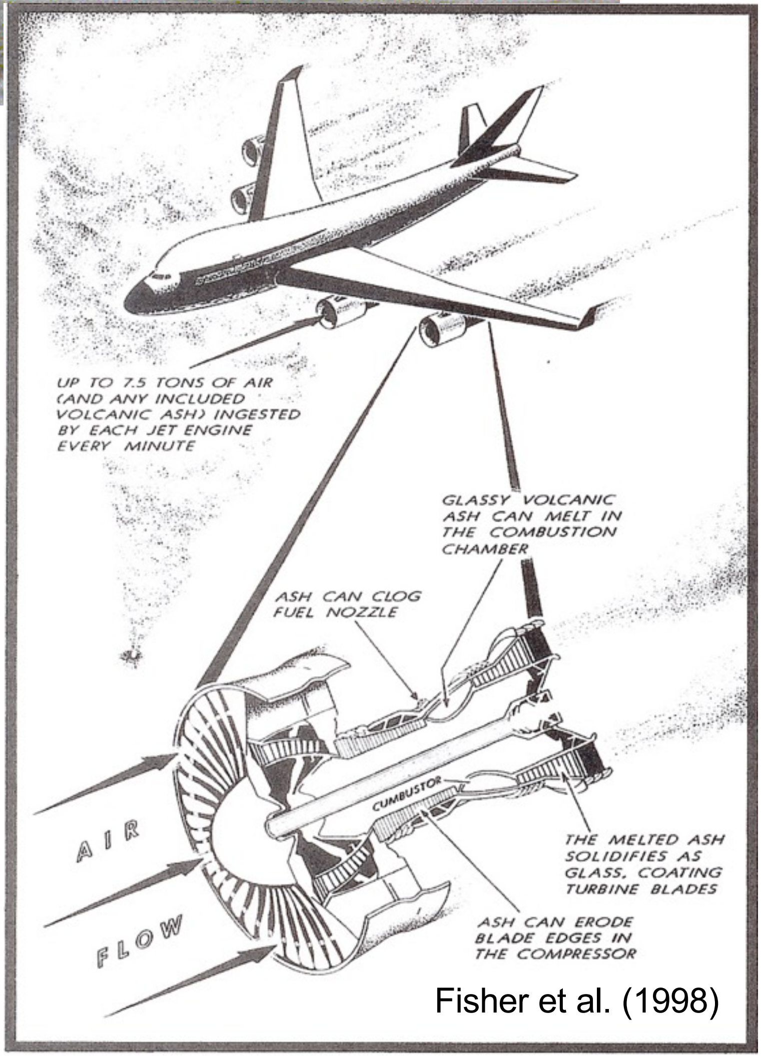

Fisher et al. (1998)

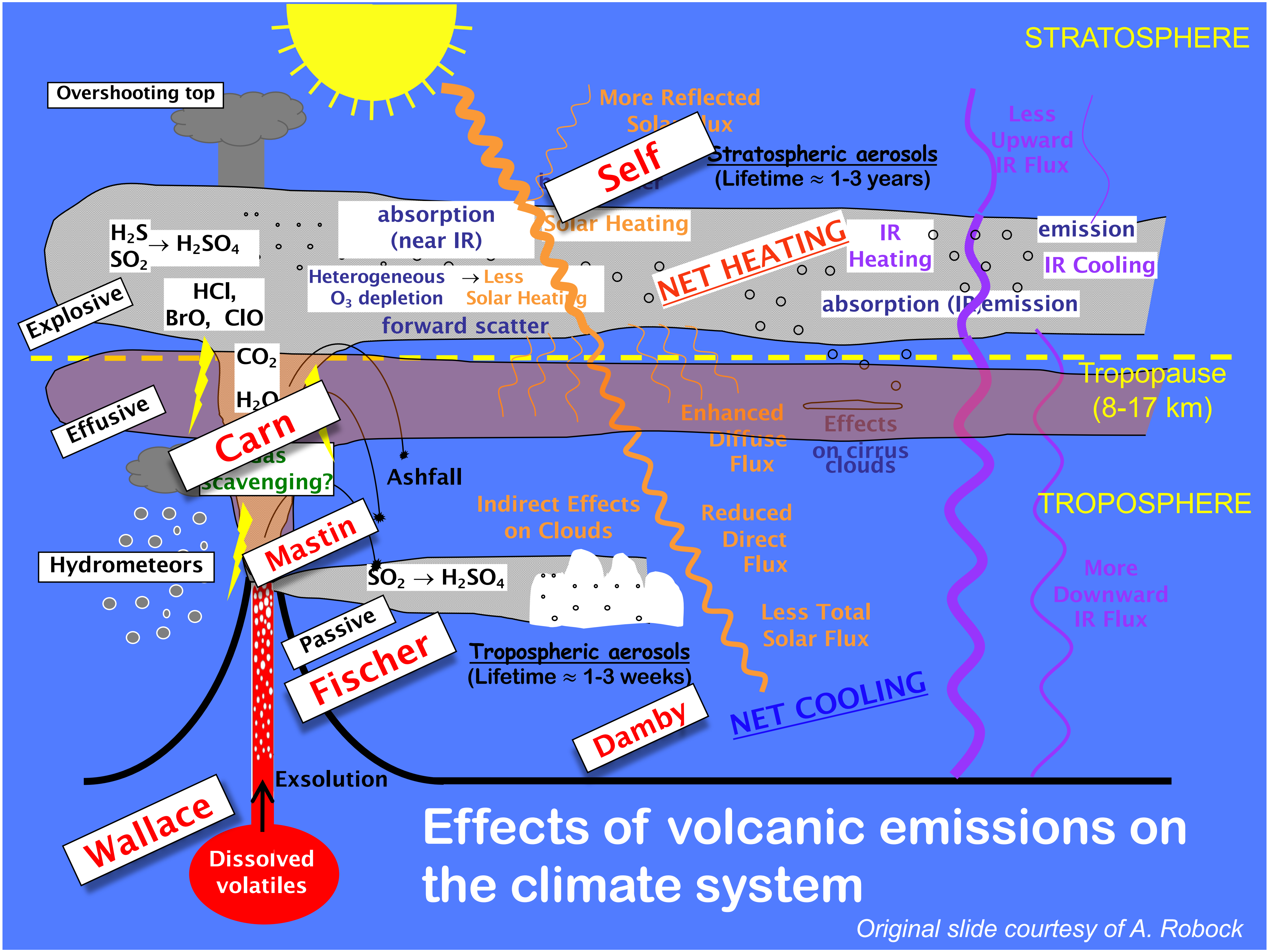

Effects of volcanic emissions on the climate system

Original slide courtesy of A. Robock

Outline

- Electromagnetic (EM) radiation
  - What do remote sensing techniques detect?
- Principles of satellite remote sensing
  - Ultraviolet (UV) and Infrared (IR) measurements
  - Spatial and temporal resolution
- Satellite remote sensing of volcanic eruptions
  - What information can satellites provide during eruptions?
  - What gas species can be measured?
- Synthesis of global eruptive SO_2 measurements
  - Degassing and deformation
- Passive volcanic degassing from space
  - New global database of volcanic emissions

Maxwell’s equations – what is light?

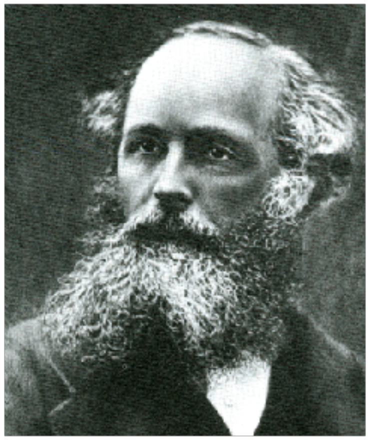

James Clerk Maxwell

$$\nabla \bullet E = 0$$

Gauss’s Law for Electricity

$$\nabla \bullet B = 0$$

Gauss’s Law for Magnetism

E = electric field

B = magnetic field

$\nabla\bullet$ = Divergence

$\nabla\times$ = Curl

$$\nabla \times E = -\frac{\partial B}{\partial t}$$

Faraday’s Law of Induction

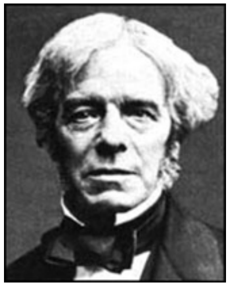

- ε_0 (electric permittivity of free space) = 8.854188×10^{-12} Farad m^{-1}
- μ_0 (magnetic permeability of free space) = 1.2566×10^{-6} T m A^{-1}

$$\nabla \times B = \varepsilon_0 \mu_0 \frac{\partial E}{\partial t}$$

Ampere’s Law

The speed of light

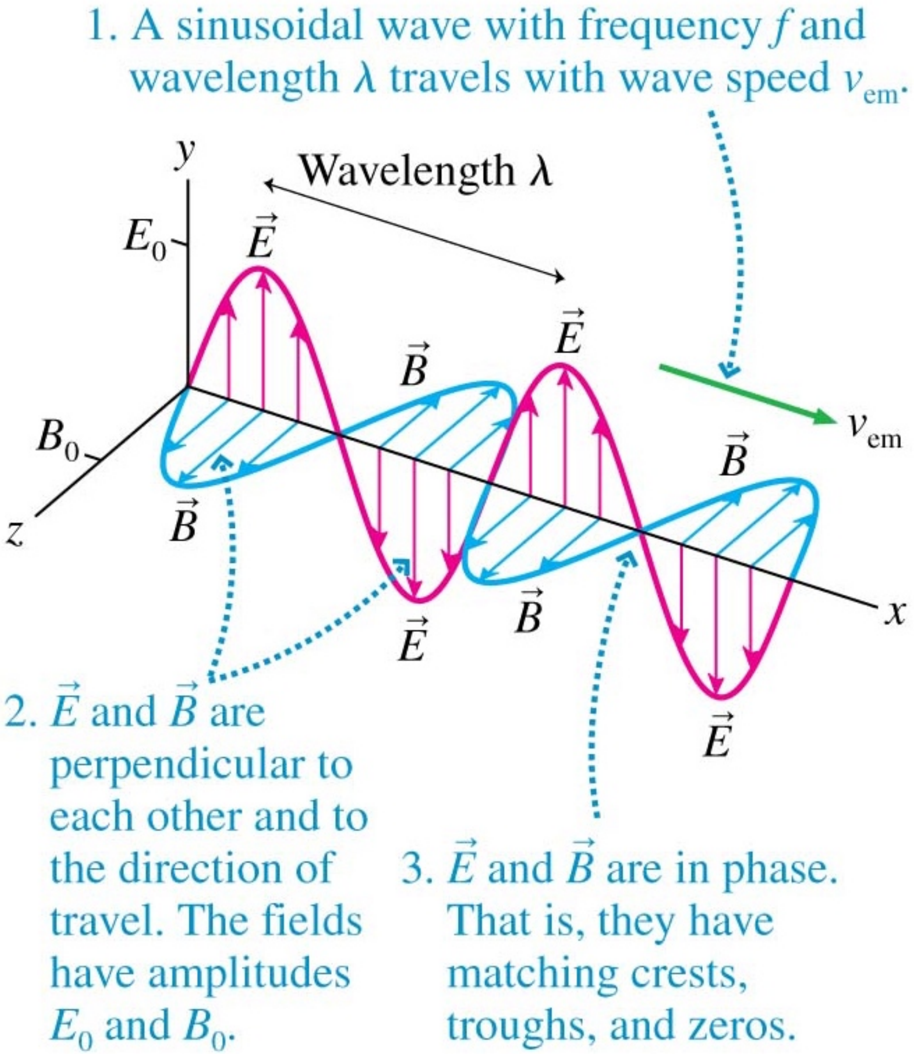

1. A sinusoidal wave with frequency f and wavelength λ travels with wave speed v_{em}.

2. $\vec{E}$ and $\vec{B}$ are perpendicular to each other and to the direction of travel. The fields have amplitudes E_0 and B_0.

3. $\vec{E}$ and $\vec{B}$ are in phase. That is, they have matching crests, troughs, and zeros.

$$v = f\lambda$$

Solution to Maxwell's Equations:

$$\nabla^2 \vec{E} = \mu\varepsilon \frac{\partial^2 \vec{E}}{\partial t^2}$$

Wave equation

$$\nabla^2 u = \frac{1}{v^2}\frac{\partial^2 u}{\partial t^2}$$

So for EM waves, $v = \dfrac{1}{\sqrt{\mu\varepsilon}}$

$$v = c = 2.998\times10^{8}\ \mathrm{m\ s^{-1}}$$

Electromagnetic wave generation

- There is no fundamental constraint on the frequency of electromagnetic (EM) radiation, provided an oscillator with the right natural frequency and/or an energy source with the minimum required energy is present

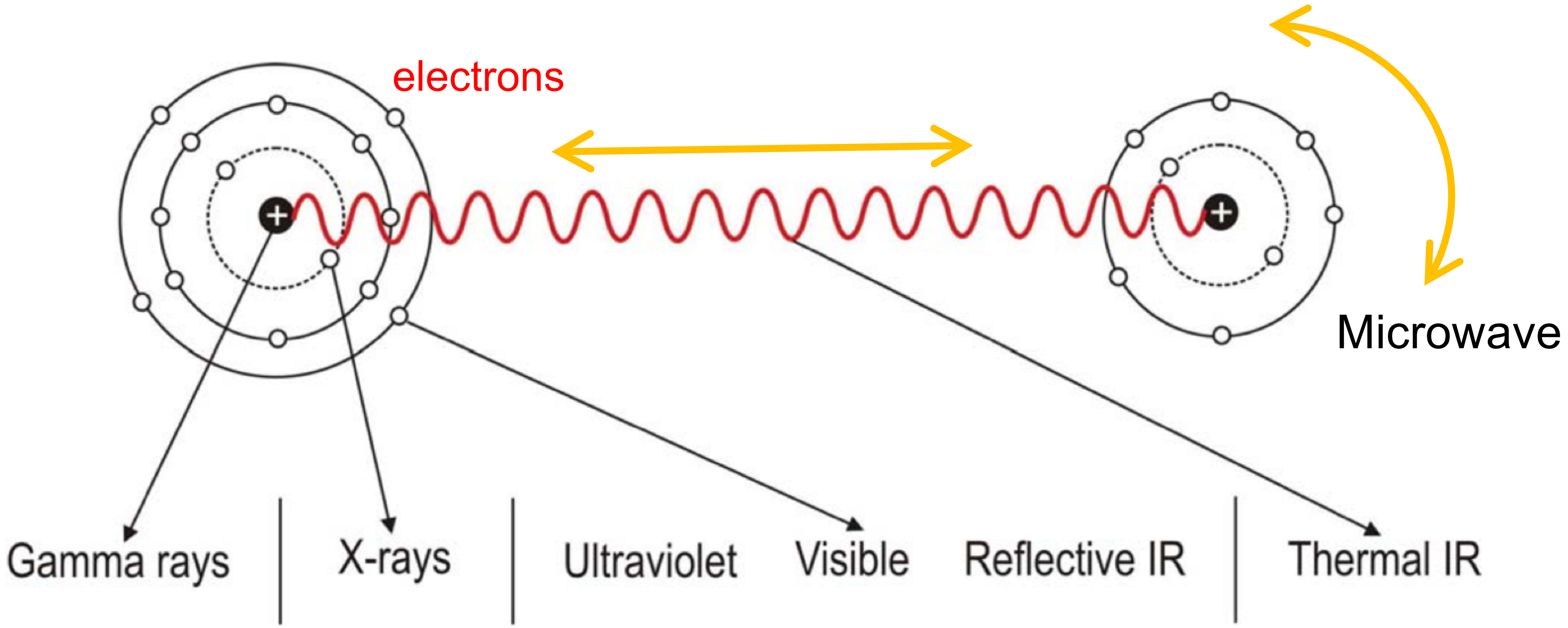

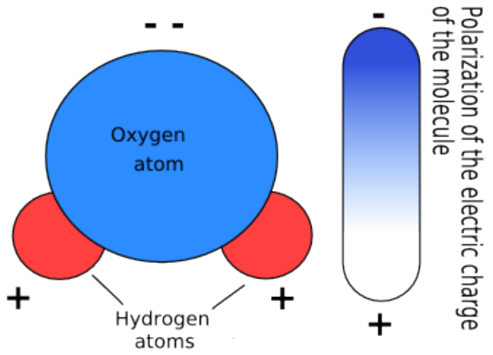

Water molecule (dipole)

The Electromagnetic Spectrum

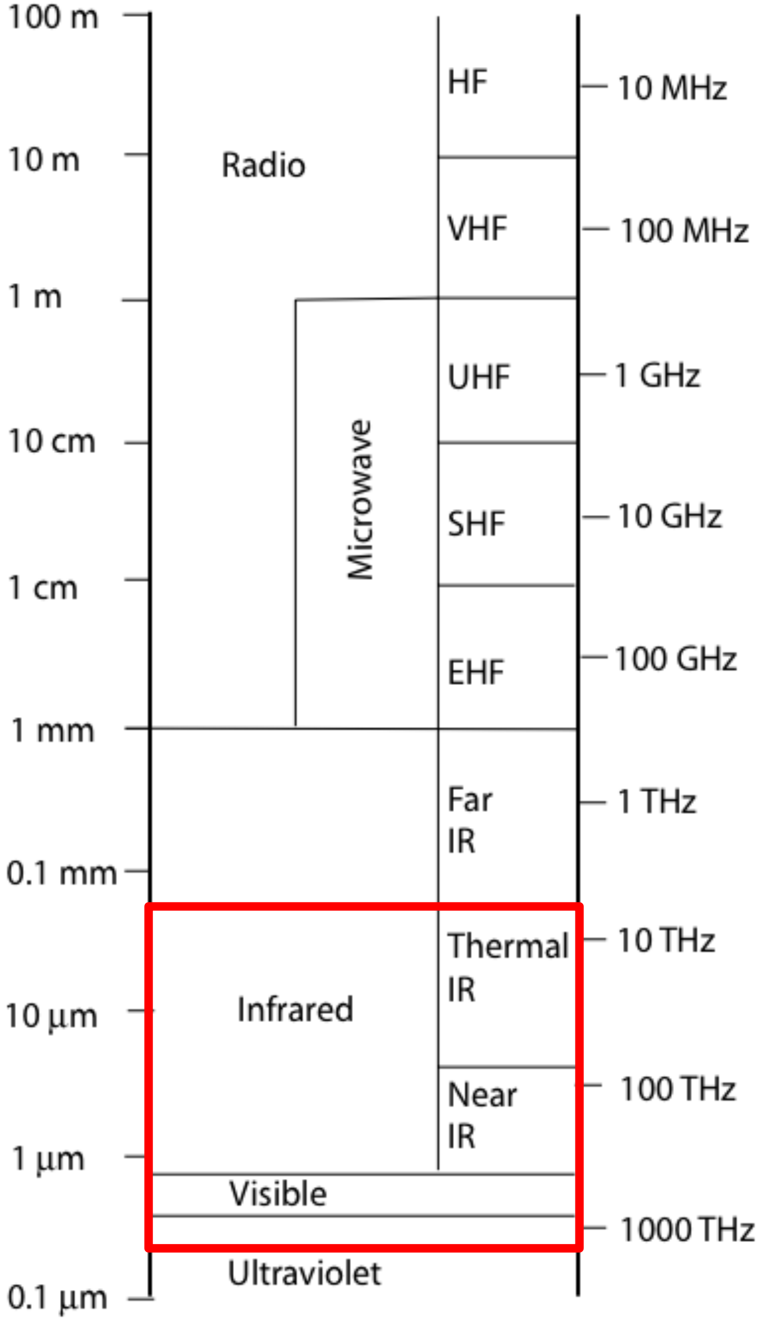

The EM spectrum is subdivided into a few discrete spectral bands*.*

EM radiation spans an enormous range of frequencies; the bands shown here are those most often used for remote sensing.

Boundaries between bands are arbitrary and have no physical significance, except for the *visible band.*

Absorption of UV radiation by atmospheric gases

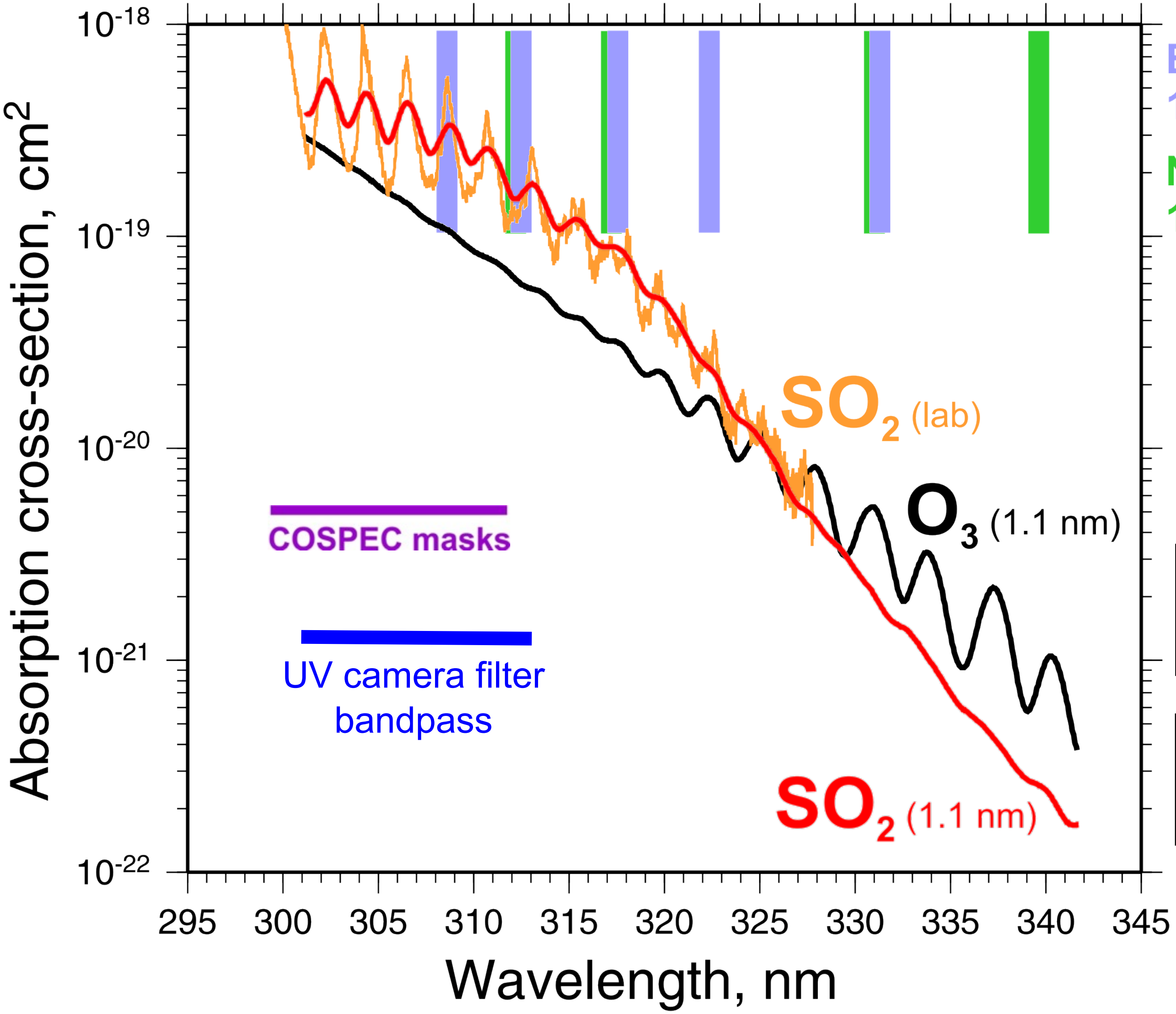

Earth Probe TOMS 1996-

Nimbus-7 TOMS 1978-93

- UV radiation absorbed by electronic transitions in SO_2 and O_3

Multi-spectral
Discrete bands

Hyperspectral
Full spectrum

- Spectral resolution affects sensitivity

Absorption of IR radiation by atmospheric gases

Fundamental or normal modes

ν_1 Symmetric stretch

ν_2 Bend (Scissoring)

ν_3 Asymmetric stretch

A normal mode is IR-active if the dipole moment changes during mode motion.

Overtones, combinations and differences of fundamental vibrations are also possible (e.g., $2v_1$, v_1+v_3 etc.)

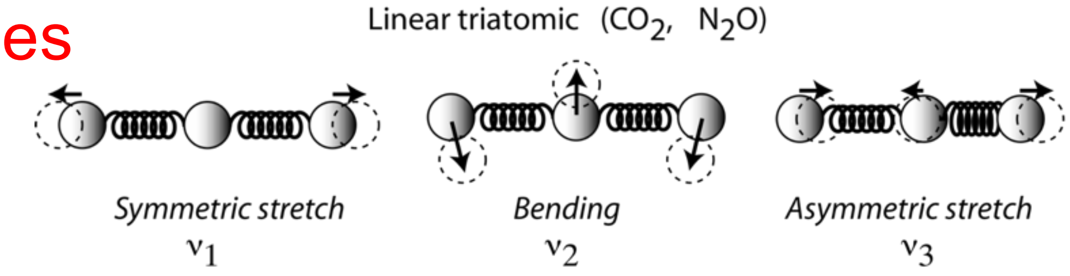

Non-linear triatomic (O_3, SO_2, H_2O)

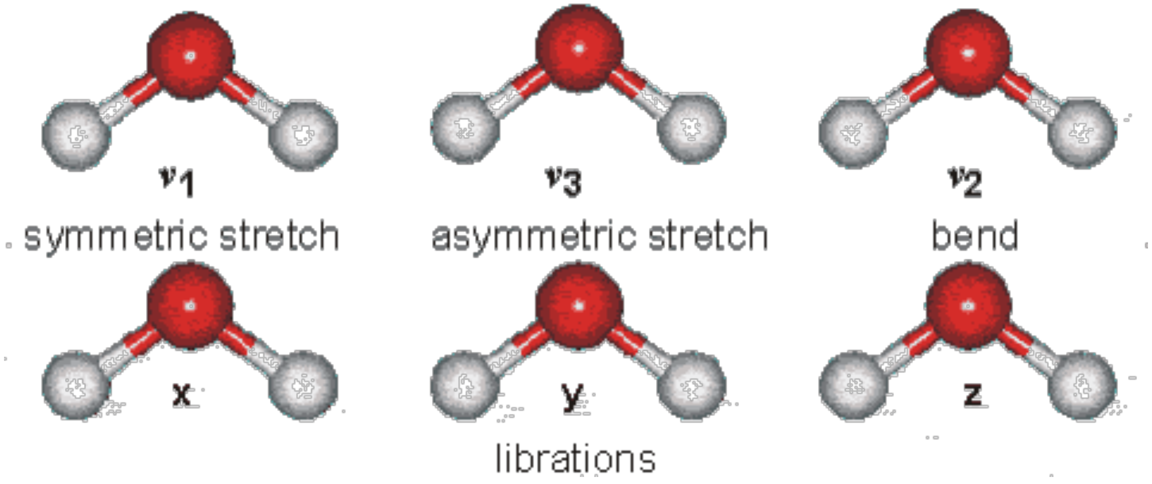

SO$_2$
'Accessible bands'

v_1: 1151 cm^{-1}, 8.6 μm

v_3: 1361 cm^{-1}, 7.3 μm – high altitude SO_2

v_1+v_3: 2500 cm^{-1}, 4 μm

Volcano remote sensing – spectral bands

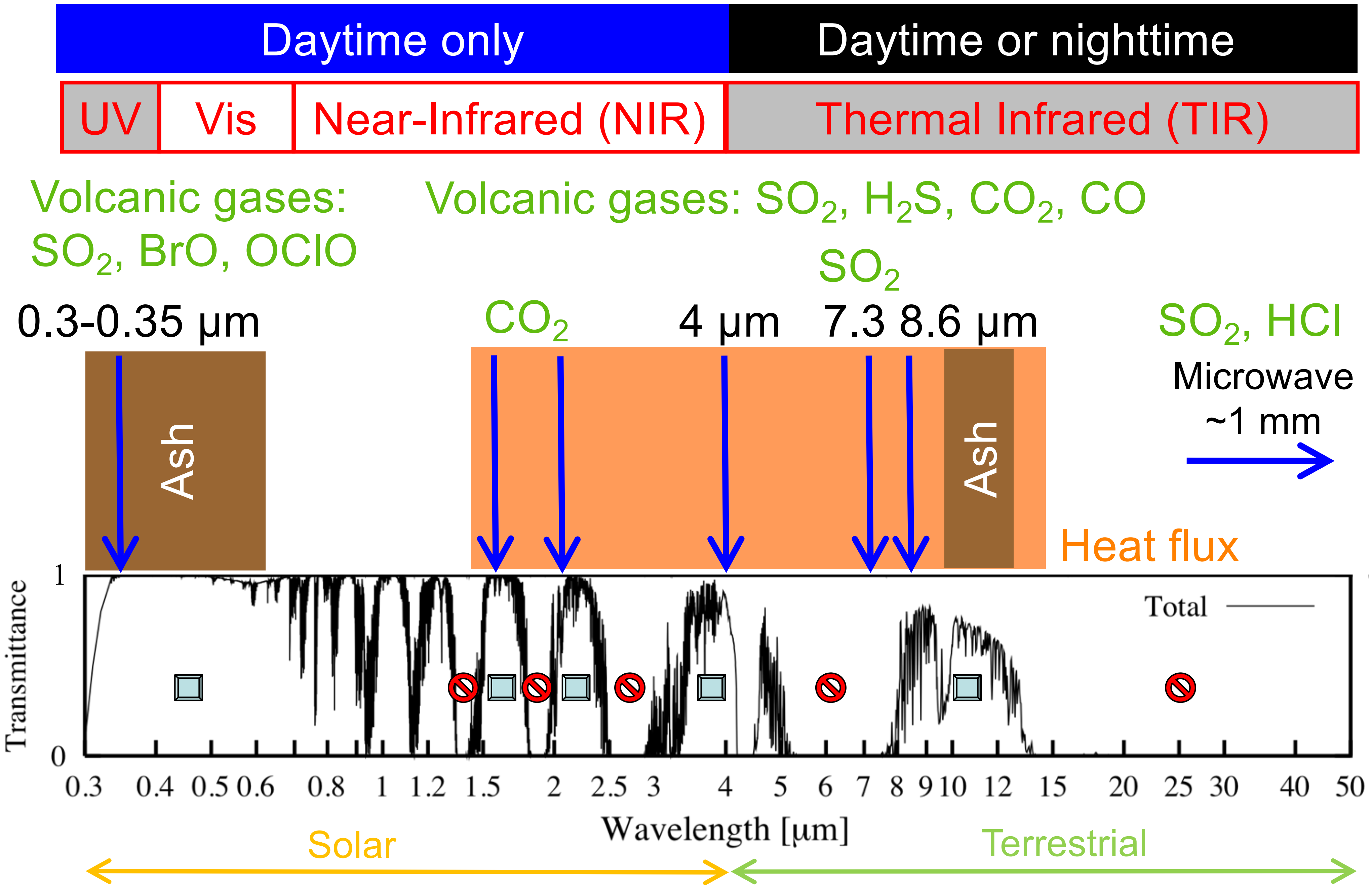

Daytime only

Daytime or nighttime

UV | Vis | Near-Infrared (NIR) | Thermal Infrared (TIR)

Volcanic gases: SO_2, BrO, OClO

Volcanic gases: SO_2, H_2S, CO_2, CO

SO_2

0.3-0.35 µm

CO_2

4 µm

7.3 8.6 µm

SO_2, HCl

Microwave ~1 mm

Ash

Ash

Heat flux

Solar

Terrestrial

UV and IR satellite remote sensing

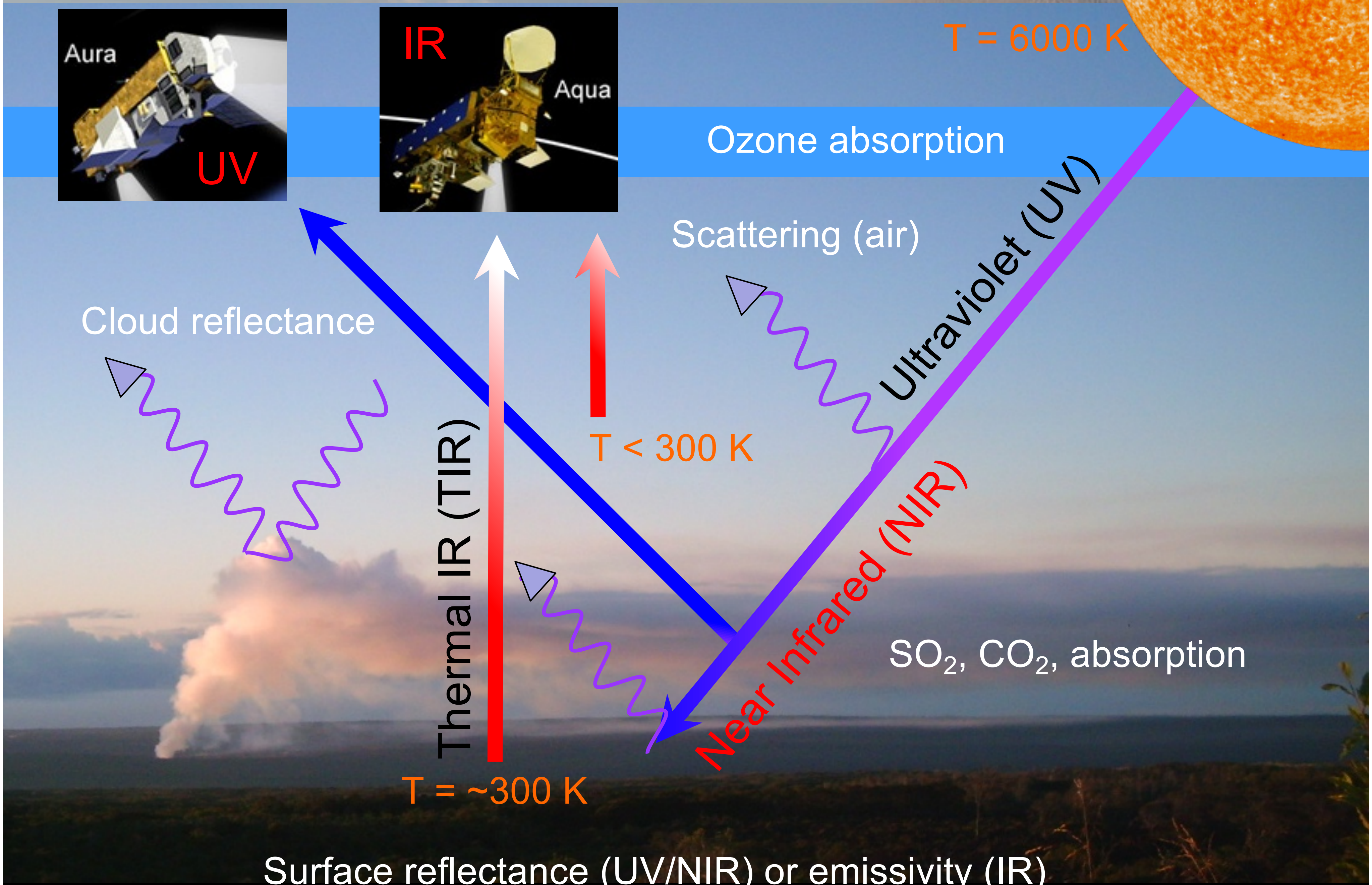

T = 6000 K

Ozone absorption

Scattering (air)

Ultraviolet (UV)

Cloud reflectance

Thermal IR (TIR)

T < 300 K

Near Infrared (NIR)

SO_2, CO_2, absorption

T = ~300 K

Surface reflectance (UV/NIR) or emissivity (IR)

Beer-Bouguer-Lambert (Beer's) Law

For a gaseous absorber, absorbance (A) is equal to the product of an absorption cross-section (σ, cm^2), the number density of absorbers (N, molecules cm^{-3}) and the path length (d):

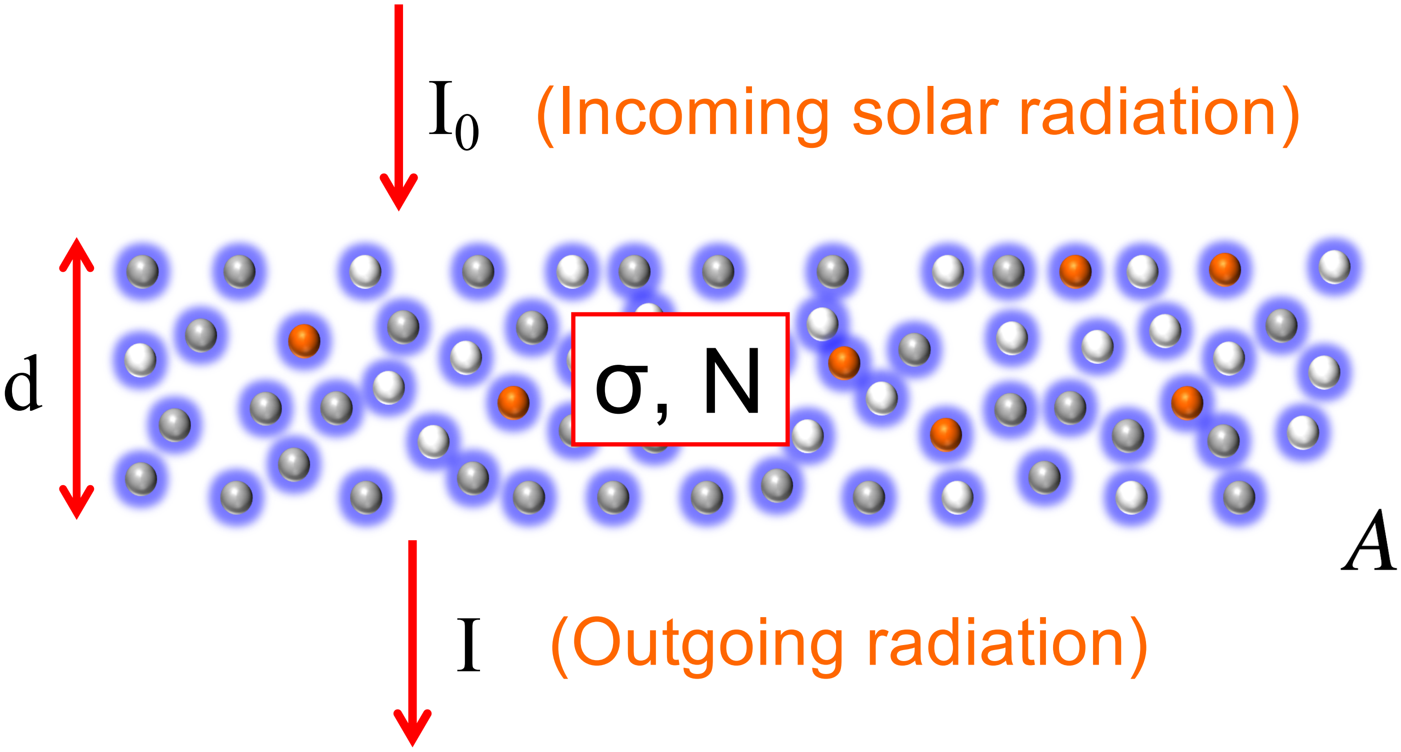

$$t = \frac{I}{I_0} = e^{-\sigma N d}$$

Transmittance

$$A = -\ln \frac{I}{I_0} = \sigma N d$$

Absorbance

- Absorption is dependent on gas temperature/pressure, hence volcanic SO_2 retrievals must use an a-priori plume vertical profile
- Lower troposphere (~3 km; TRL), mid-troposphere (~8 km; TRM) and upper troposphere to lower stratosphere (~17 km; STL) typically used

Satellite measurements of trace gases

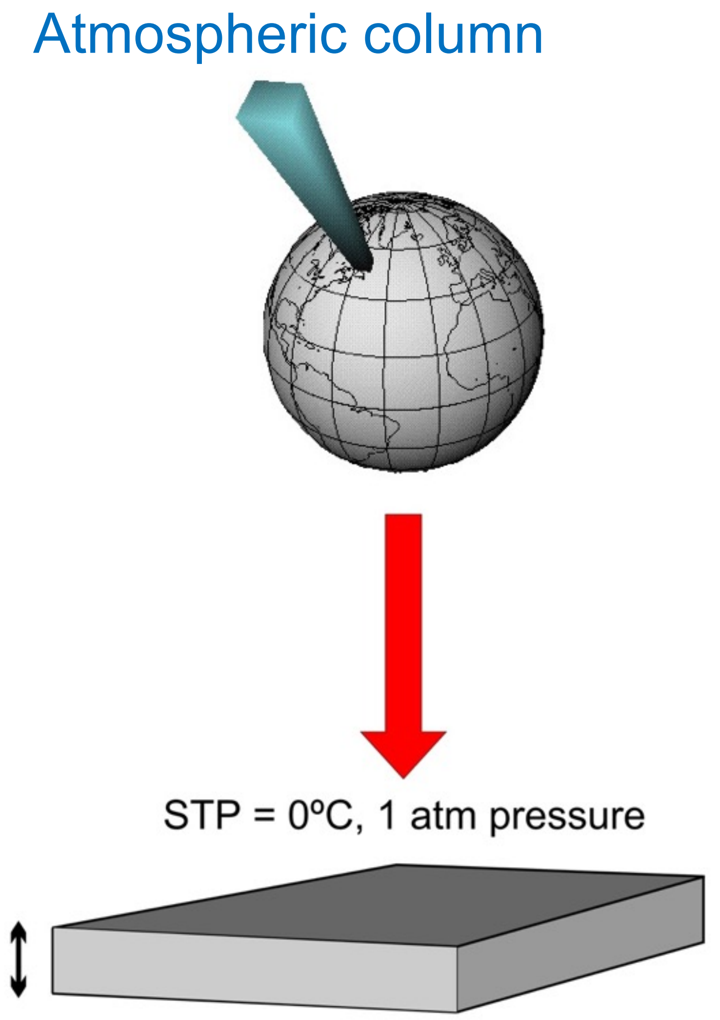

Atmospheric column

STP = 0ºC, 1 atm pressure

1 Dobson Unit (DU) = 1 Milli Atm cm
1 DU = 0.01 mm thickness at STP
e.g. 800 DU = 8 mm thick layer
1 DU = 10 ppmm at STP

- Satellites measure the 'column amount' or 'total column' of a gas
  - US units: Dobson Unit (DU)
  - 1 DU = 2.69×10^{16} molecules cm^{-2} = 0.0285 g m^{-2} SO_2
  - Averaged over satellite footprint (km^2)
- Typical SO_2 columns in volcanic clouds
  - Fresh eruption cloud: 100s – 1000+ DU
  - Passive degassing: <20 DU
  - Measured column depends on spatial resolution of sensor
  - Can be converted to mass or concentration (if cloud thickness is known)
- Sensitivity decreases towards surface
  - Snow cover can enhance sensitivity (in the UV)

Relative sensitivity of UV and IR measurements

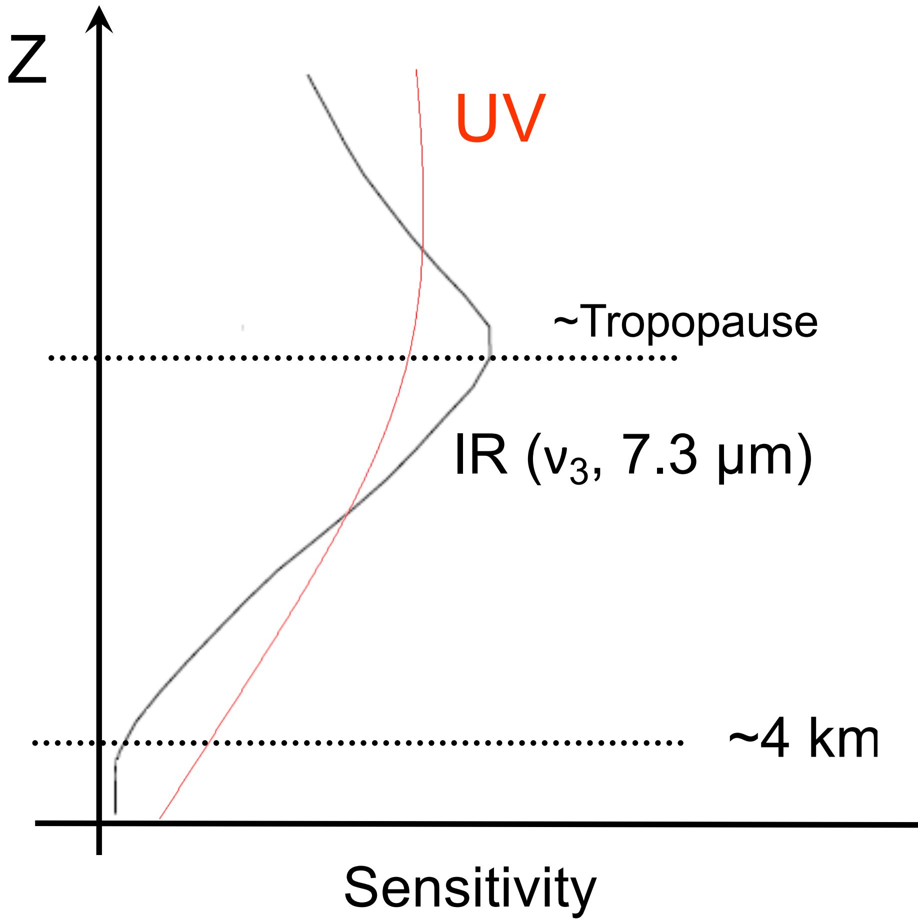

Courtesy of L. Clarisse, ULB

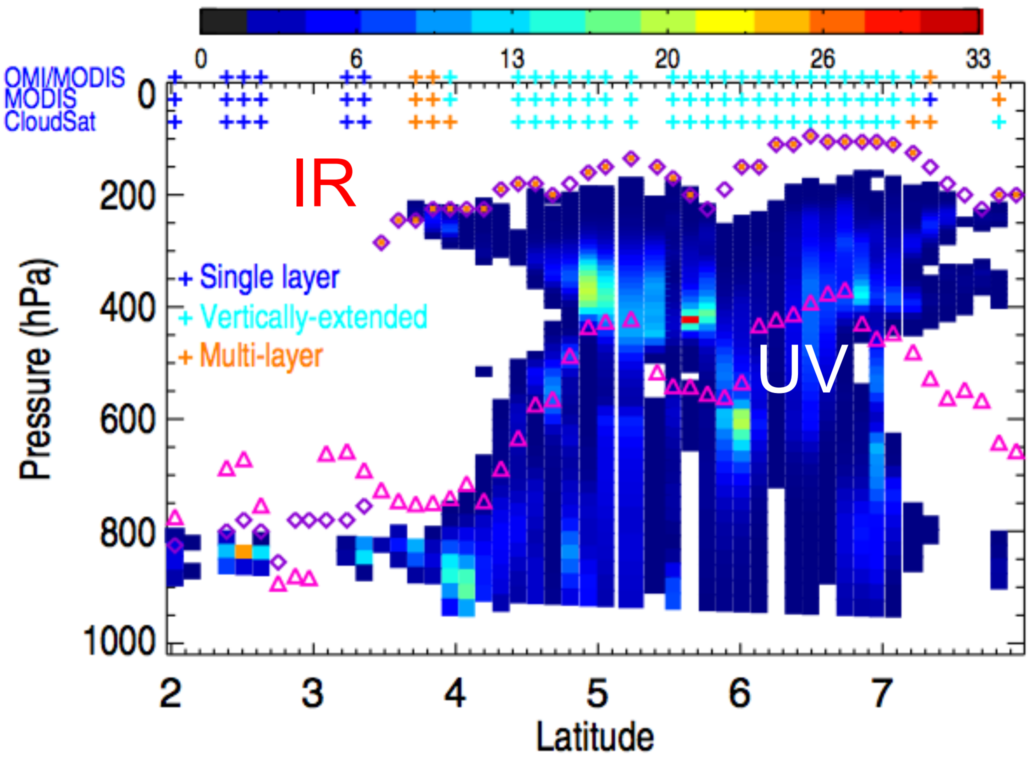

Fig. 7. CloudSat 2B-Tau cross section of cloud extinction (km^{-1}) along OMI orbit 12 402 (western track in tropical Pacific highlighted in Fig. 6); Averaged along-track over OMI pixel (~13 km); Pink triangles: OMI optical centroid cloud pressure; Purple diamonds: MODIS minimum cloud-top pressure within closest passive sensor footprint, orange-filled where MODIS maximum multi-layer flag >2.

Joiner et al. (2009)

- IR cloud top ≠ UV cloud pressure

- SO_2 altitude can be directly retrieved in some cases (UV and IR)
- Satellite sensitivity increases with altitude in the troposphere
- UV measurements more sensitive to passive degassing (low altitude)

Satellite orbits and temporal resolution

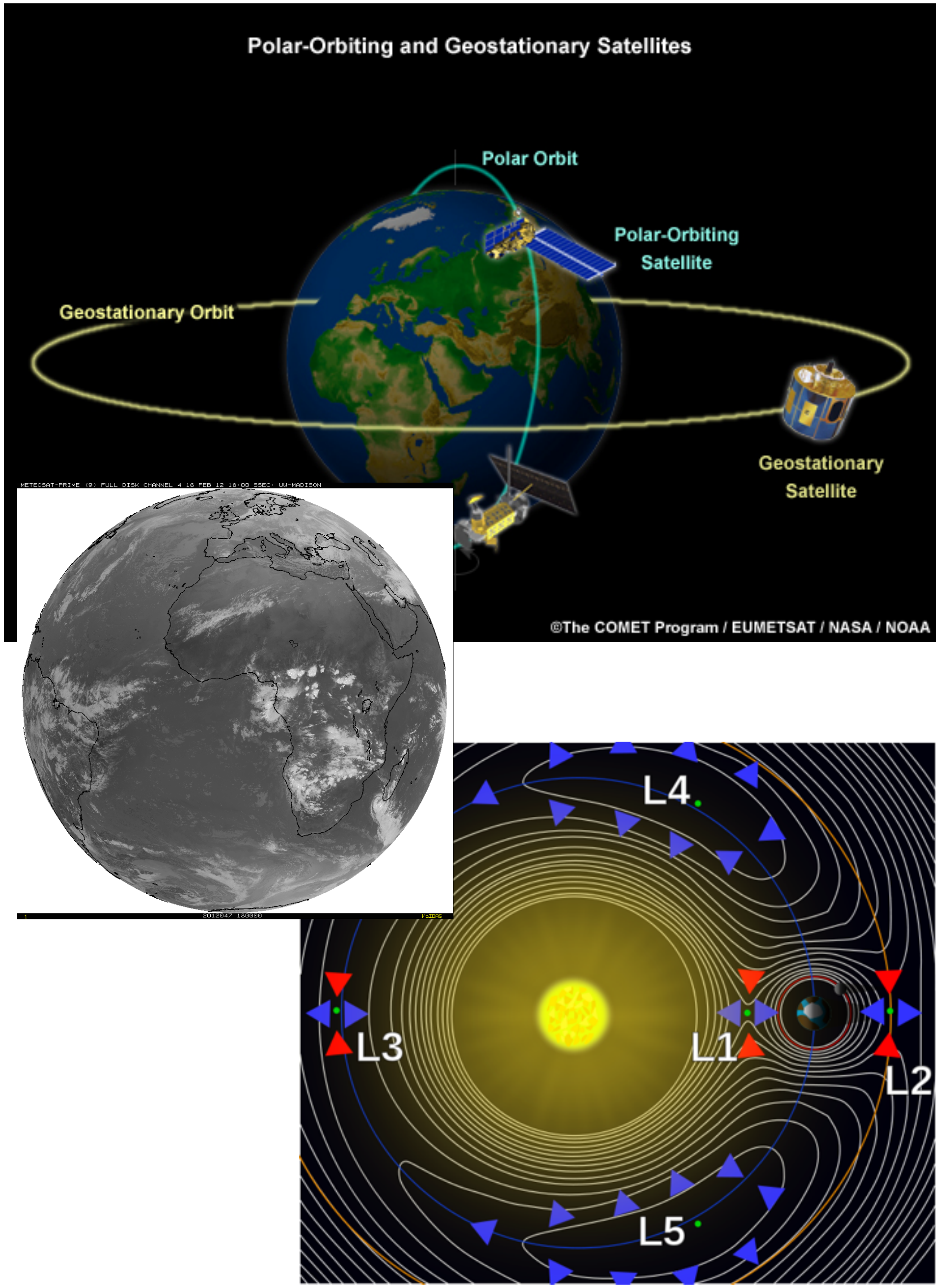

- Geostationary (GEO)
  - ~36,000 km altitude
  - Continuous view of one hemisphere
  - High temporal resolution (~1-15 min)
  - Low spatial resolution (~3 km+)
  - Poor high-latitude coverage (>55º)

- Polar-orbiting (LEO)
  - ~700-800 km altitude
  - 14-15 orbits per day
  - Low temporal resolution (hours-days)
  - Higher spatial resolution (m, km)
  - Coverage of polar regions

- L_1 Lagrange point
  - ~1.5 million km from Earth
  - Continuous view of sunlit Earth disk

Aura (2004-)

OMI - SO_2, NO_2, BrO

TES - SO_2

MLS - strat. SO_2, HCl

CloudSat (2006-)

CPR (radar) – precipitation, hydrometeors

Aqua (2002-)

MODIS - SO_2, ash, sulfate

AIRS - UTLS SO_2, ash

Volcanic CO_2?

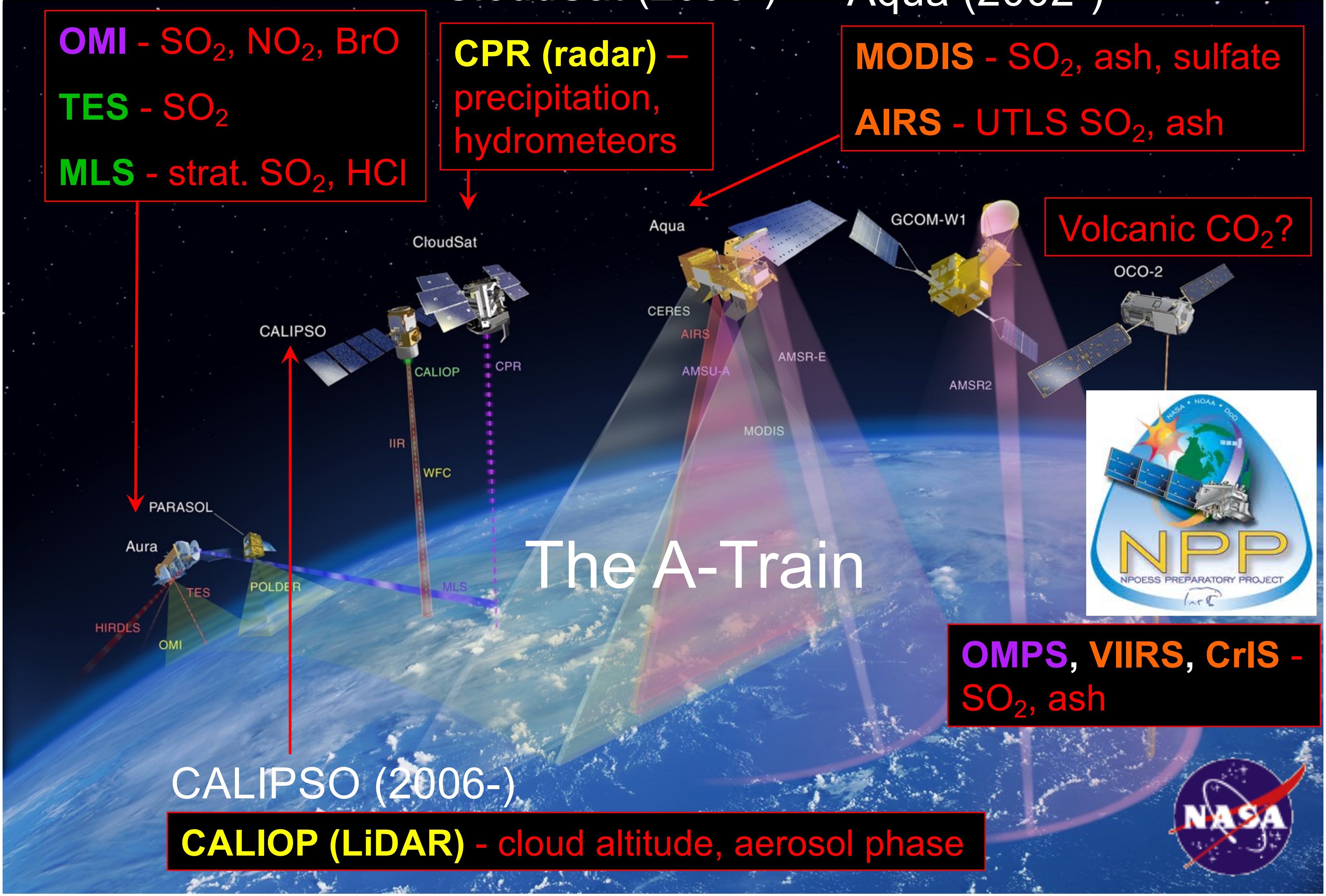

OMPS, **VIIRS**, **CrIS** - SO_2, ash

CALIPSO (2006-)

CALIOP (LiDAR) - cloud altitude, aerosol phase

Deep Space Climate Observatory (DSCOVR) at L_1

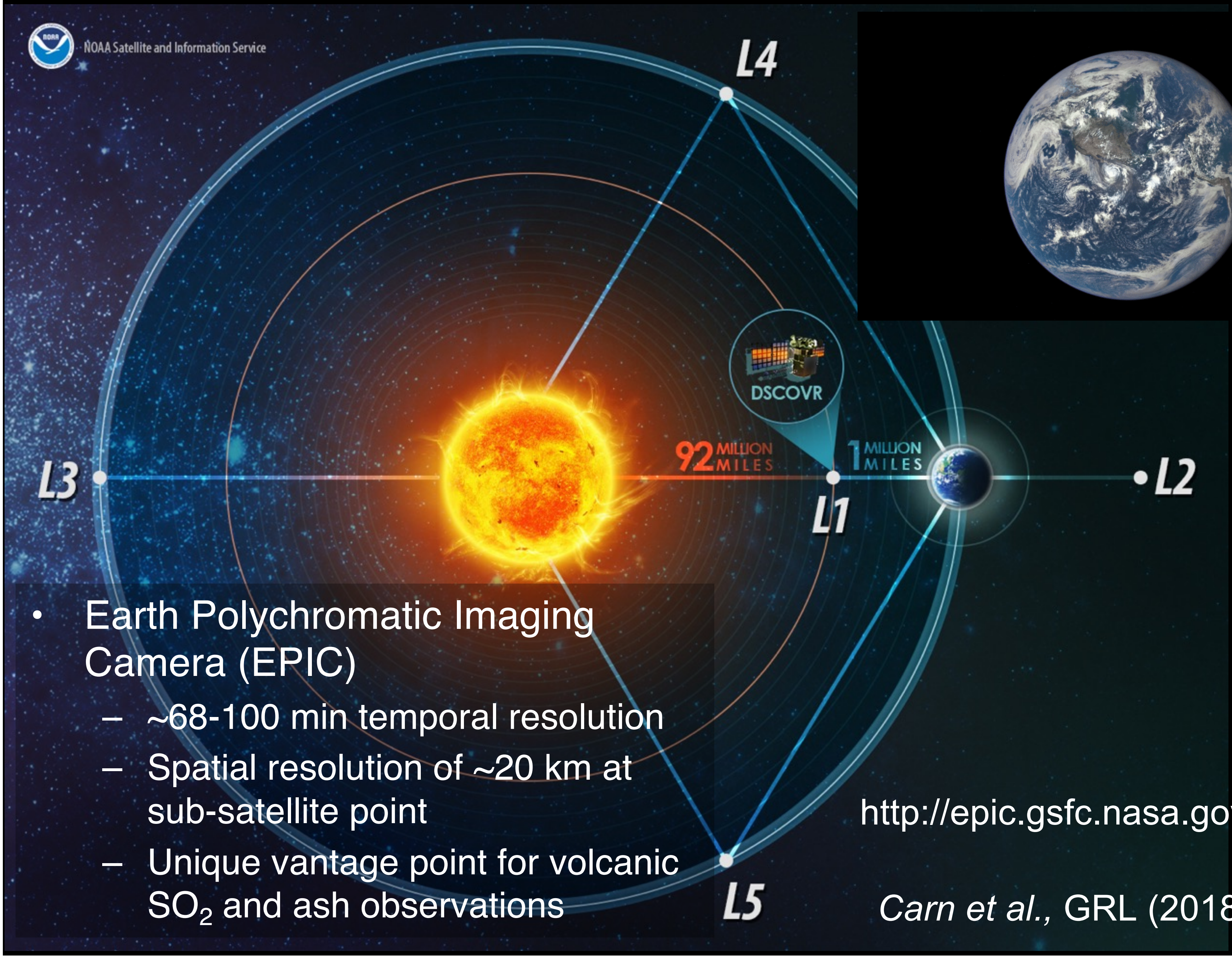

- Earth Polychromatic Imaging Camera (EPIC)
  - ~68-100 min temporal resolution
  - Spatial resolution of ~20 km at sub-satellite point
  - Unique vantage point for volcanic SO_2 and ash observations

http://epic.gsfc.nasa.gov

Carn et al., GRL (2018)

Sierra Negra

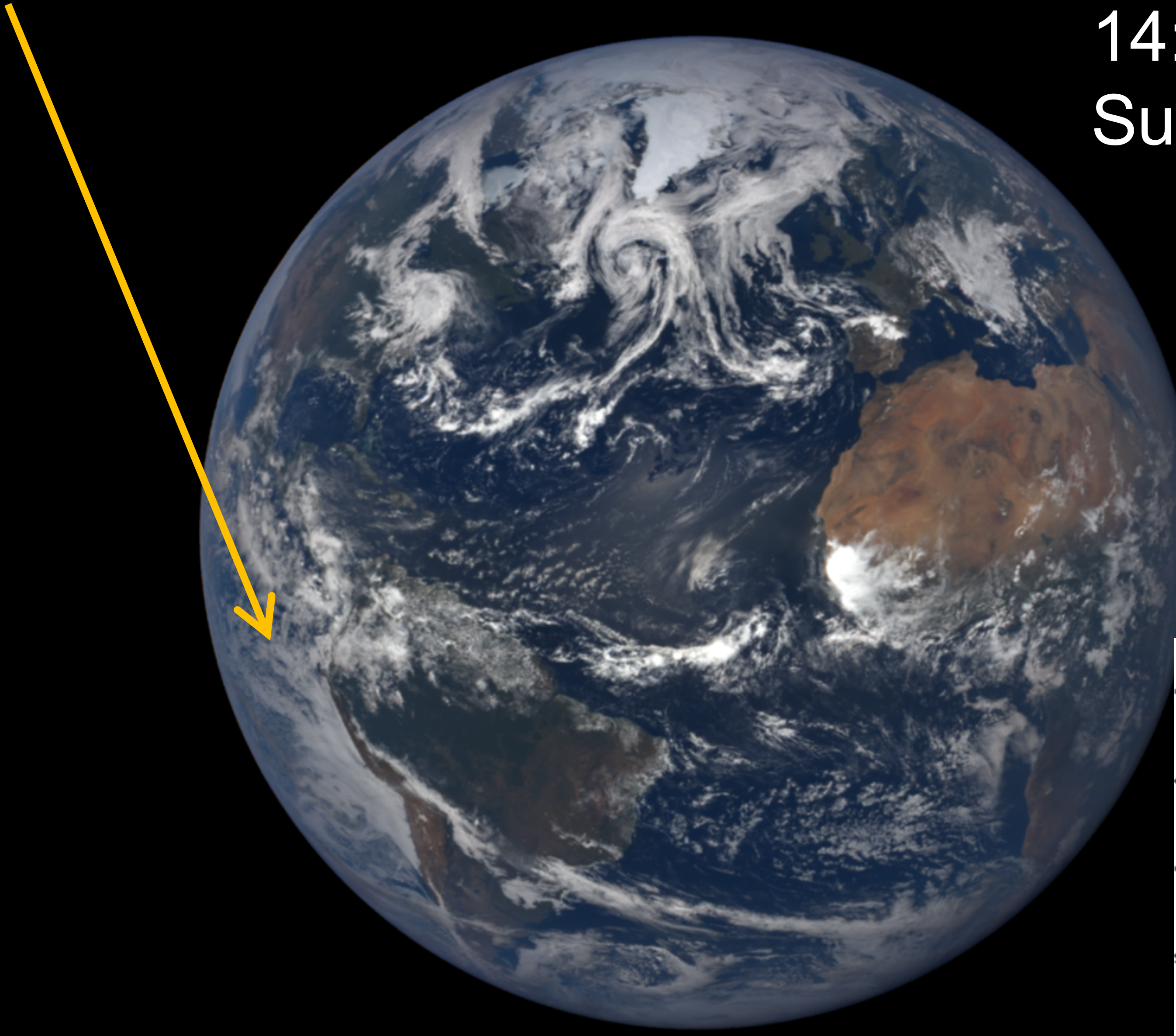

Jun 26, 2018
14:38 UT
Sunrise

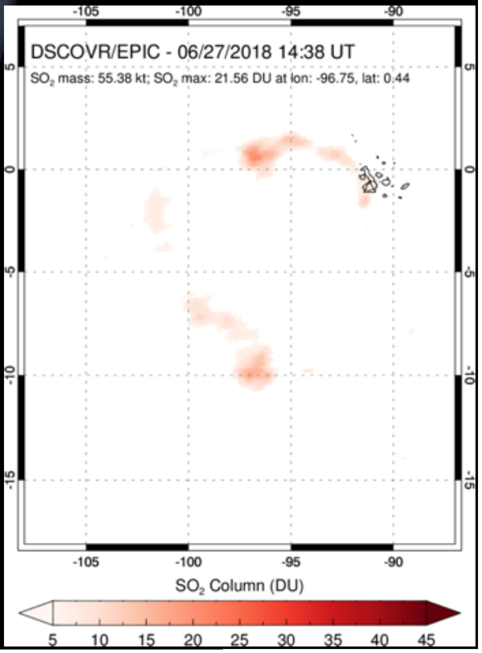

Jun 26, 2018
15:43 UT

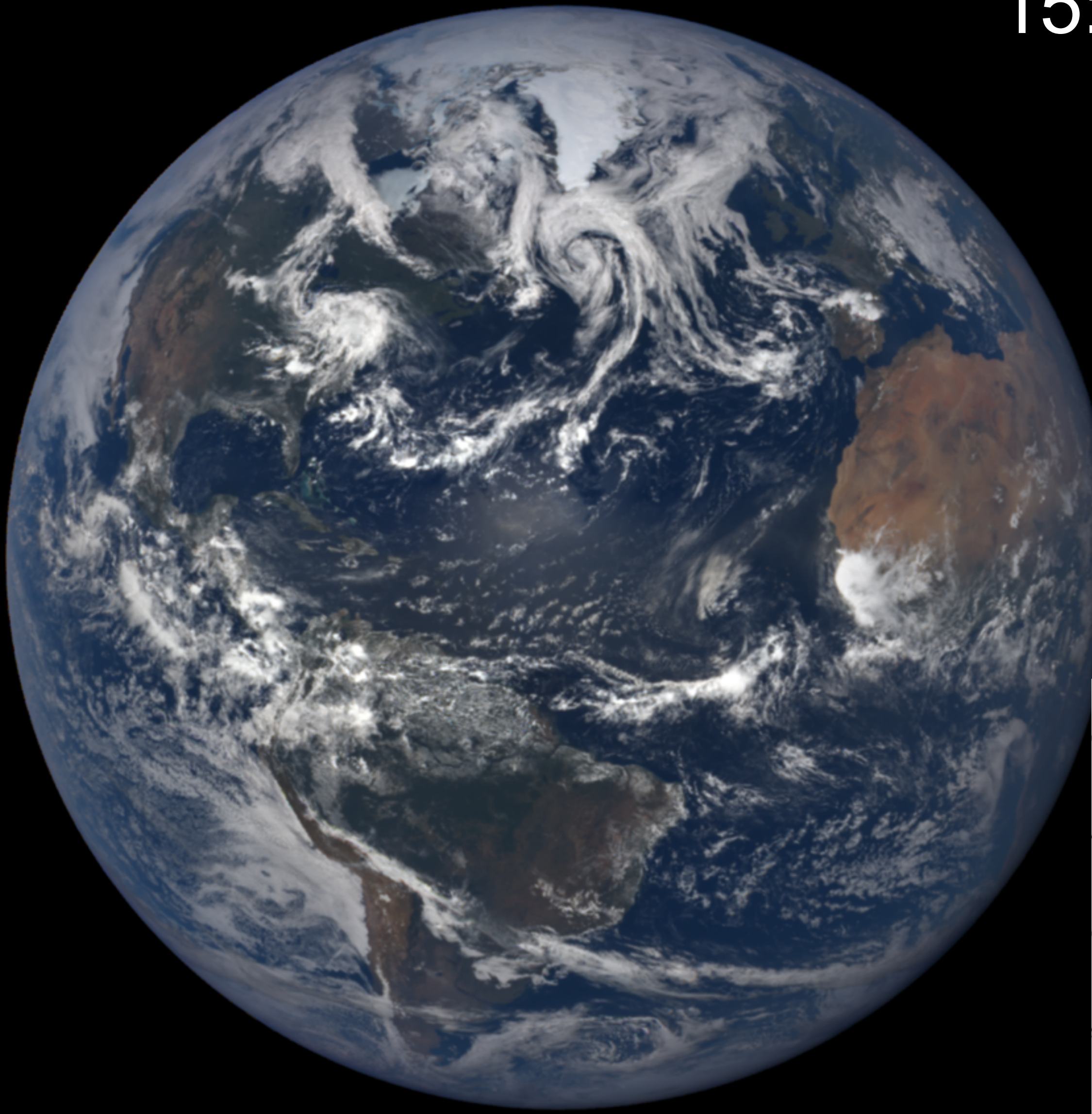

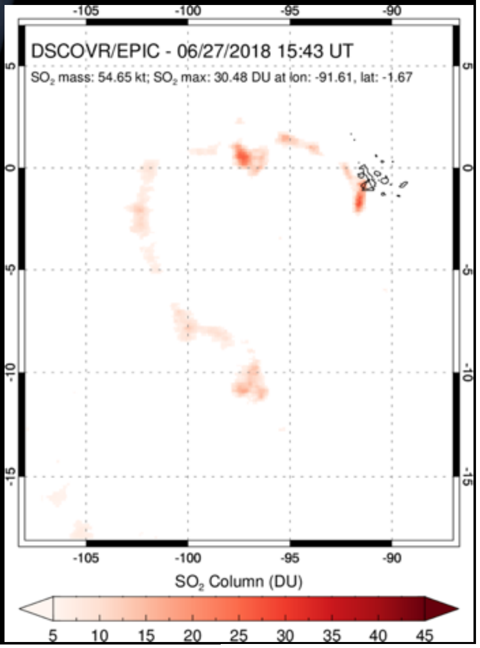

Jun 26, 2018
16:49 UT

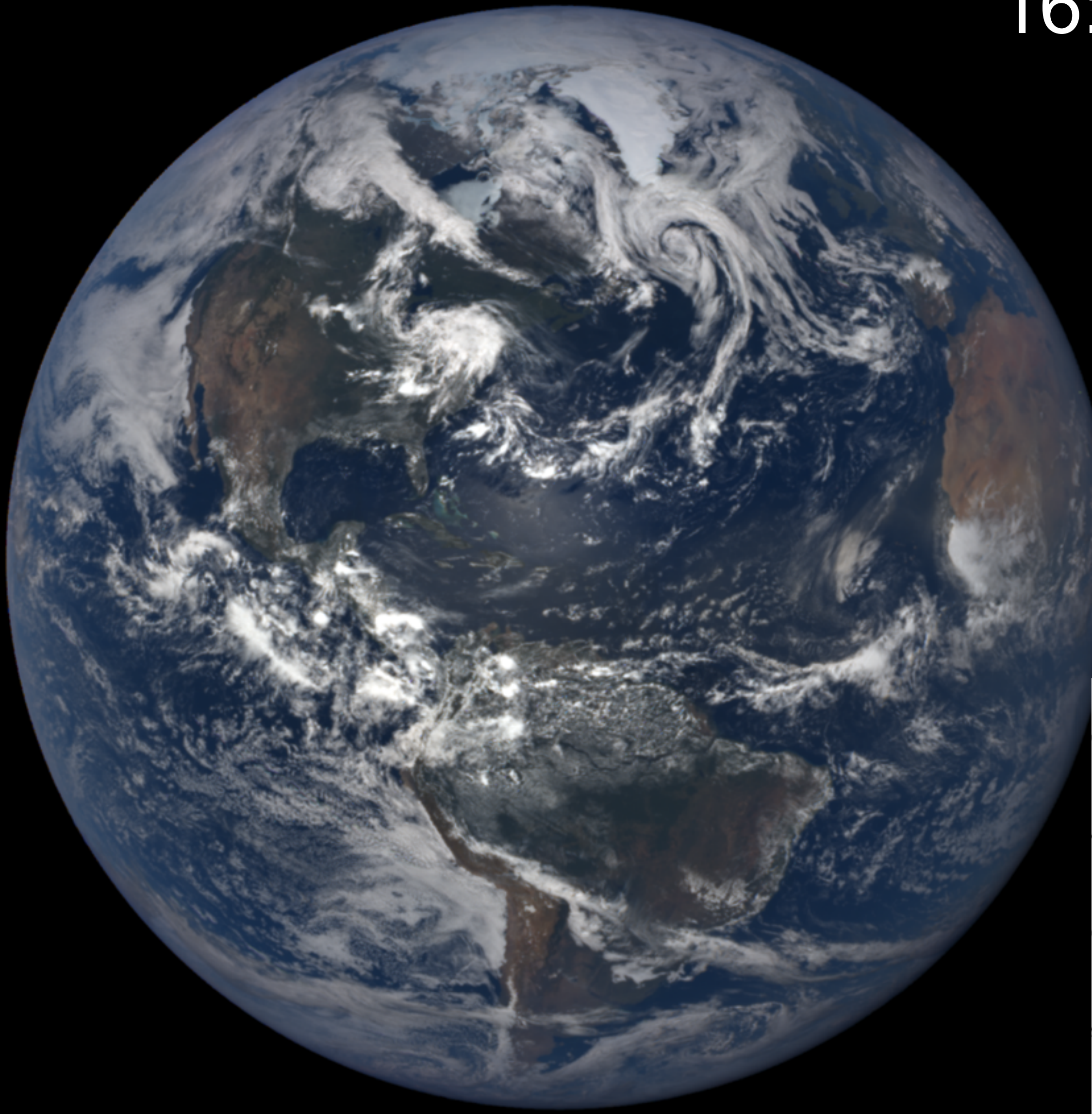

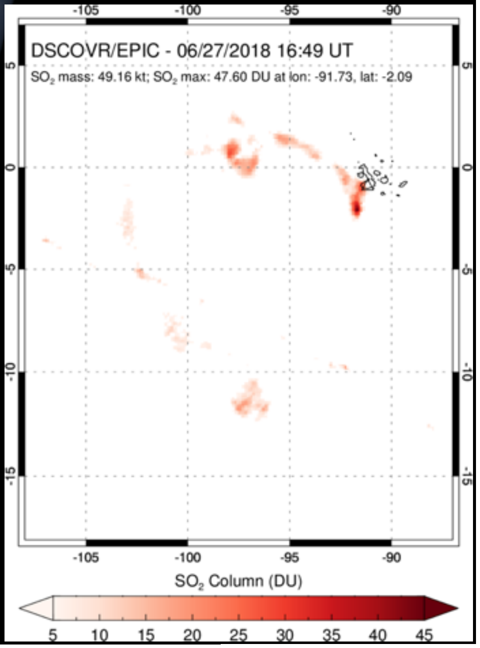

DSCOVR/EPIC - 06/27/2018 16:49 UT

SO_2 mass: 49.16 kt; SO_2 max: 47.60 DU at lon: -91.73, lat: -2.09

Jun 26, 2018
17:54 UT

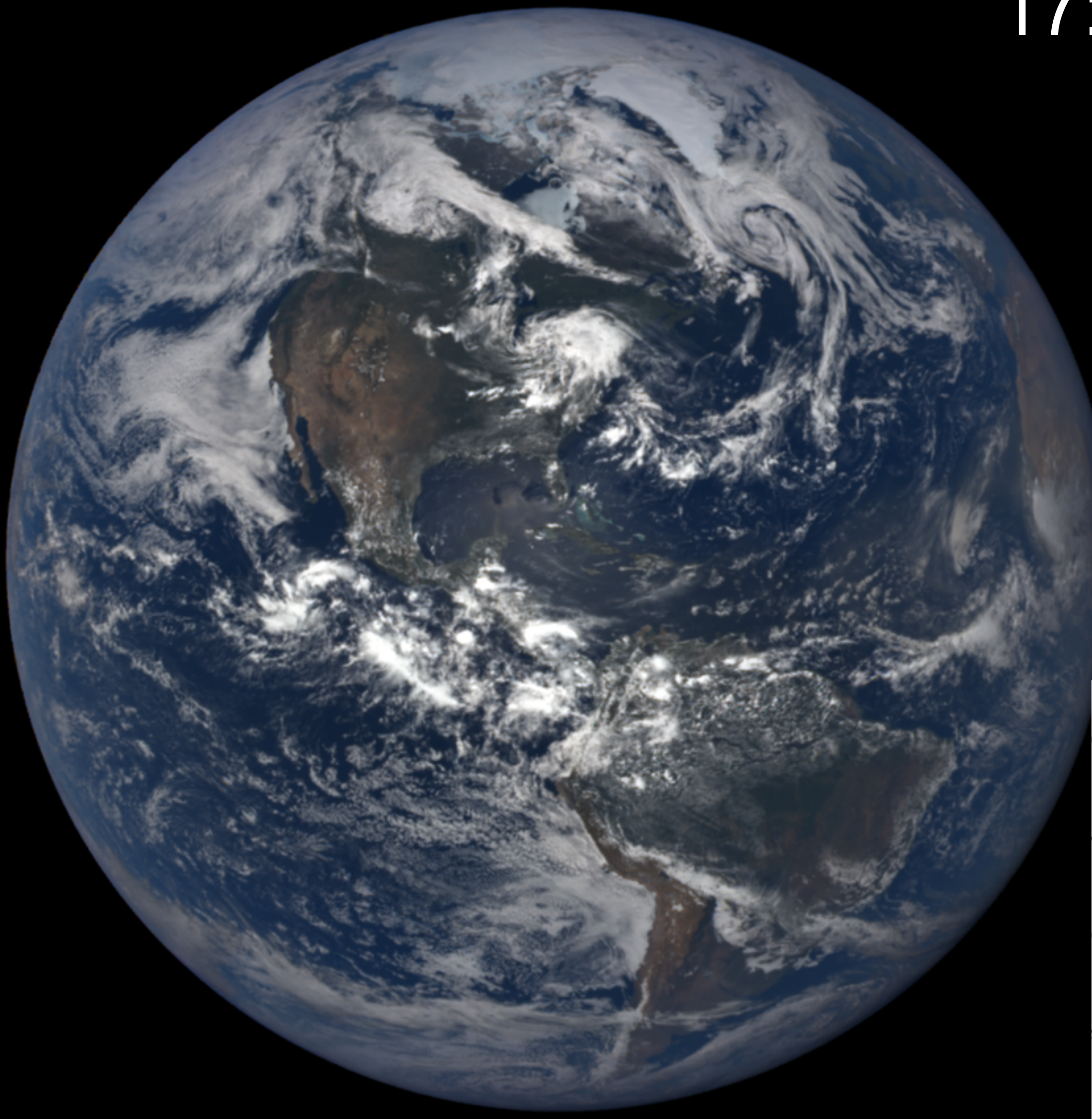

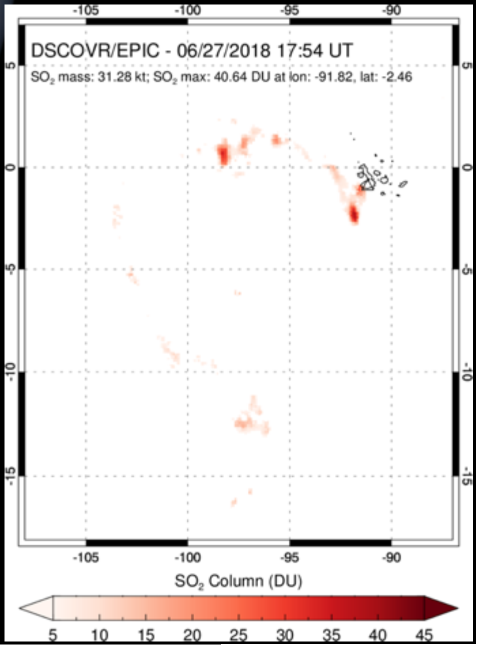

Jun 26, 2018
19:00 UT

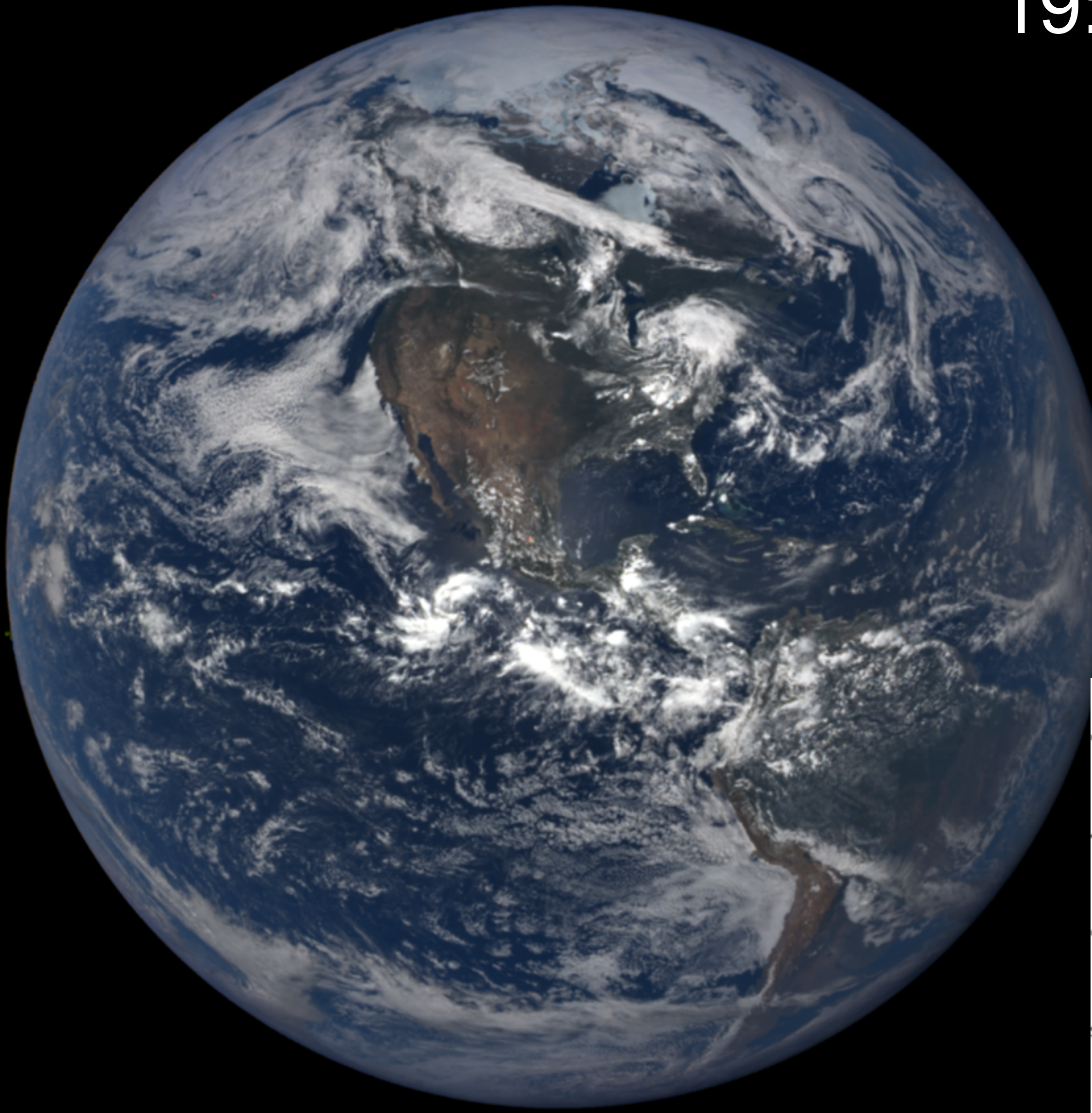

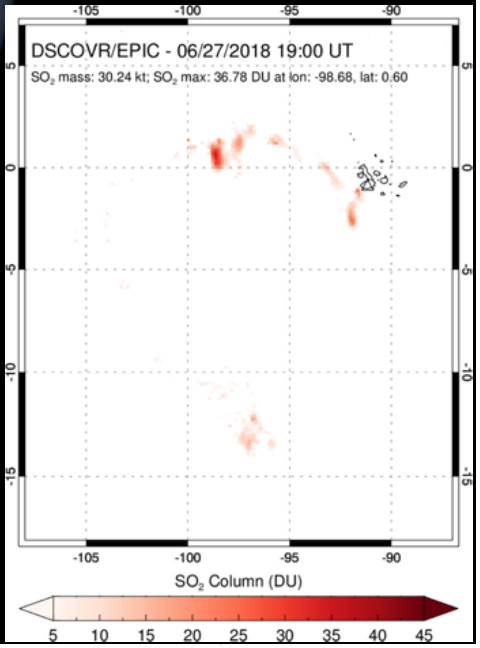

DSCOVR/EPIC - 06/27/2018 19:00 UT

SO_2 mass: 30.24 kt; SO_2 max: 36.78 DU at lon: -98.68, lat: 0.60

Jun 26, 2018
20:05 UT

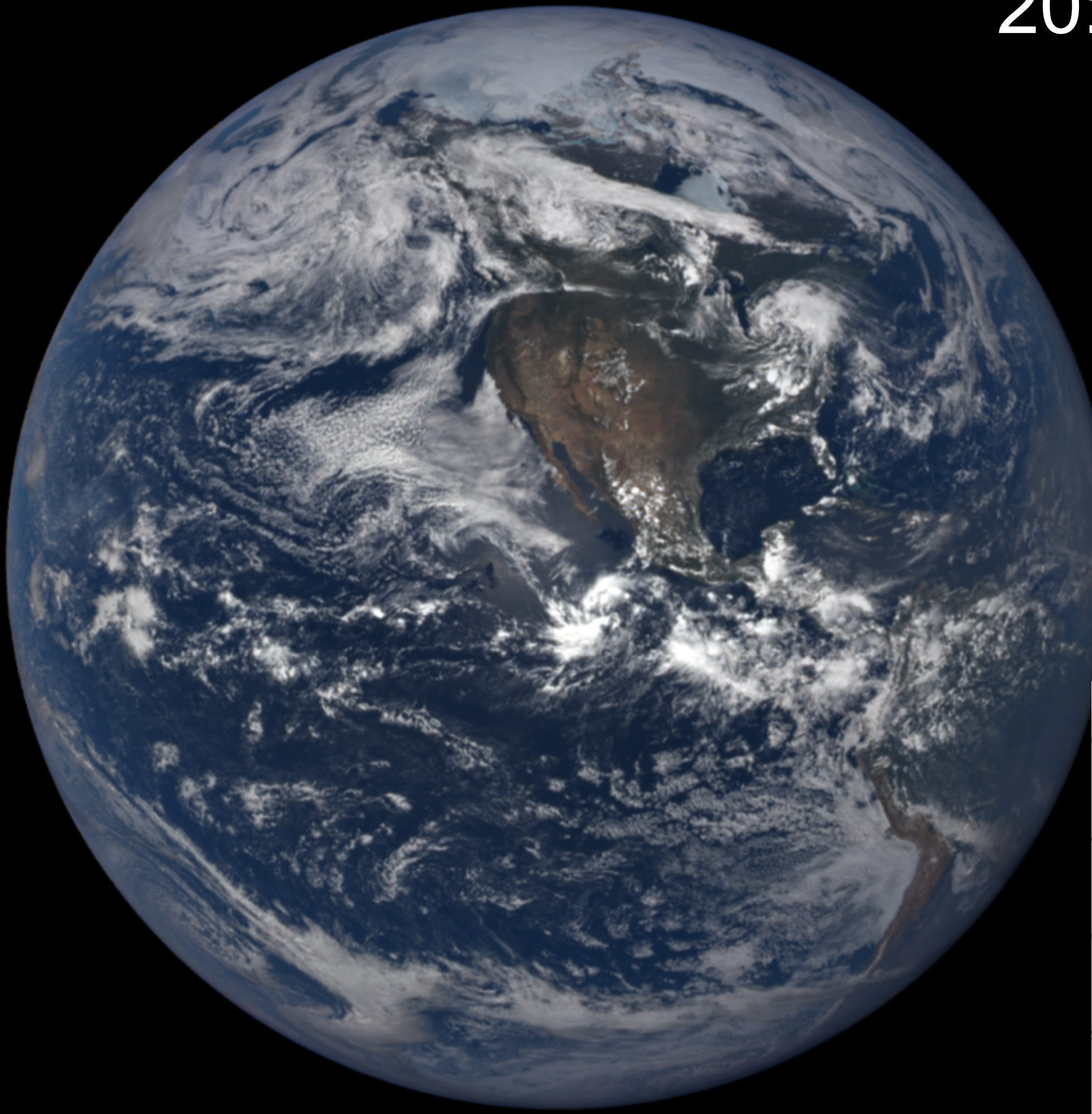

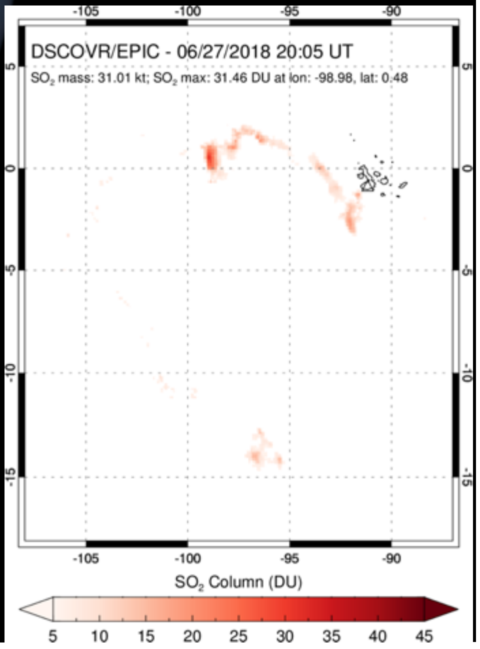

DSCOVR/EPIC - 06/27/2018 20:05 UT

SO$_2$ mass: 31.01 kt; SO$_2$ max: 31.46 DU at lon: -98.98, lat: 0.48

Jun 26, 2018
21:11 UT

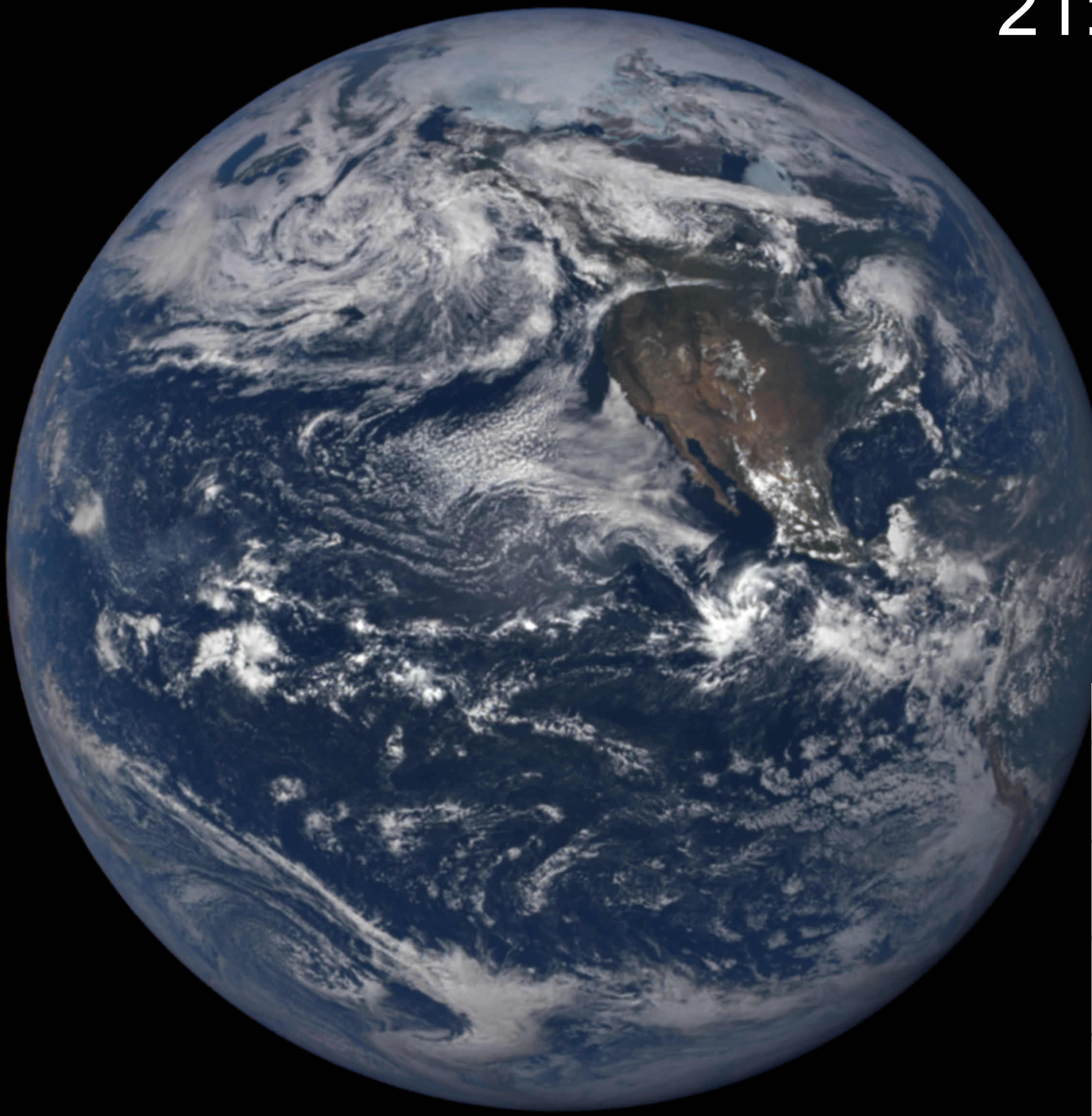

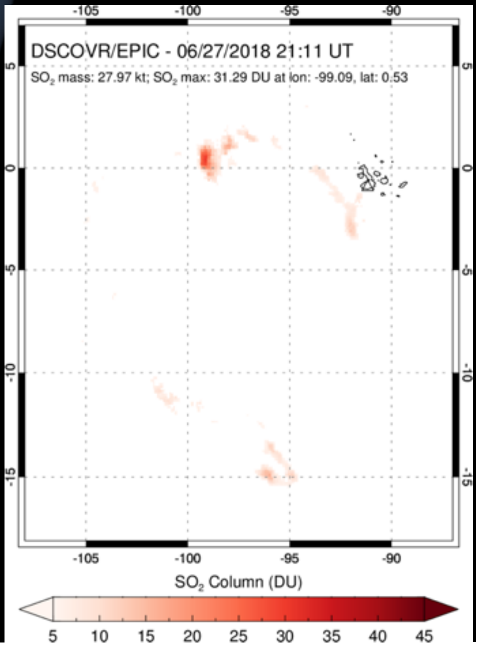

Jun 26, 2018
22:16 UT

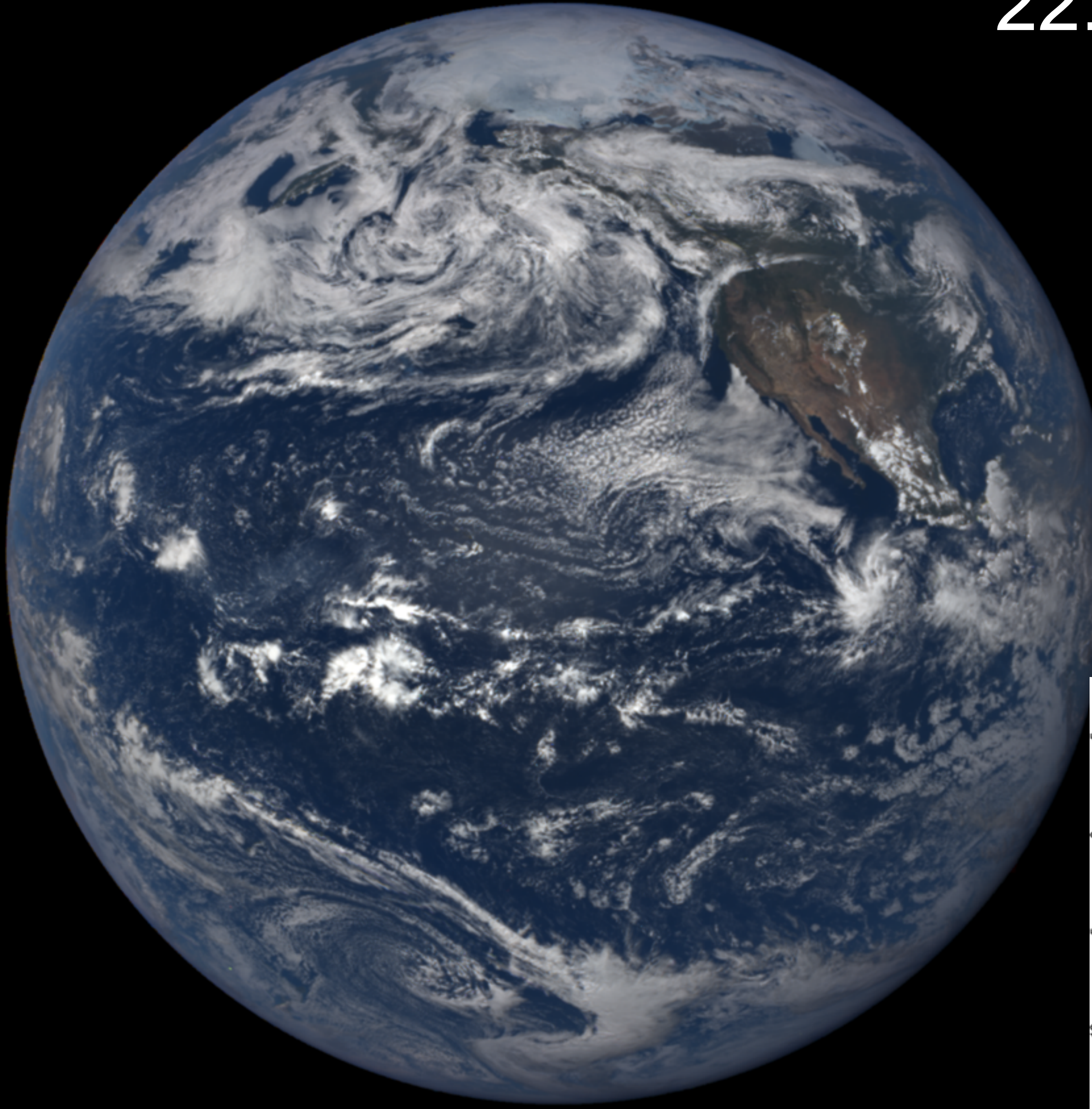

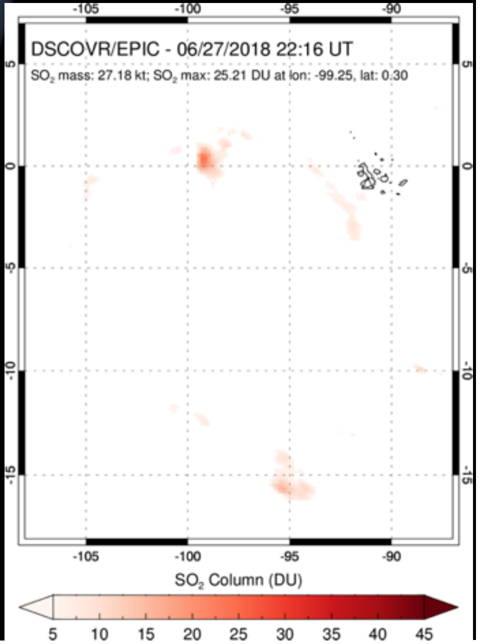

Jun 26, 2018
23:21 UT
Sunset

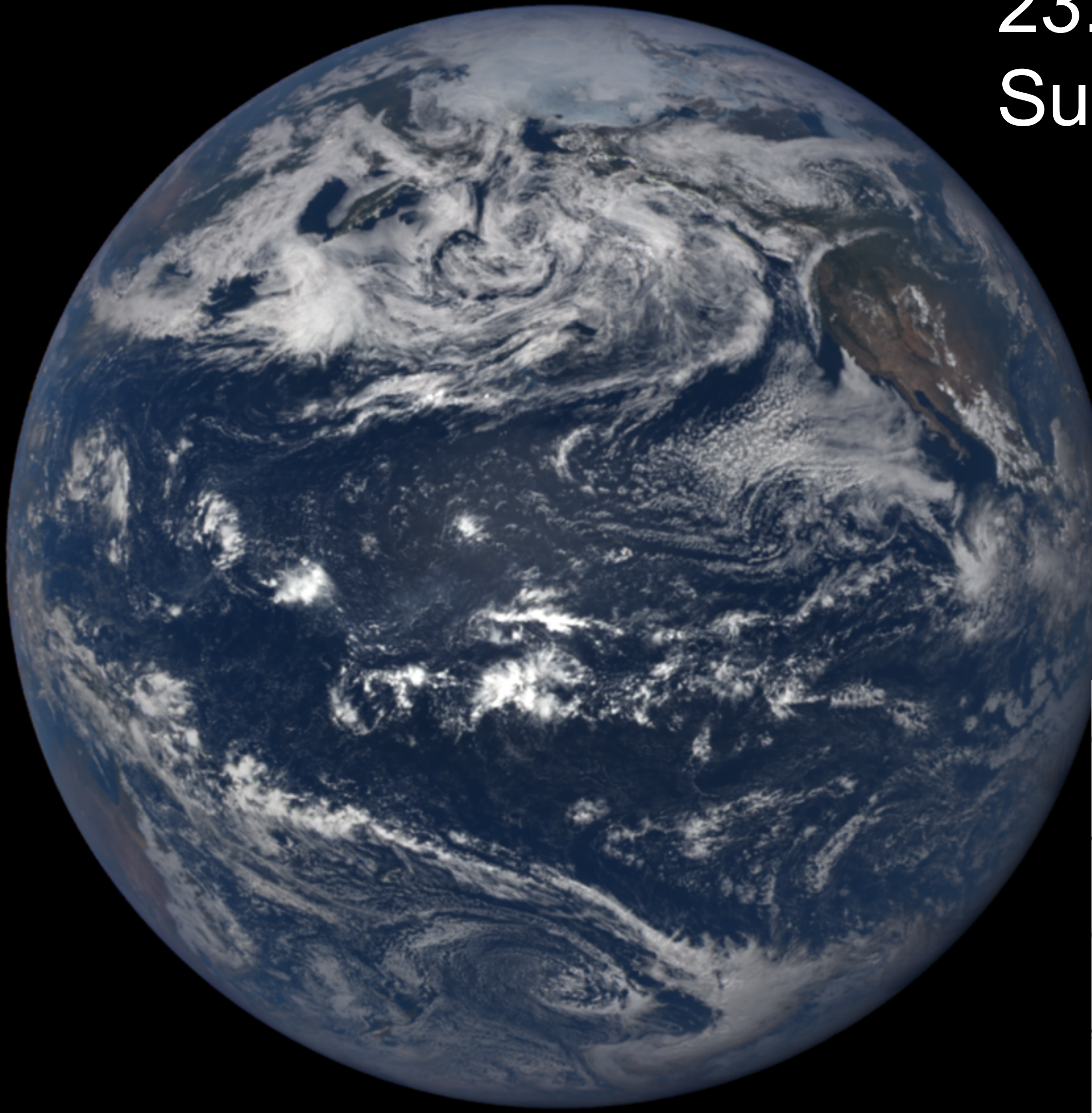

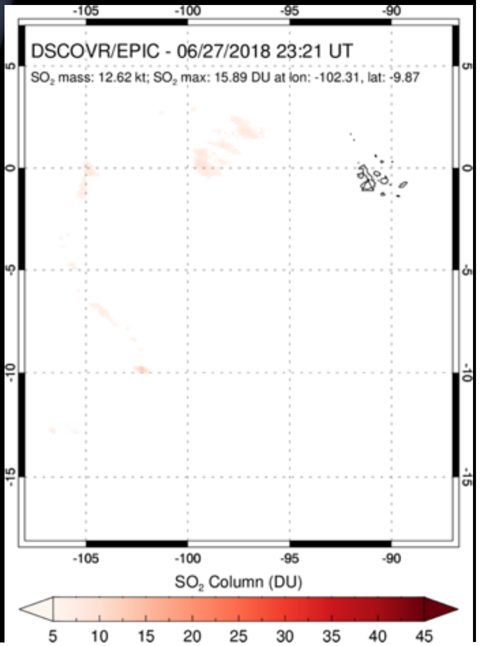

Satellite instrument spatial resolution

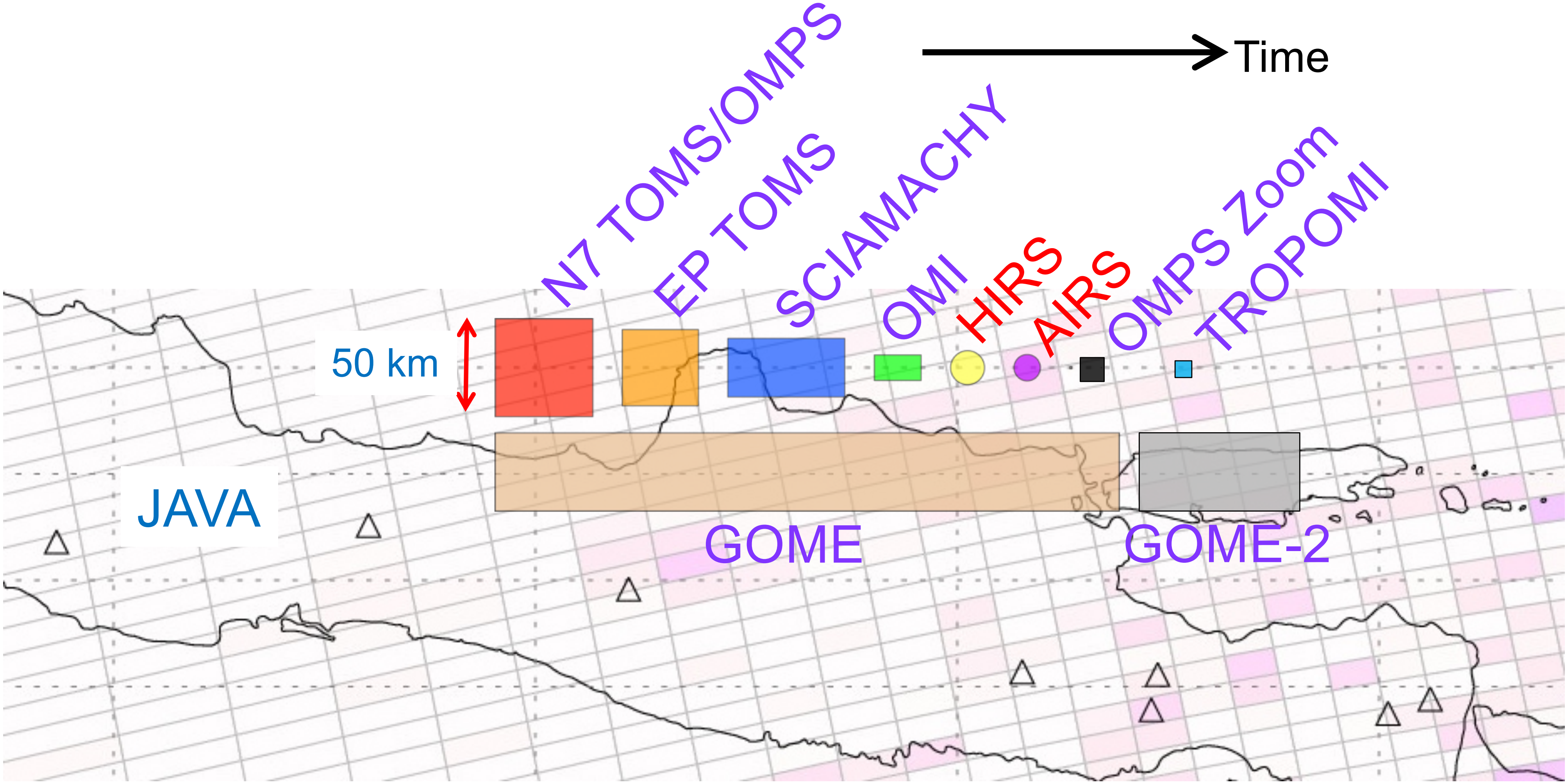

- Detection requires that a volcanic plume cover a large fraction of the sensor pixel or instantaneous field of view (IFOV)
- For most instruments, IFOV size also varies across the swath
- For large volcanic clouds (>IFOV), footprint size is less important
- Pixel size is ultimately constrained by the available photon flux

Sentinel-5P TROPOMI SO_2 measurements

- ESA Sentinel-5P TROPOMI instrument (launched Oct 2017)
- Improved volcanic plume resolution (in the UV) with 7 x 3.5 km pixel size
- Some IR sensors (e.g., ASTER) have higher spatial resolution but lower SO_2 sensitivity and temporal resolution

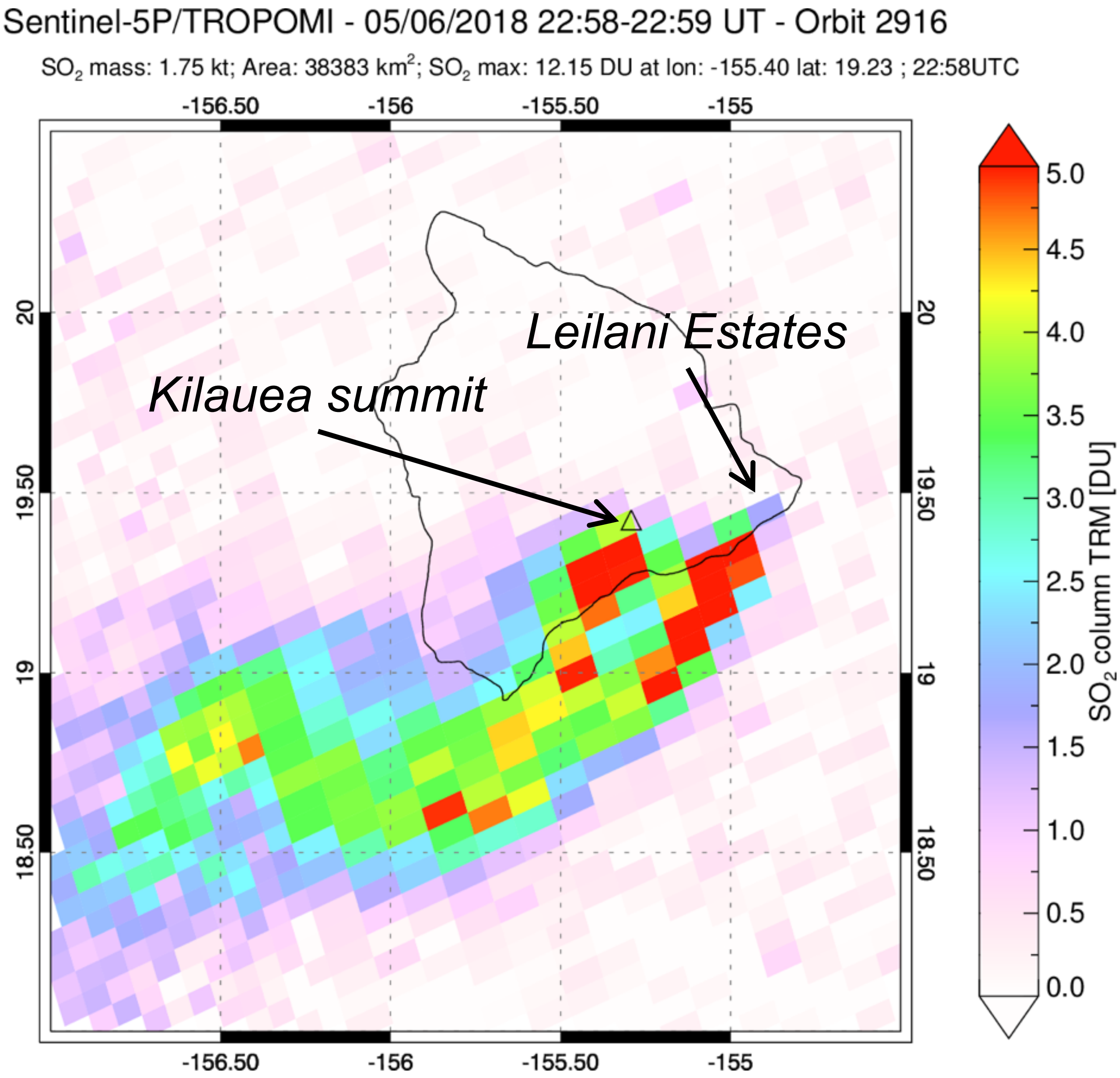

Volcanic gases detected from space

	Volatile species											
UV/IR Sensor[a]	H_2O	CO_2	CO	SO_2	H_2S	NO_2	HCl	BrO	OClO	IO	CH_3Cl	Timespan
TOMS*				🟥								1978-2005
SBUV* (P)				🟥								1978-present
HIRS*				🟥								1978-present
GOME	▨			🟥		▨		▨	▨			1995-2003
MODIS*	▨			🟥								1999-present
ASTER				🟥								1999-present
MOPITT			🟥									1999-present
SCIAMACHY (L)	▨	▨	▨	🟥		▨		🟥	🟥	🟥		2002-2012
MIPAS (L)				🟥								2002-2012
AIRS	▨	▨	▨	🟥								2002-present
ACE (L)	▨	▨	▨	🟥			▨				▨	2003-present
SEVIRI				🟥								2004-present
OMI				🟥		🟥		🟥	🟥	🟥		2004-present
MLS* (L)	▨		▨	🟥			🟥	▨	▨		🟥	1991-2001; 2004-present
TES (P)				🟥								2004-present
GOME-2*	▨			🟥		▨		🟥	🟥	🟥		2006-present
IASI*	▨	▨	🟥	🟥	🟥							2006-present
OMPS*				🟥		▨		▨	▨	▨		2011-present
VIIRS				🟥								2011-present
CrIS				▨								2011-present
AHI				▨								2015-present
GOSAT (P)		▨		▨								2009-present
OCO-2		🟥										2014-present

* = Multiple sat.
P = Profiler
L = Limb
🟥 = Confirmed
▨ = Possible?

- Compositional bias towards SO_2
- >20 daily polar-orbiting SO_2 sensor overpasses

Carn et al. (2016)

What can satellites measure during volcanic eruptions?

Calbuco Chile, April 2015 (C. Gutierrez/AP)

Vertical growth anomalies in volcanic plumes

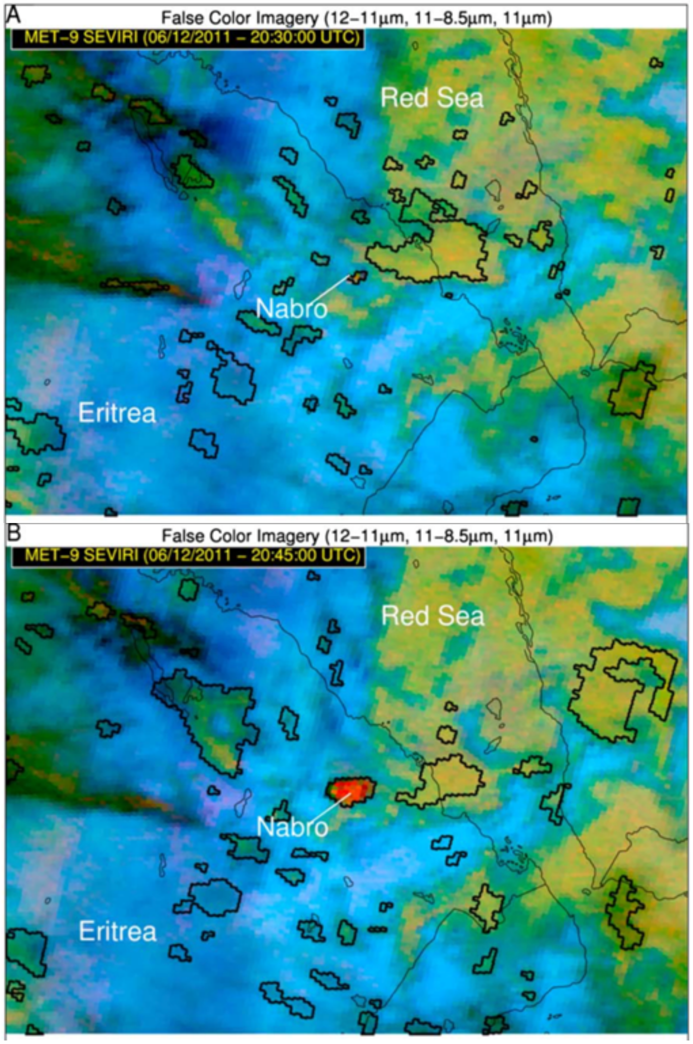

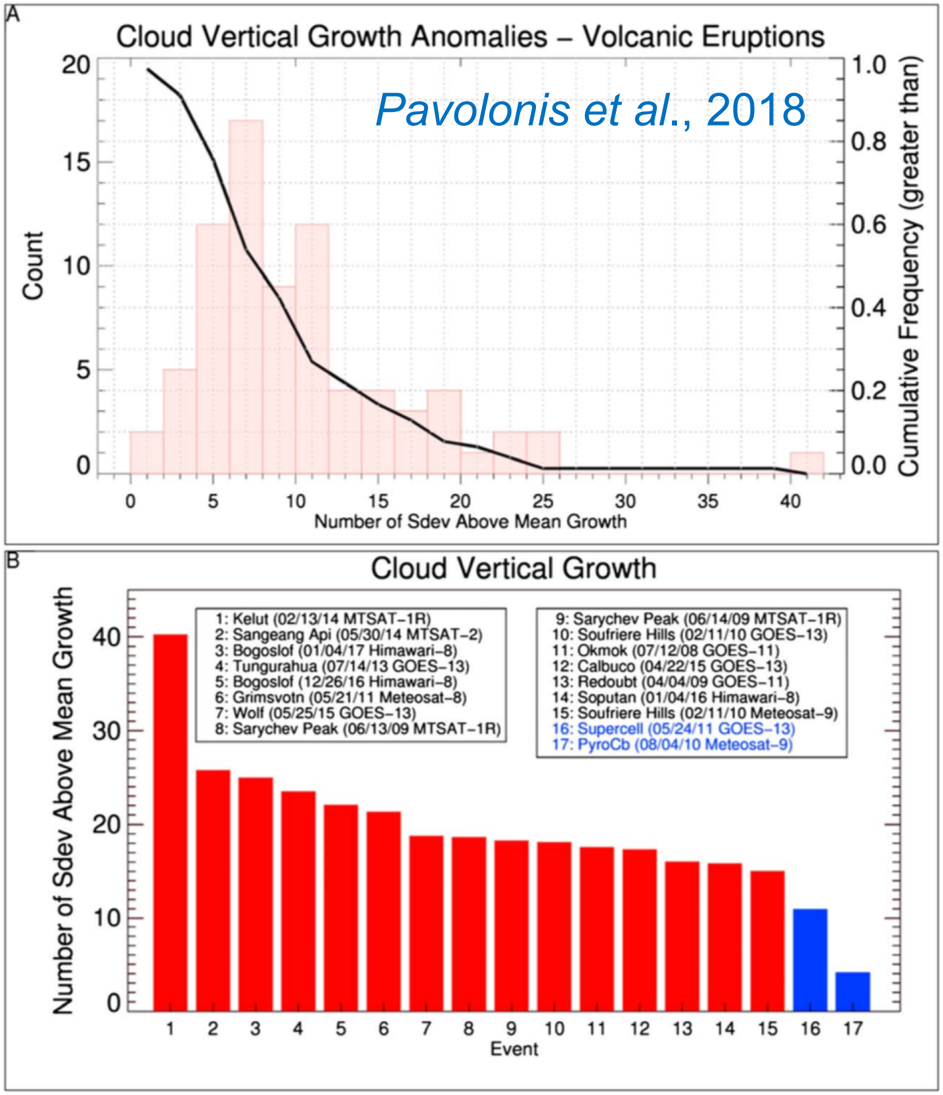

Pavolonis et al., 2018

- Anomalous vertical growth rates of volcanic clouds (wrt meteorological clouds) used to detect explosive eruptions in geostationary satellite data and issue alerts
- Used operationally by some Volcanic Ash Advisory Centers (VAACs)

Volcanic ash cloud detection and alerts

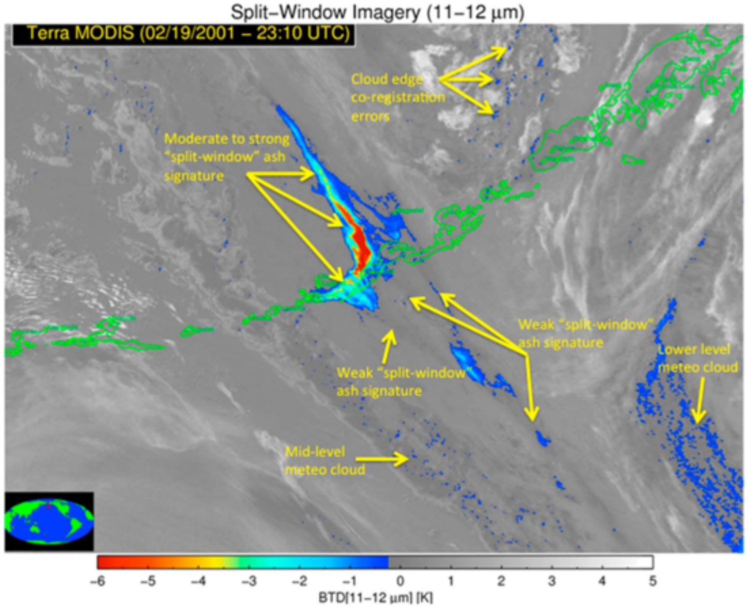

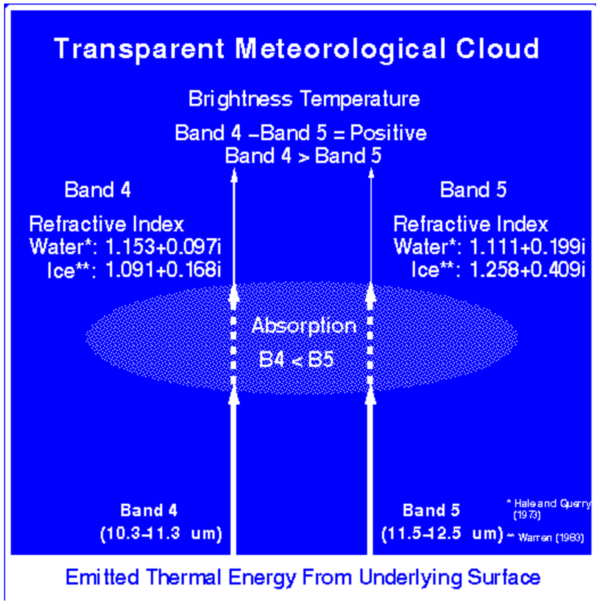

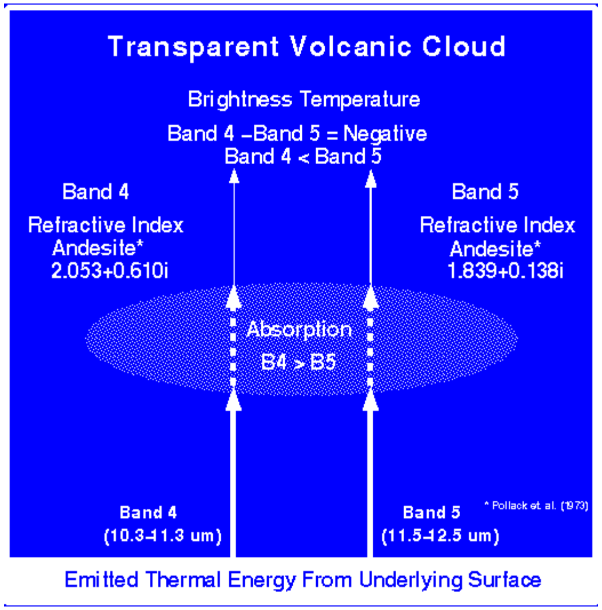

'Reverse absorption'

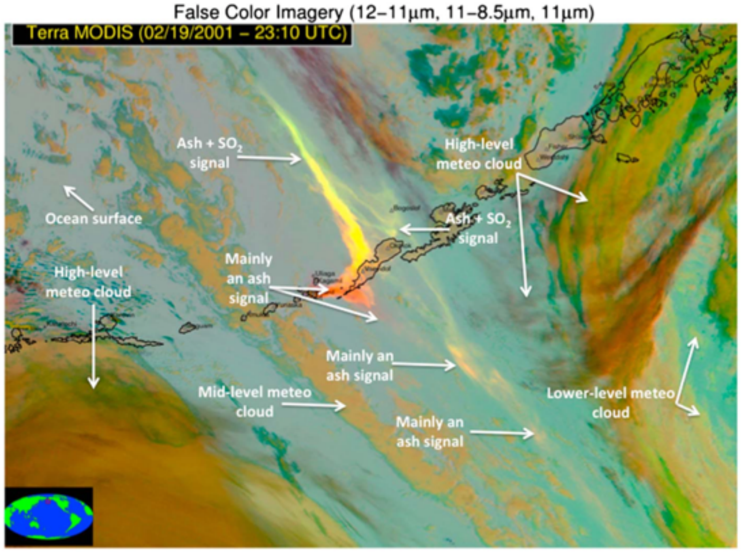

- Automated volcanic ash cloud and thermal anomaly detection conducted in 'near real-time'
- Algorithms attempt to mimic human expert analysis of satellite imagery (similar to AI)
- Improve as more satellite data for actual volcanic events is collected (algorithm training)
- Towards an 'unbiased' record of volcanic activity?
- VOLCAT: https://volcano.ssec.wisc.edu

Prata, 1989; *Pavolonis et al.*, 2015

Mass eruption rates from umbrella cloud expansion

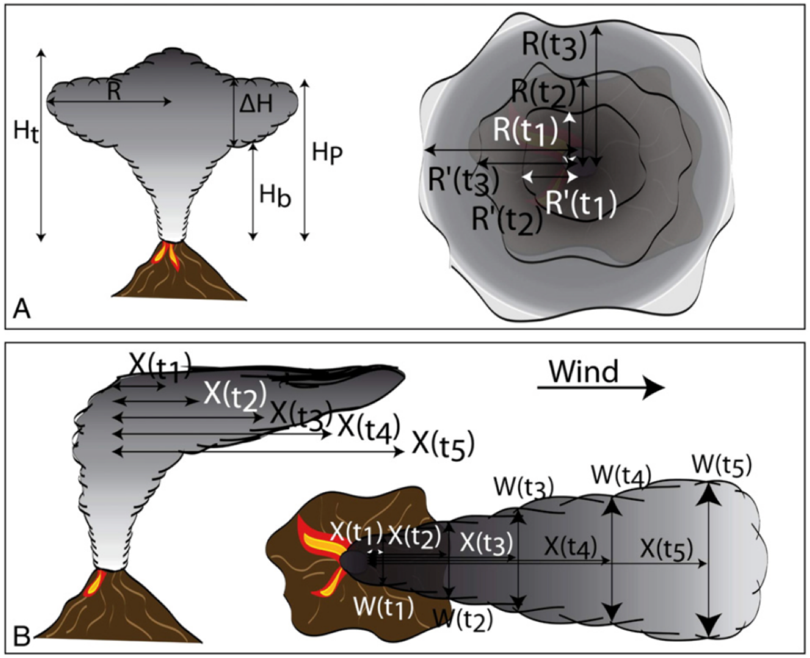

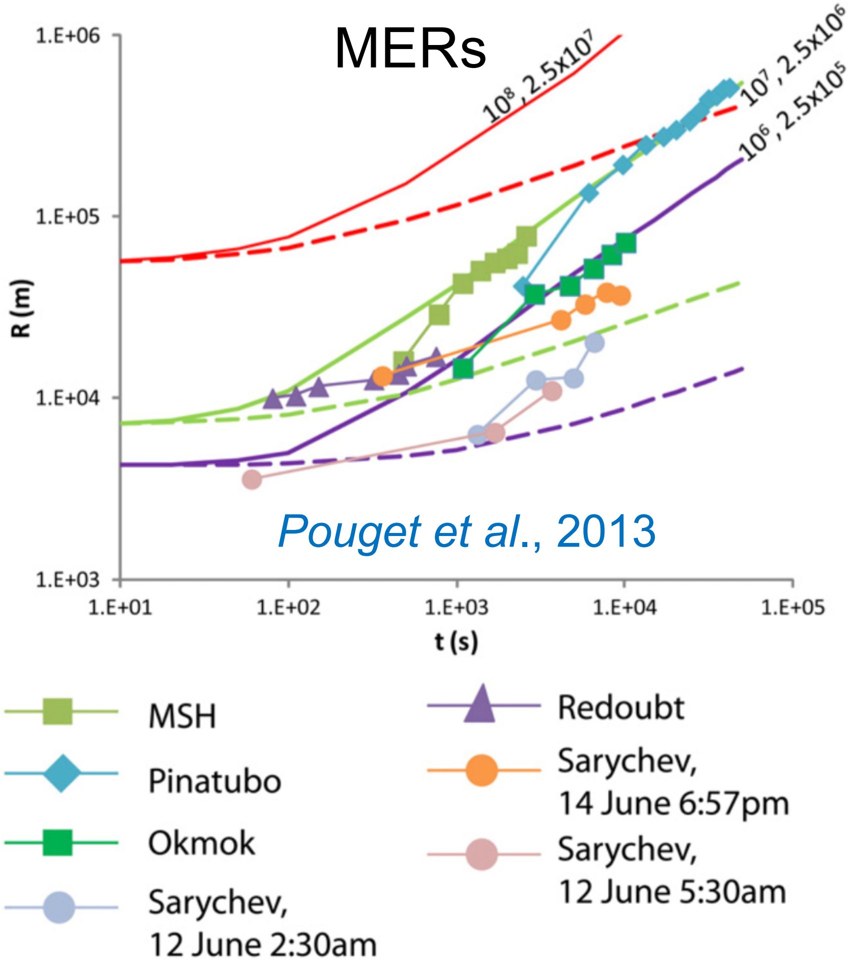

Pouget et al., 2013

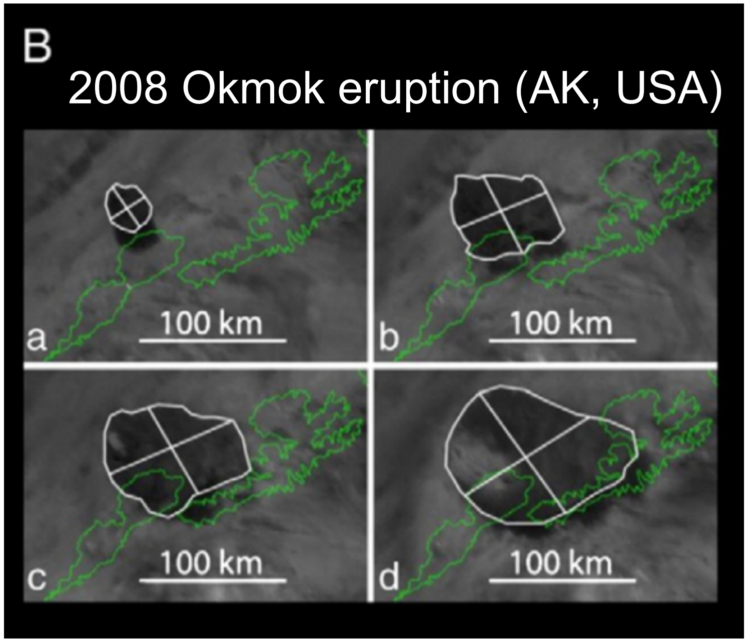

2008 Okmok eruption (AK, USA)

- Growth of umbrella clouds and downwind plumes from satellite imagery used to estimate mass eruption rates (MER)
- Faster, remote estimates of MER and its temporal variation

A-Train data for February 2014 Kelut eruption

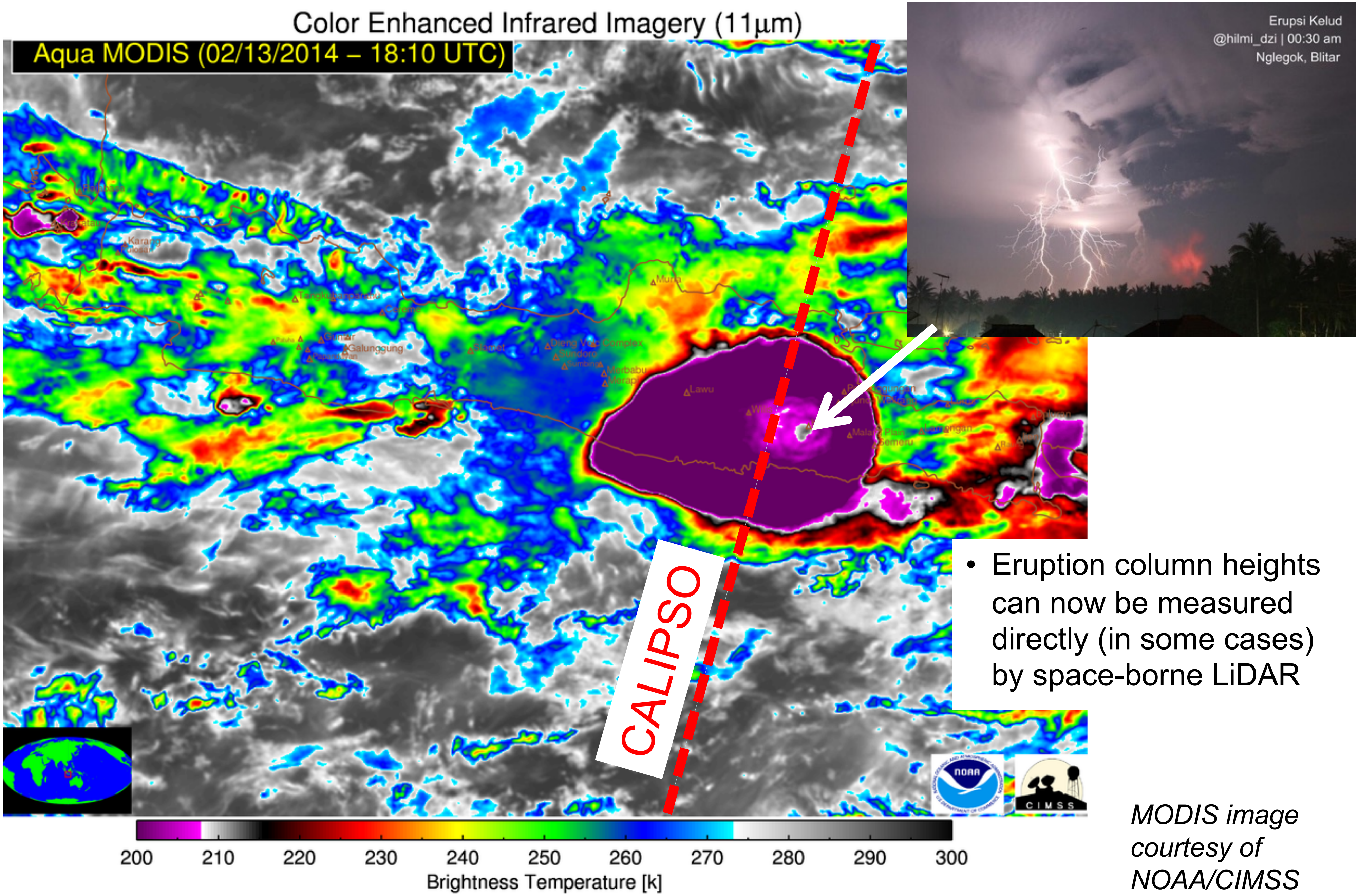

- Eruption column heights can now be measured directly (in some cases) by space-borne LiDAR

MODIS image courtesy of NOAA/CIMSS

A-Train data for February 2014 Kelut eruption

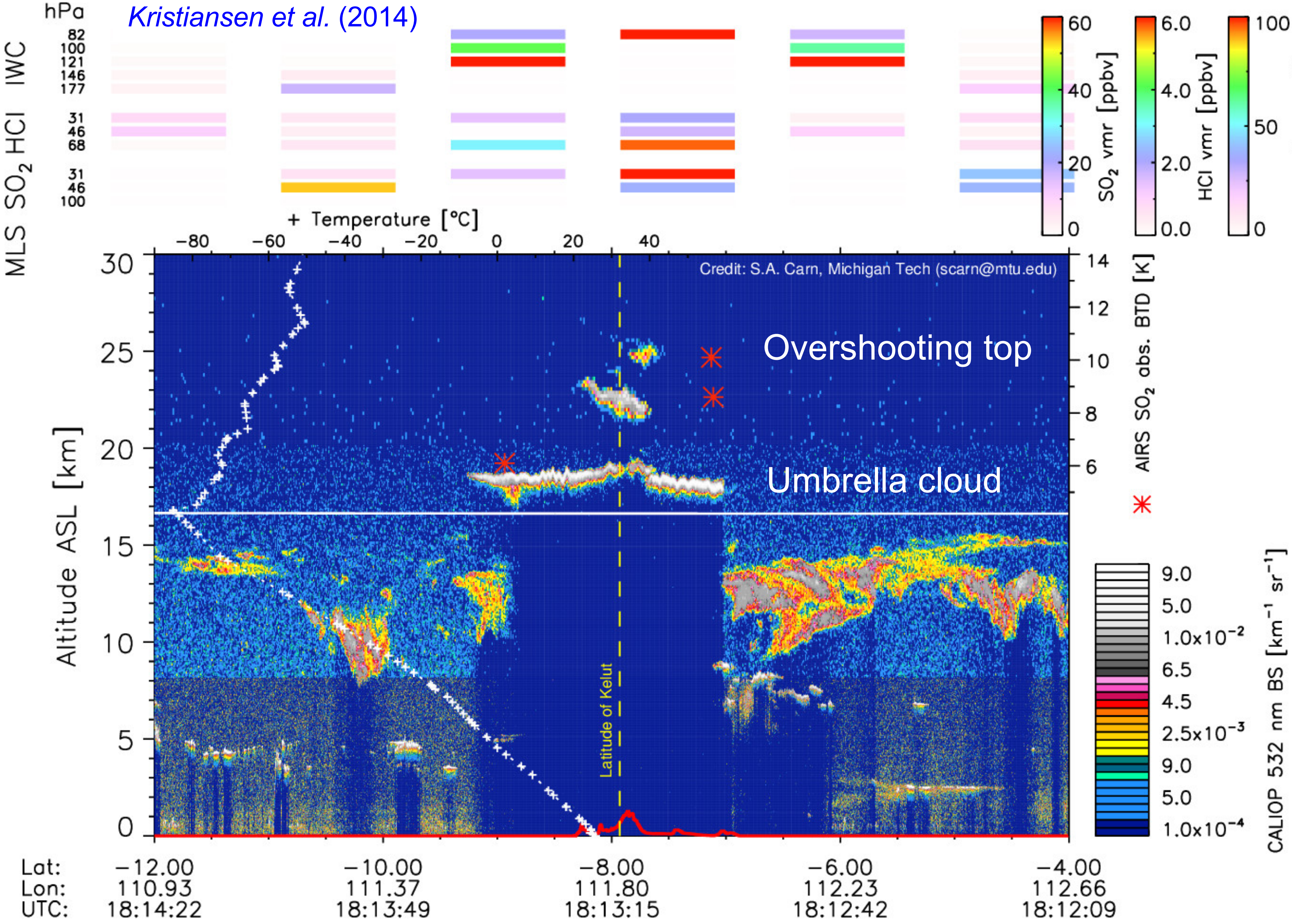

Kristiansen et al. (2014)

Credit: S.A. Carn, Michigan Tech (scarn@mtu.edu)

Eruptive SO_2 emissions

Pinatubo, June 1991
~13-17 Tg SO_2
~500 Dobson Units (DU) SO_2

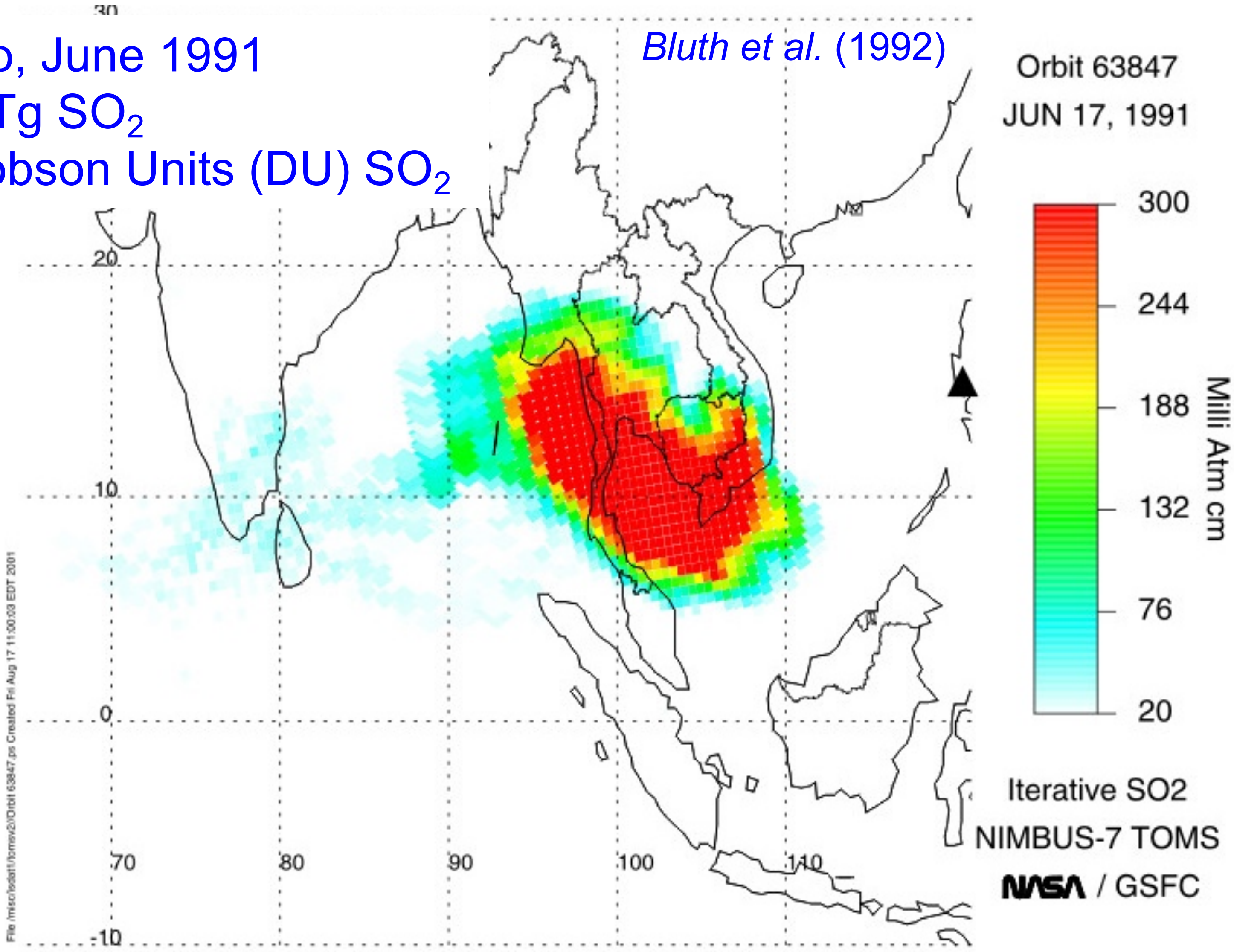
Bluth et al. (1992)

- Satellites measure ‘snapshot’ SO_2 mass rather than flux
- Pinatubo SO_2 mass retrievals still being refined (*Fisher et al.*, 2019)
- Image archive: NASA global SO_2 monitoring website (http://so2.gsfc.nasa.gov)

Ambae (Vanuatu) eruption

July 26, 2018

Suomi NPP – Ozone Mapping and Profiler Suite (OMPS)

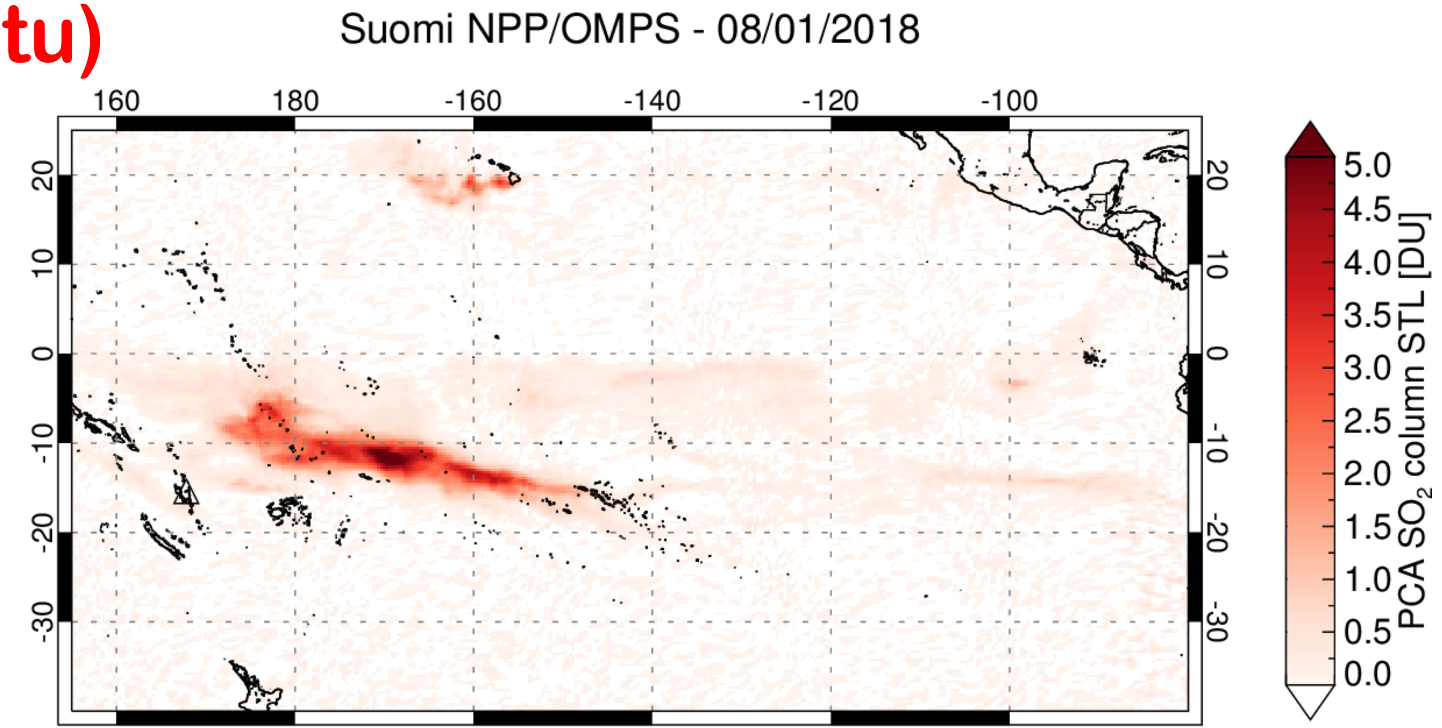

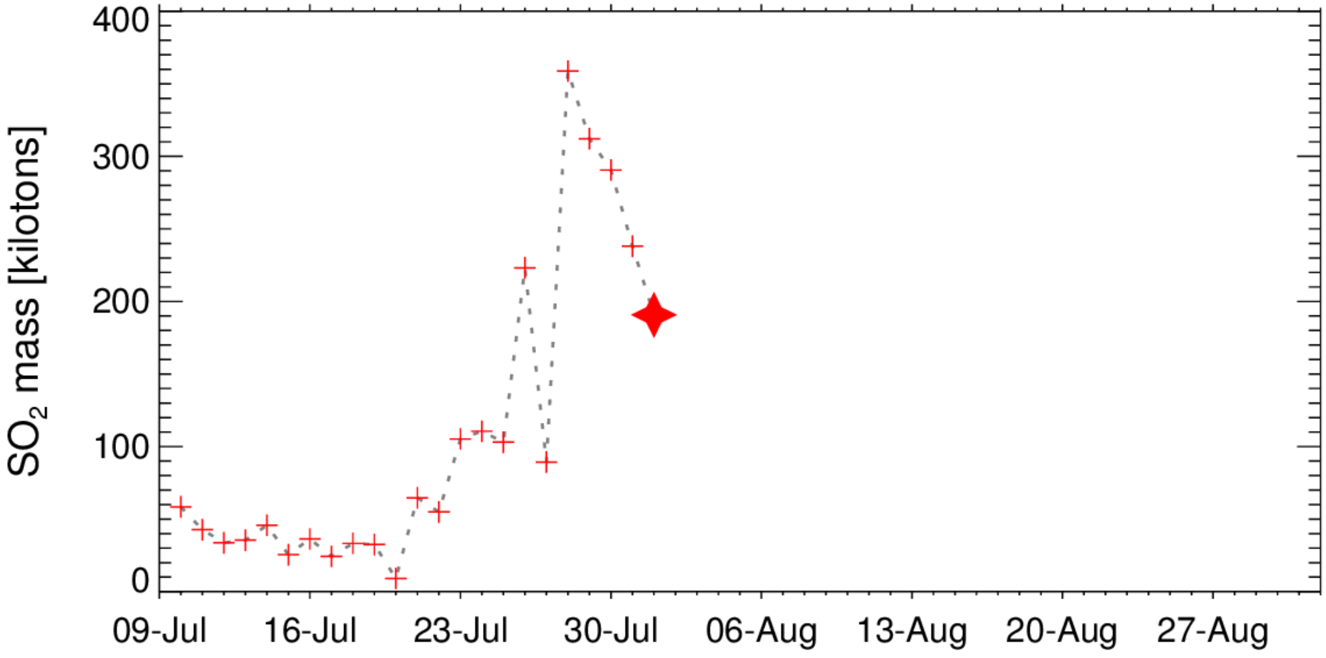

Galápagos eruption
June - August 2018

Suomi NPP – Ozone Mapping and Profiler Suite (OMPS)

- Typical 'waxing-waning' emission trend – proxy for effusion rate
- Fernandina (16 June)
  - ~2 day eruption
  - ~3 km plume altitude
  - ~100 kt SO_2
- Sierra Negra (26 June)
  - Unrest since July 2017 (seismicity, uplift)
  - SO_2 detected from 26 June – 19 August
  - Several pulses of higher SO_2 emissions

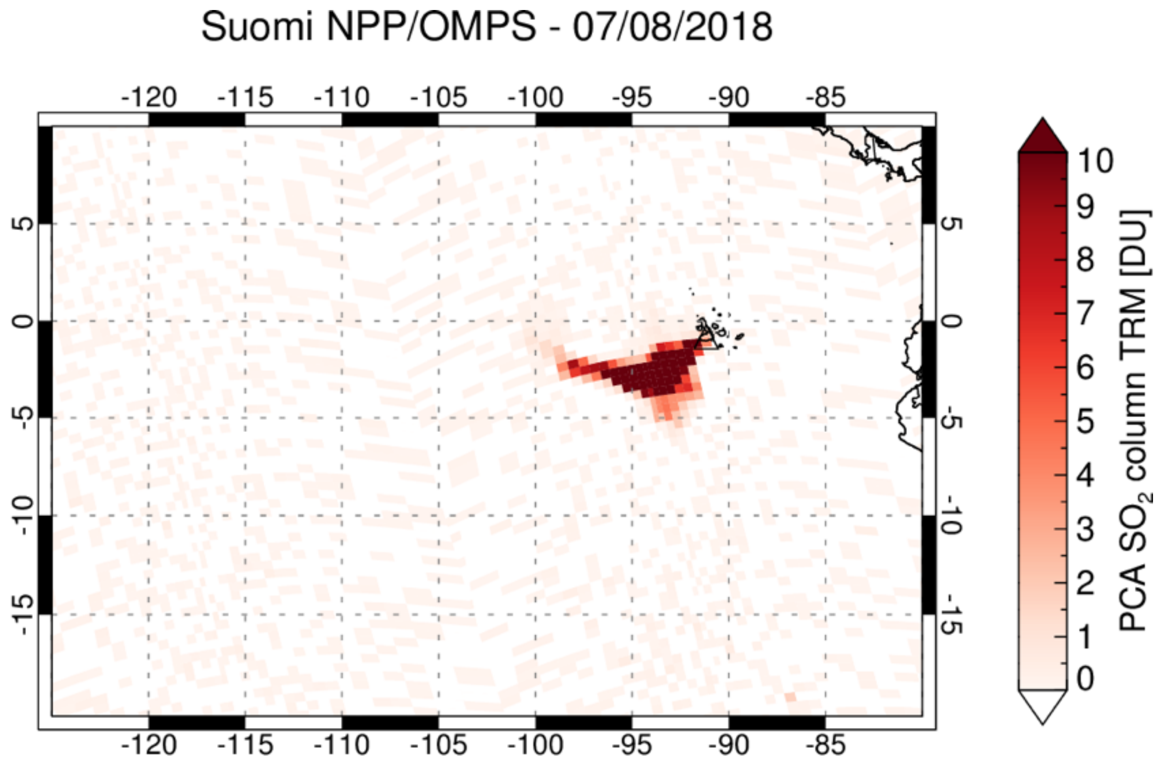
Suomi NPP/OMPS - 07/08/2018

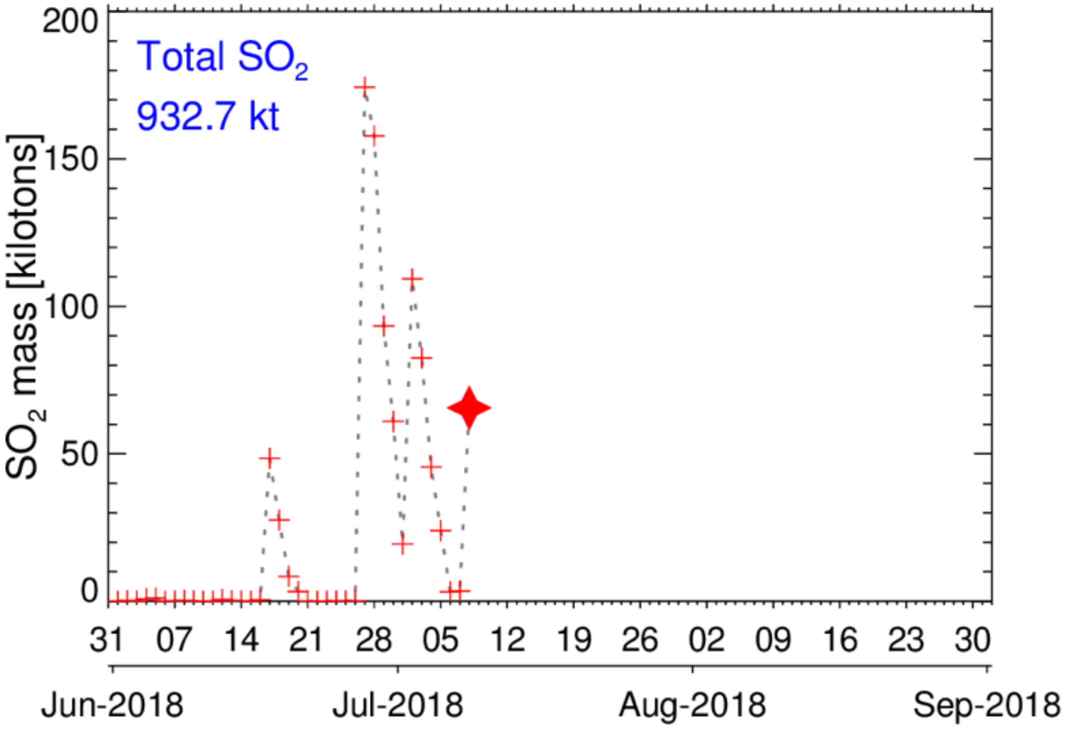

Ash composition detected from space

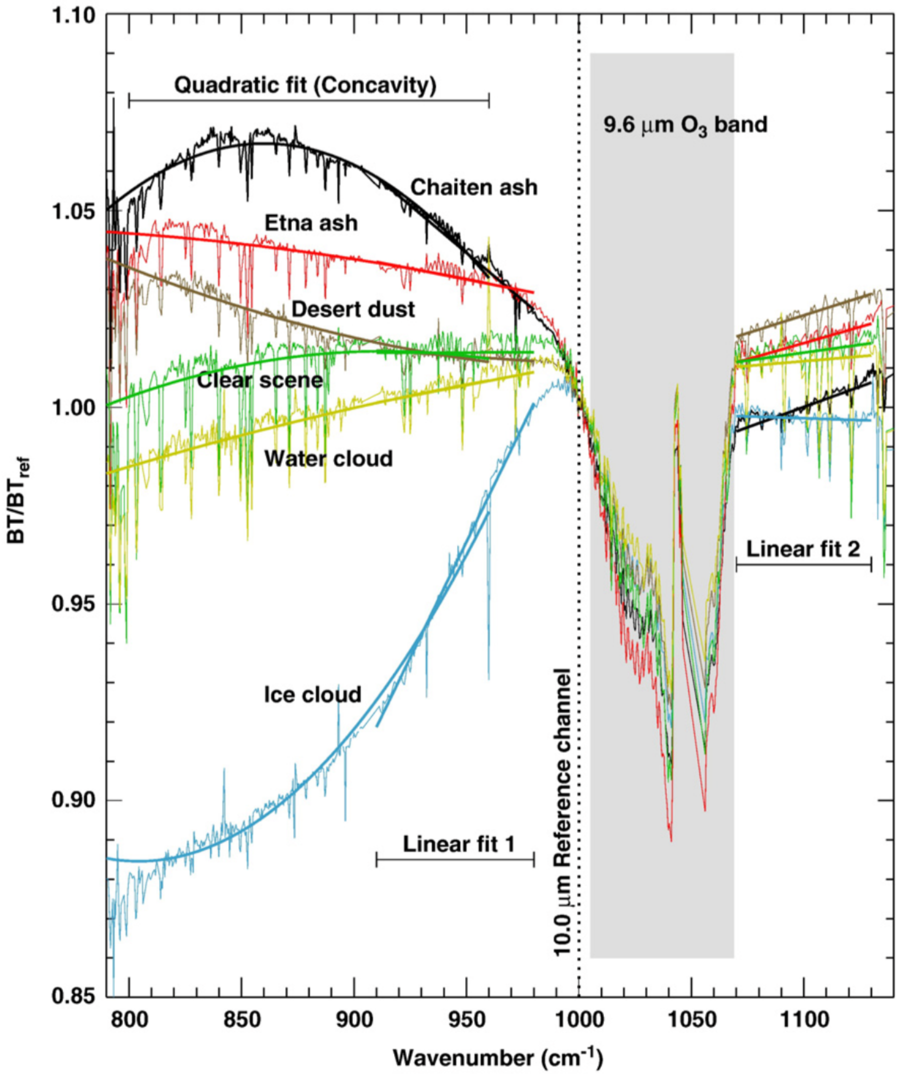

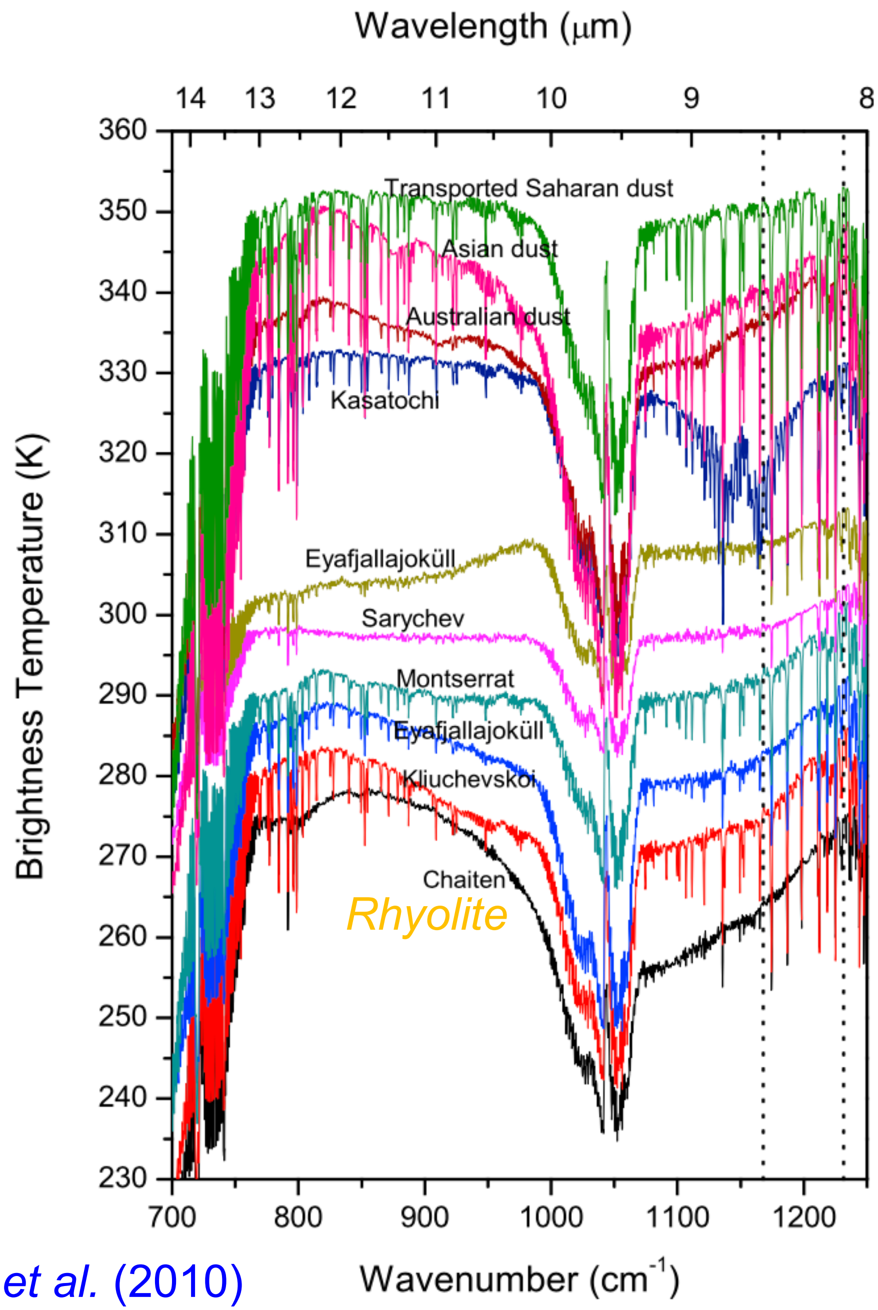

- IR spectral shape is sensitive to volcanic ash composition and differentiates ash from dust and water/ice clouds

Gangale et al. (2009); *Clarisse et al.* (2010)

Can we detect volcanic CO_2 from space?

Explosive eruption

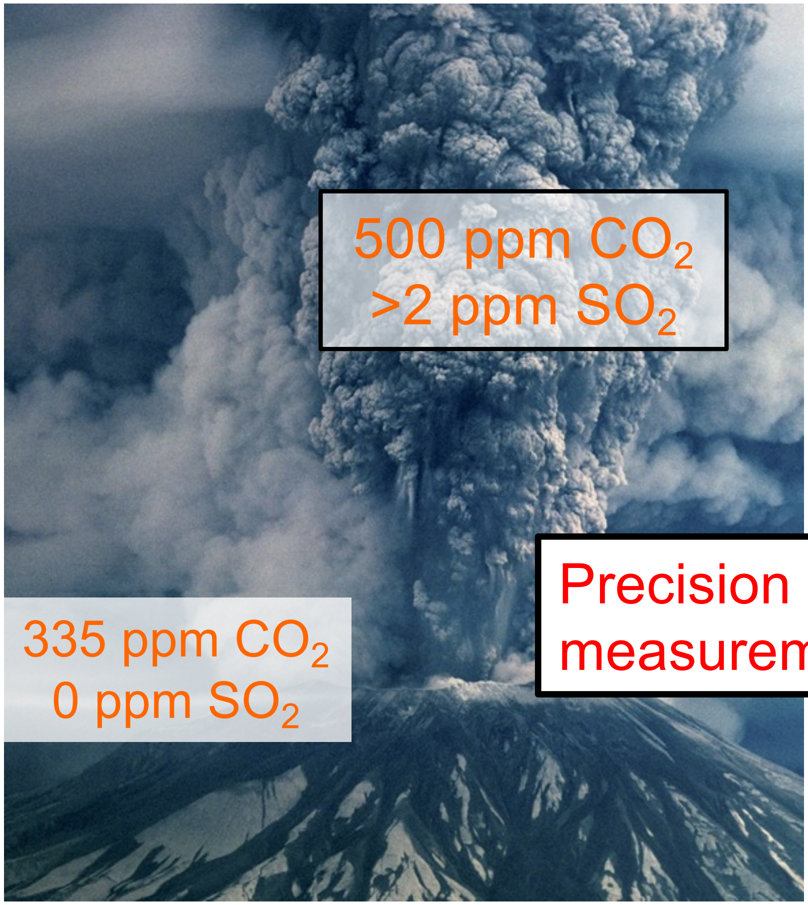

500 ppm CO_2
>2 ppm SO_2

335 ppm CO_2
0 ppm SO_2

May 1980 Mt St Helens eruption
(*Hobbs et al.*, 1982)

CO_2/SO_2 = 55 -> ~55 Tg CO_2

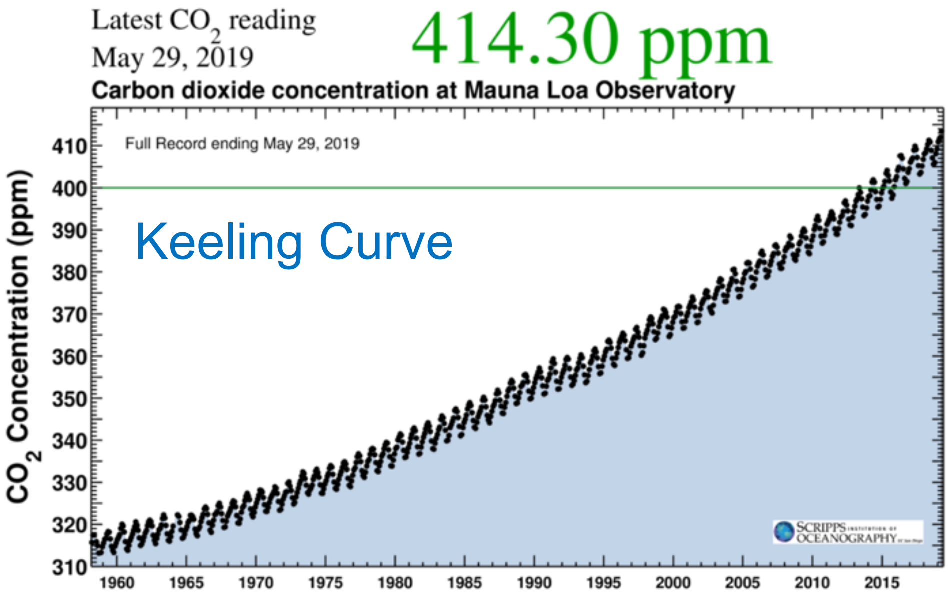

Keeling Curve

Precision of satellite CO_2 measurements: ~1-4 ppm

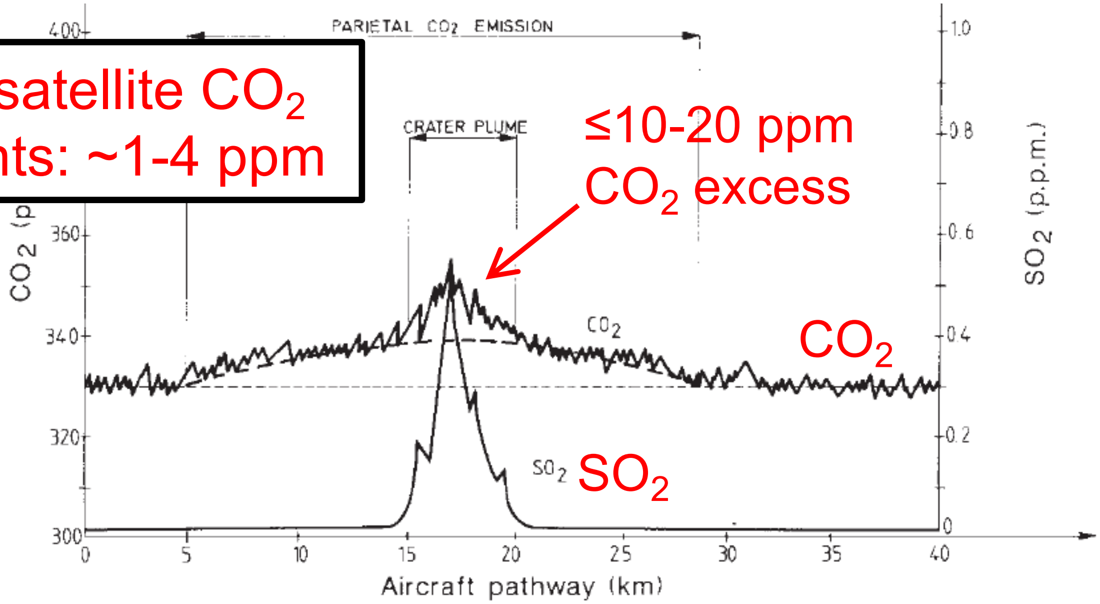

≤10-20 ppm CO_2 excess

CO_2

SO_2

Etna, Italy: 13 Tg yr^{-1} CO_2 (*Allard et al.*, 1991)

Volcanic lightning NOx and ash-gas separation

- $NO_x = NO + NO_2$
- $N_2 + O_2 \rightarrow 2NO$
- $2NO + O_2 \rightarrow 2NO_2$

Lightning NO_x (LNOx)

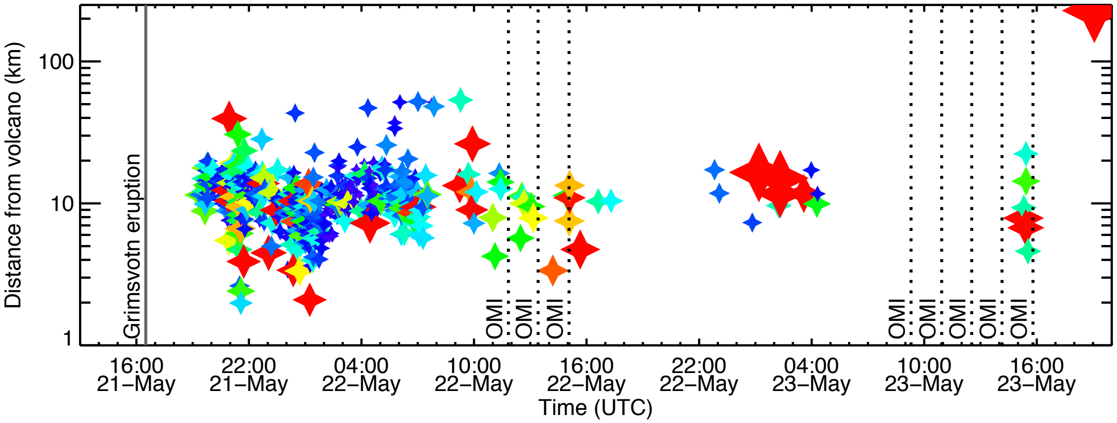

WWLLN lightning strikes during May 2011 eruption of Grimsvötn (Iceland)

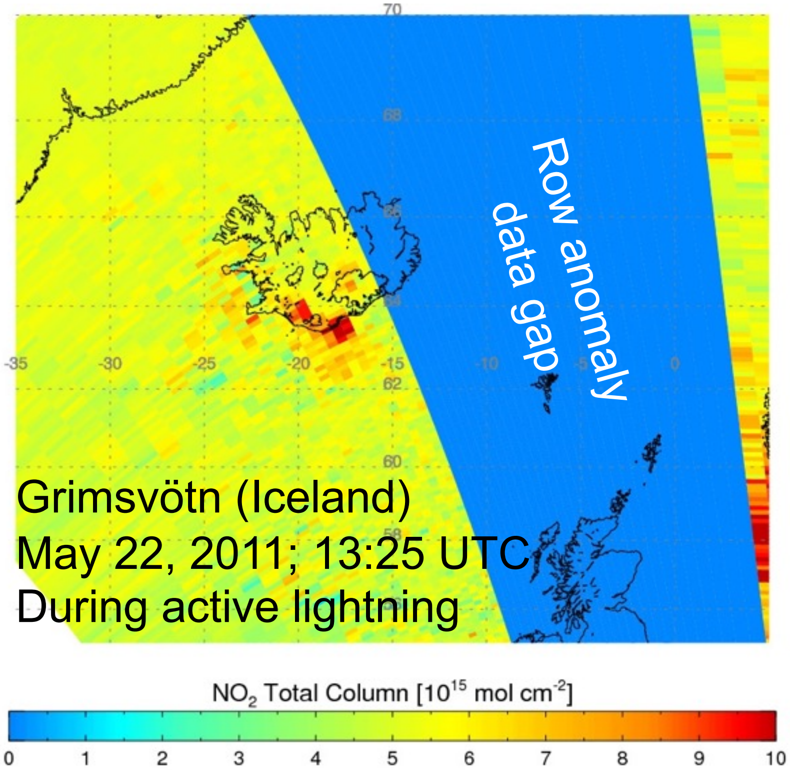

Grimsvötn (Iceland)
May 22, 2011; 13:25 UTC
During active lightning

- Volcanic lightning NO_x could provide a new way to detect hazardous volcanic clouds
- Several processes could create lightning, including fallout of ash-hydrometeor aggregates (‘dirty thunderstorm’ mechanism)

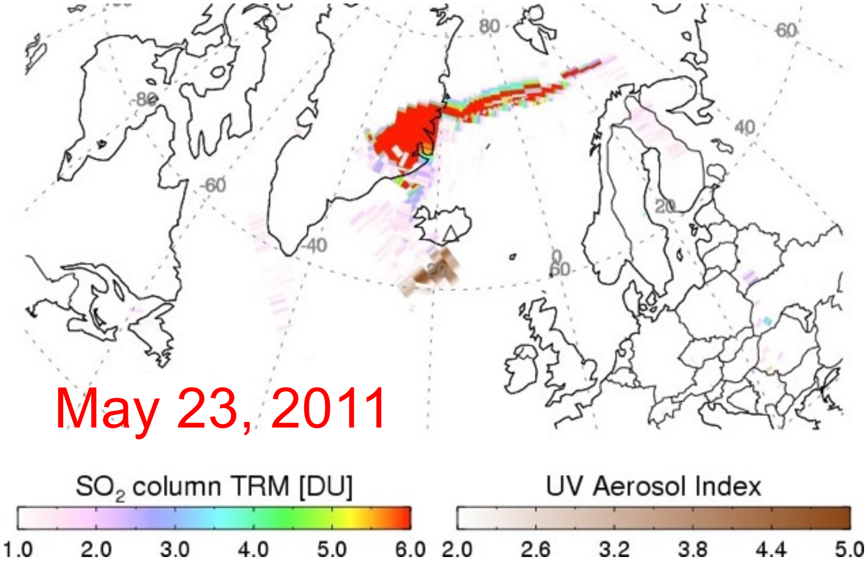

May 23, 2011

Sigmarsson et al. (2013); *Carn et al.* (2016)

Grimsvötn (Iceland) eruption plume (May 2011)

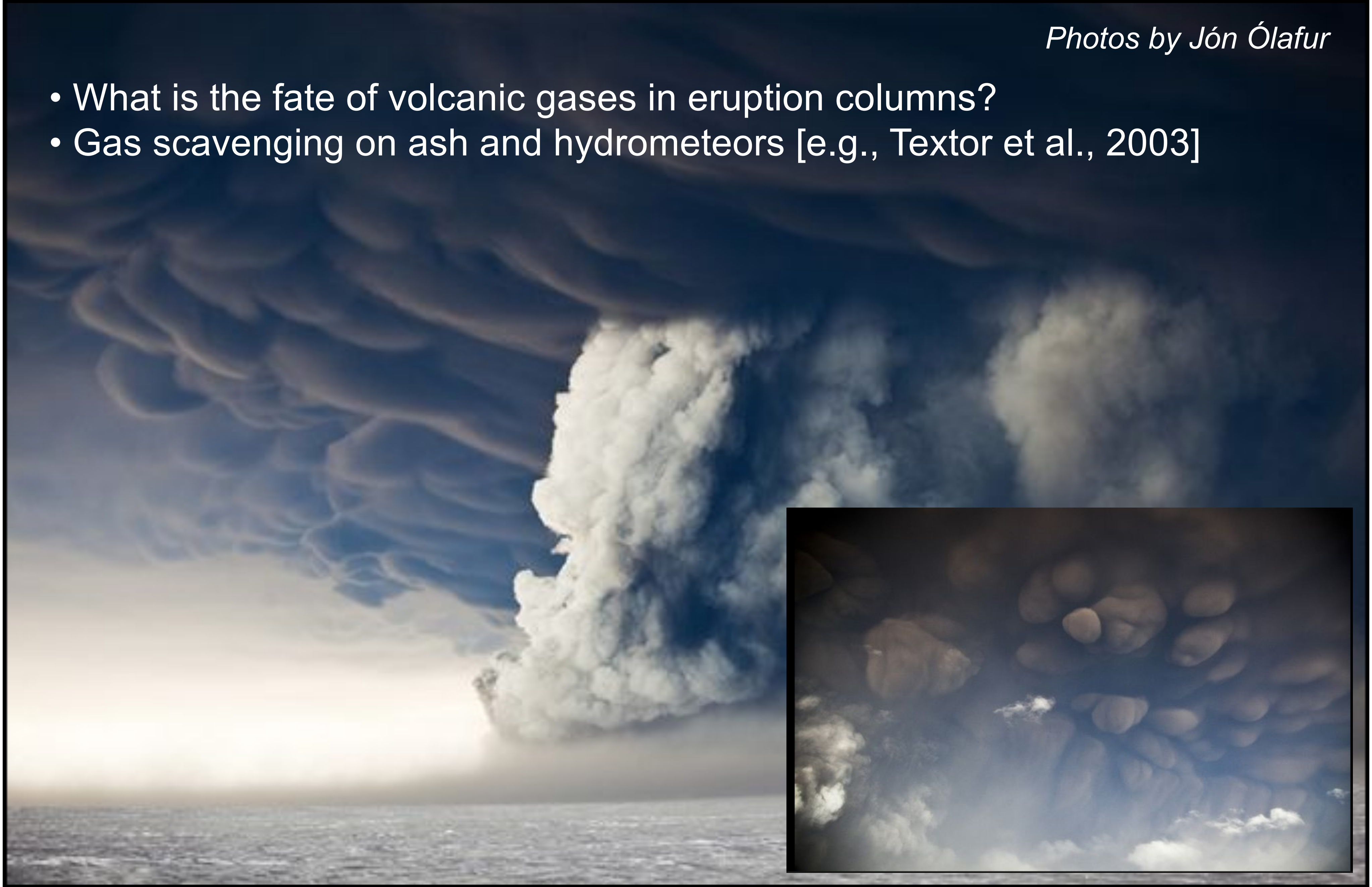

Photos by Jón Ólafur

- What is the fate of volcanic gases in eruption columns?
- Gas scavenging on ash and hydrometeors [e.g., Textor et al., 2003]

Gas scavenging in volcanic plumes

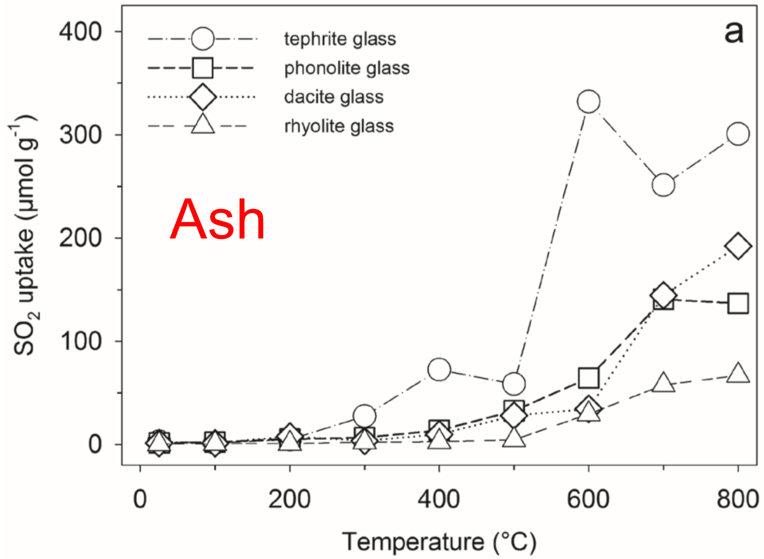

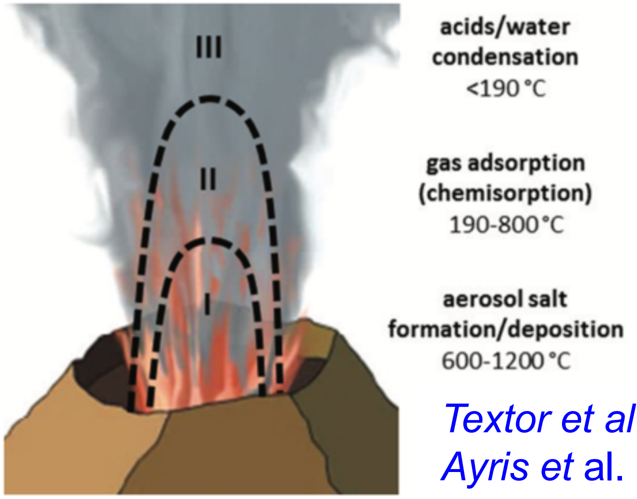

Textor et al. (2003)
Ayris et al. (2013)
Delmelle et al. (2018)

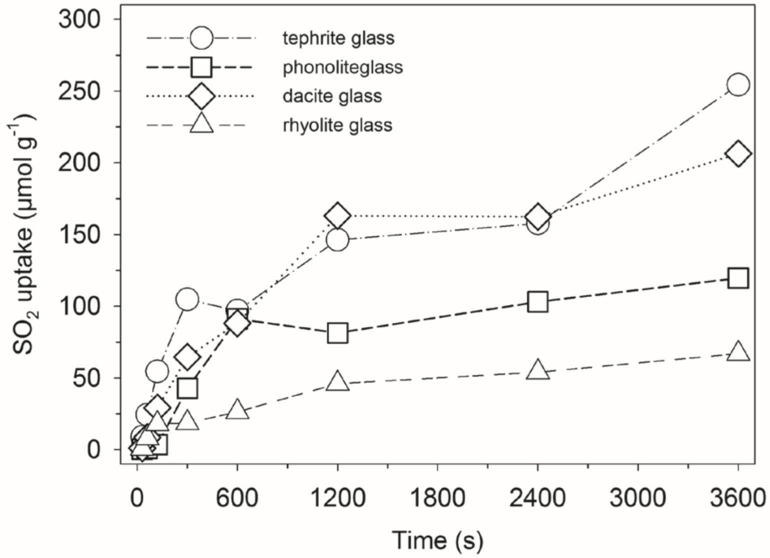

Hydrometeors

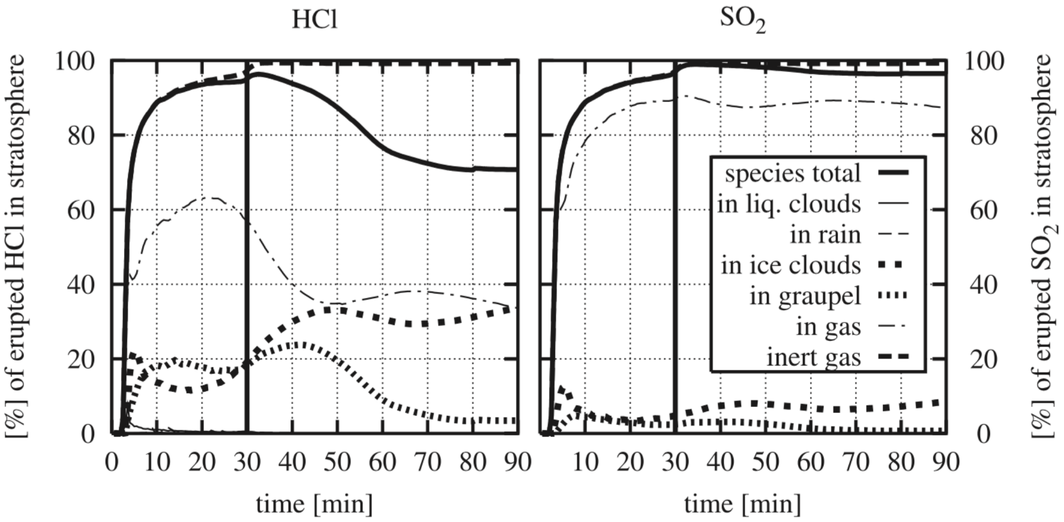

- >80% S gases and >25% HCl predicted to reach stratosphere in explosive eruptions
- Ash interactions dependent on volcanic gas-ash exposure time at high T (i.e., fragmentation depth), ash composition (Ca)

Satellite measurements of volcanic halogens

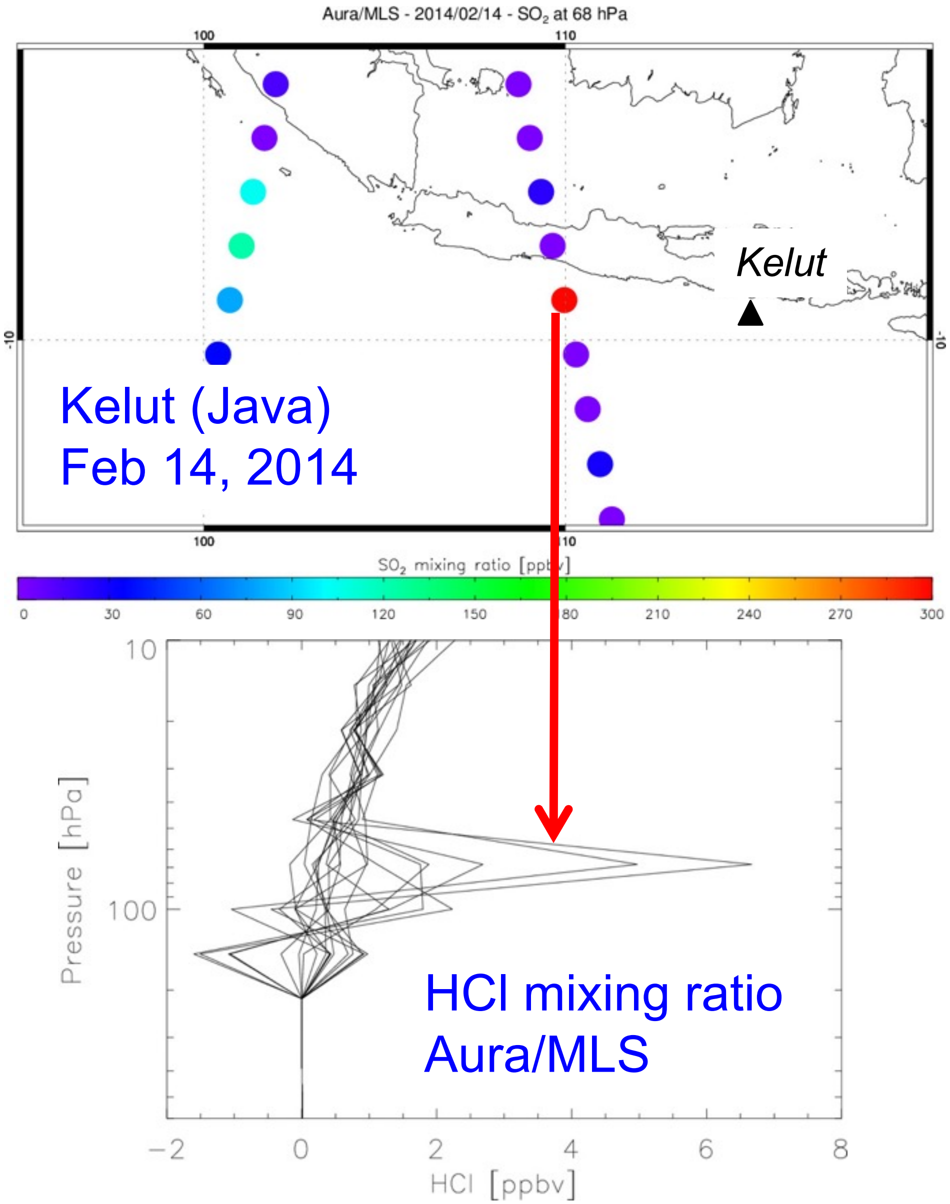

Kelut (Java)
Feb 14, 2014

HCl mixing ratio
Aura/MLS

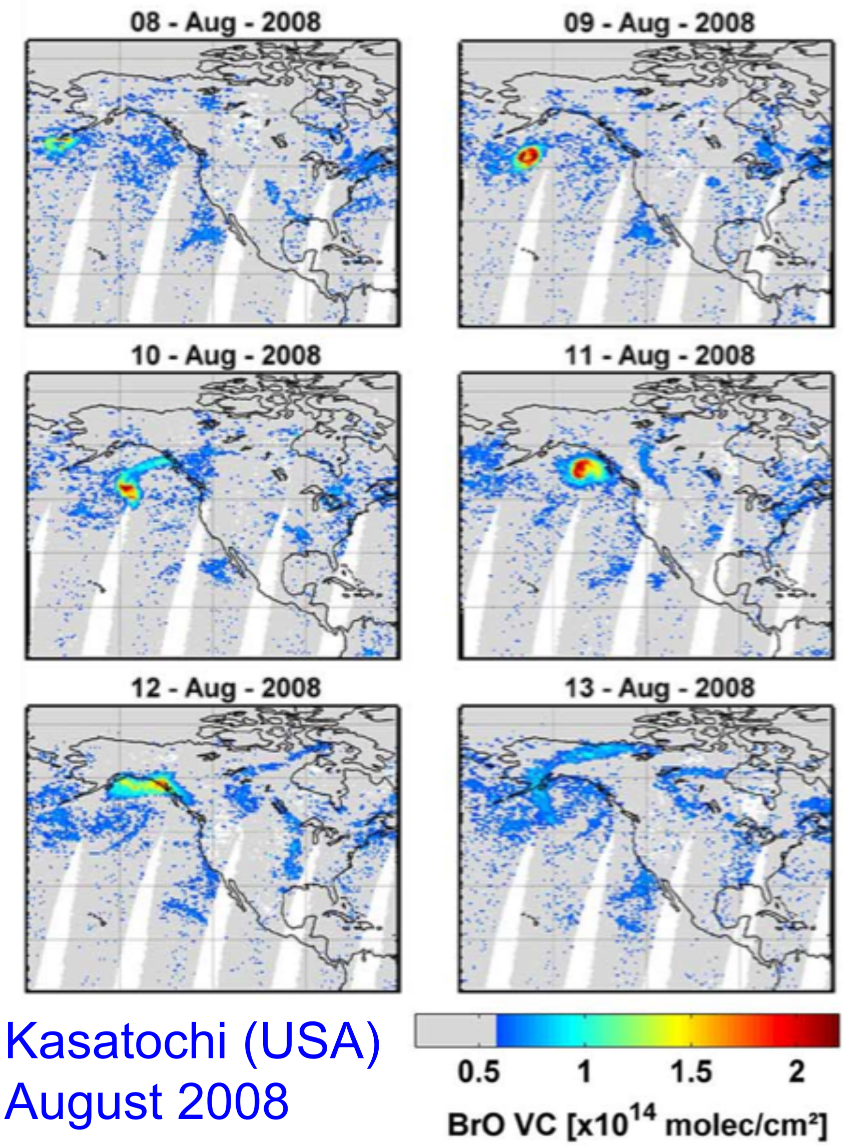

Kasatochi (USA)
August 2008

Theys et al. (2009, 2014); *Carn et al.* (2016)

- Satellites have measured HCl, BrO, and OClO in explosive volcanic eruption clouds
- Volcanic halogens can promote ozone depletion

Satellite measurement of volcanic H_2S emissions

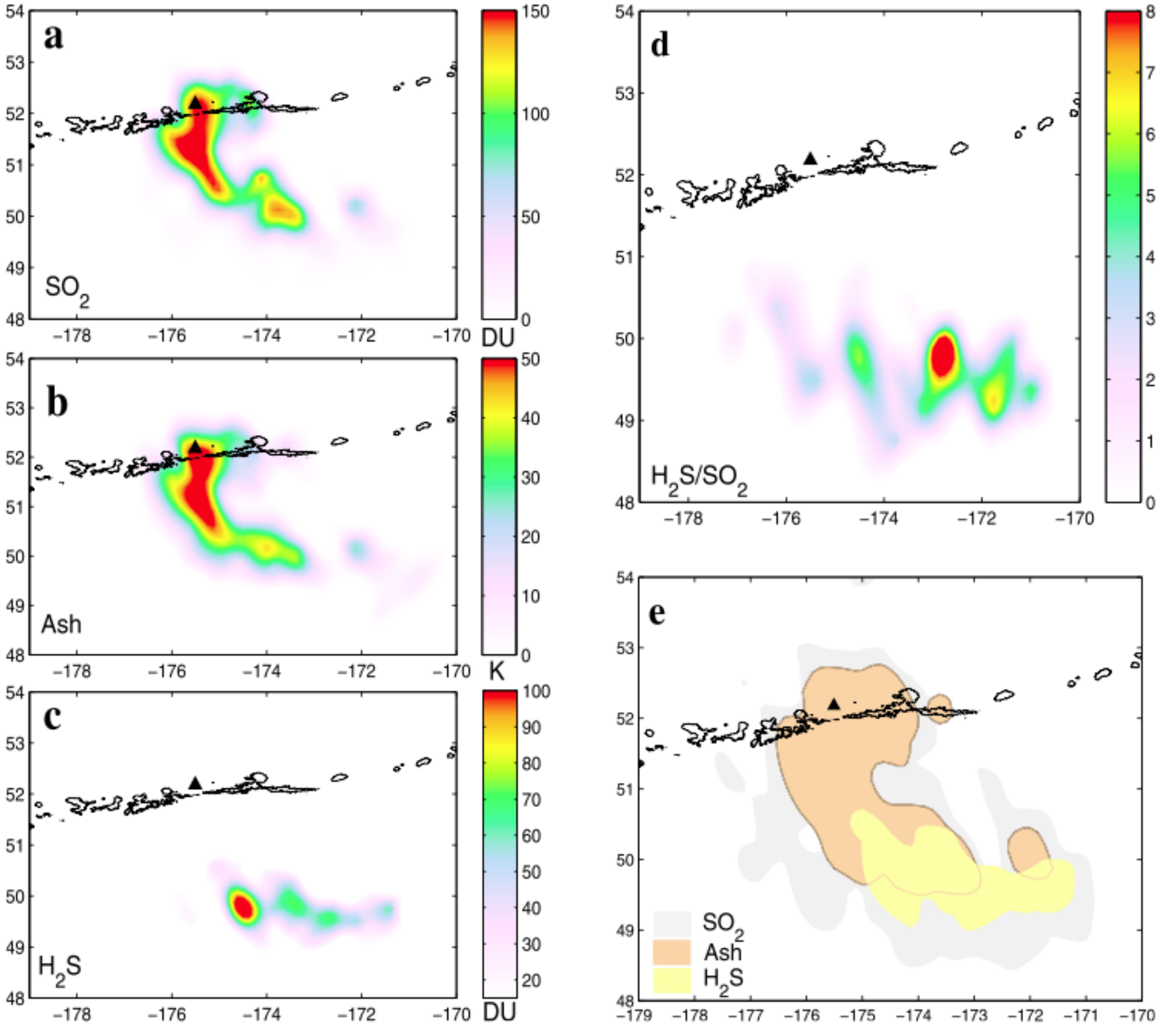

2008 Kasatochi eruption
Clarisse et al. (2011)

Pressure →

$$SO_2 + 3H_2 = H_2S + 2H_2O$$

← Temperature / fO_2

$$\log (SO_2/H_2S) = \log K_T - 3 \log (H_2/H_2O) - \log P \cdot X_{H2O}$$

Symonds et al., 1994

- May be a significant component of the total sulfur budget at some volcanoes (*Aiuppa et al.*, 2005)
- IR absorption bands are very weak, hence can only be detected from space in large eruptions (IASI; *Clarisse et al.*, 2011)

Inverse trajectory modeling of SO_2 data

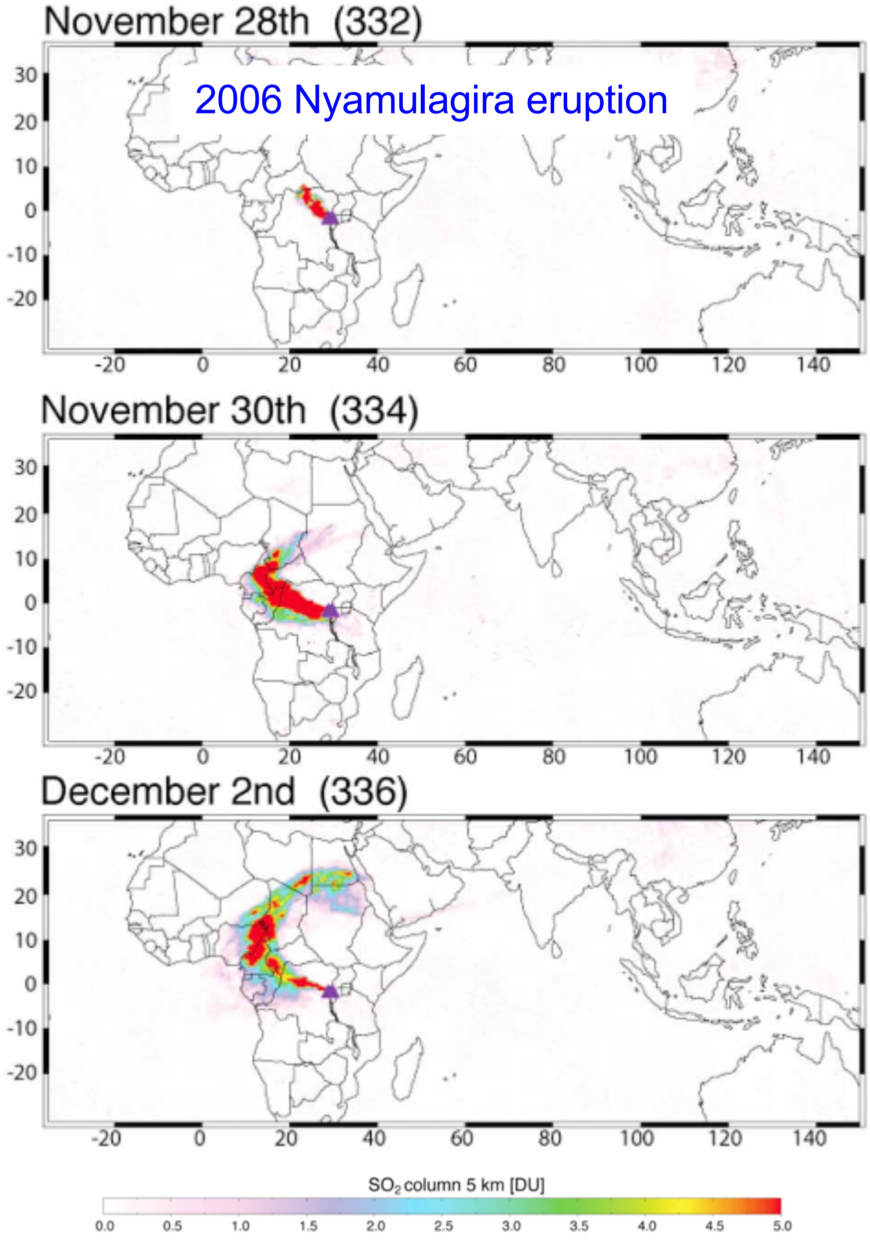
November 28th (332)

2006 Nyamulagira eruption

November 30th (334)

December 2nd (336)

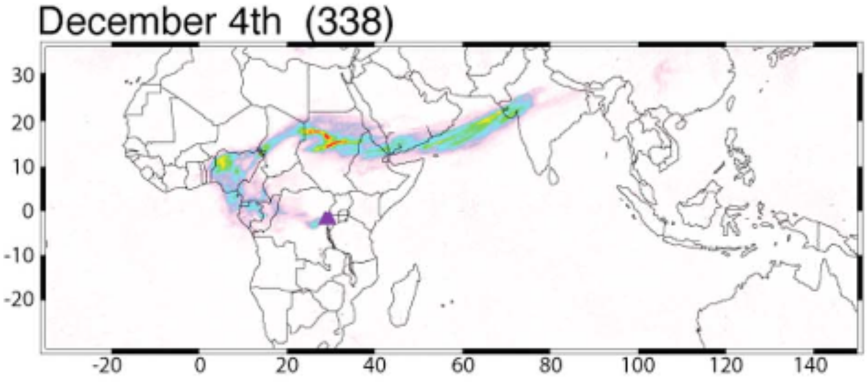
December 4th (338)

December 6th (340)

Hughes et al. (2012)

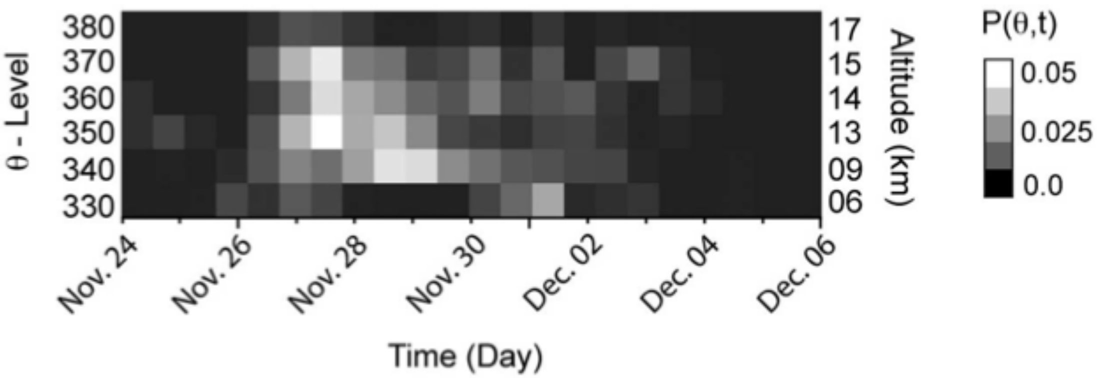

- Satellite measurements from polar-orbiting sensors have low (~daily) temporal resolution
- Initiate backward trajectories from observed locations of SO_2 cloud – select those that approach volcano
- Generate PDF of SO_2 emission altitude and time (here for an effusive erruption)

Eckhardt et al. (2008); *Kristiansen et al.* (2010, 2014); *Boichu et al.* (2013, 2014)

Inverse modeling of volcanic 'source term'

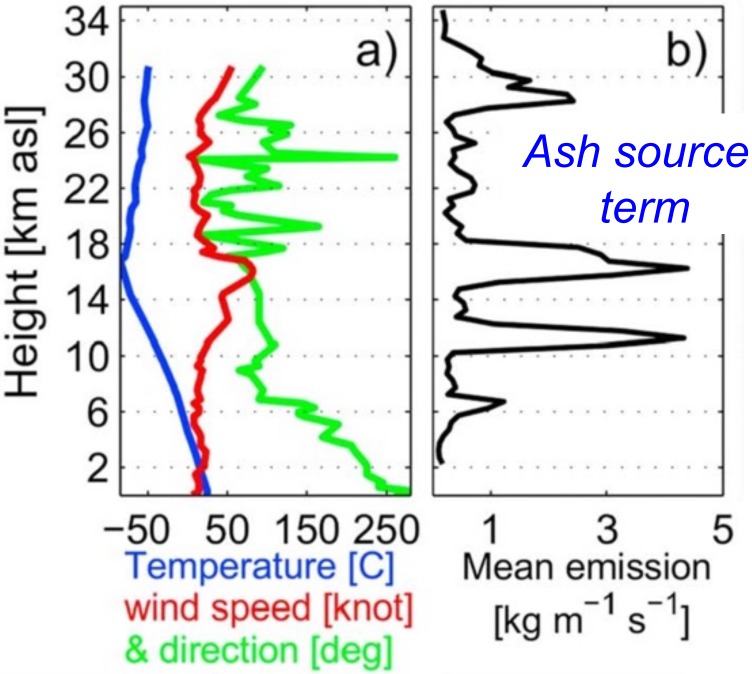

Ash source term

FLEXPART–ECMWF MODEL SIMULATION
13 Feb 2014 22:00 – 22:30 UTC

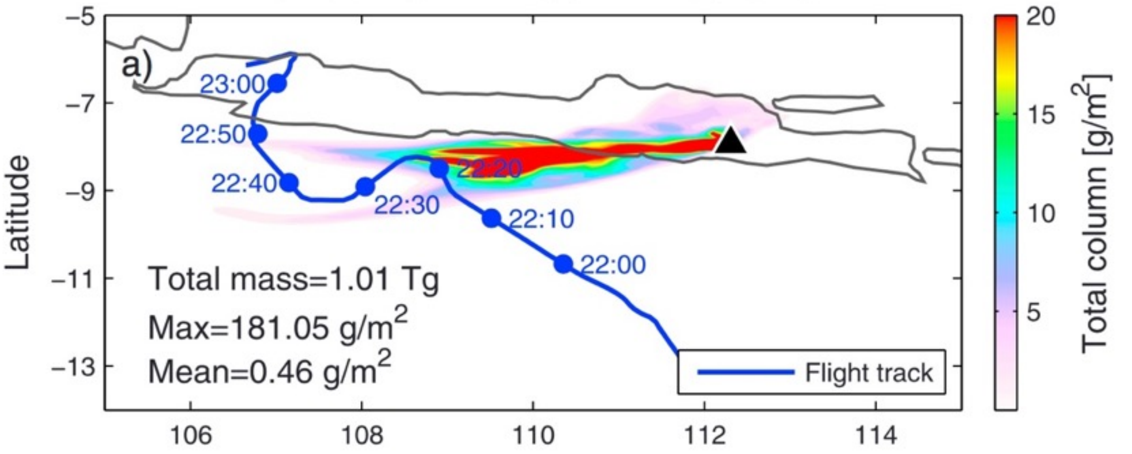

Vertical cross section along flight track

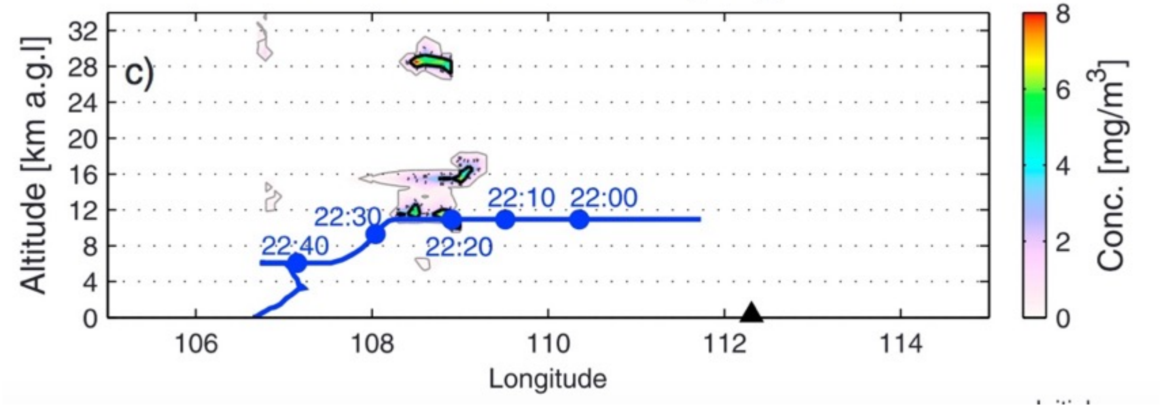

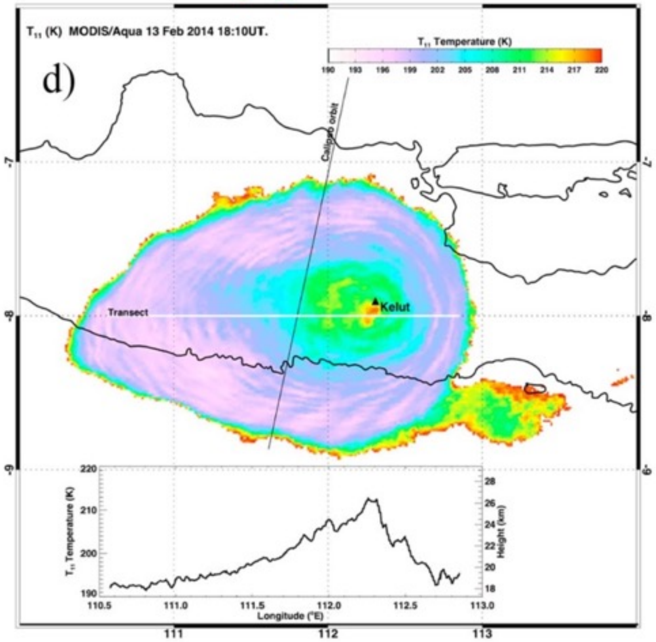

- Geostationary satellite data used to estimate volcanic ash source term, and simulate location of aircraft encounter that was not directly observed

Kristiansen et al. (2014)

Evolution of SO_2 mass after volcanic eruptions

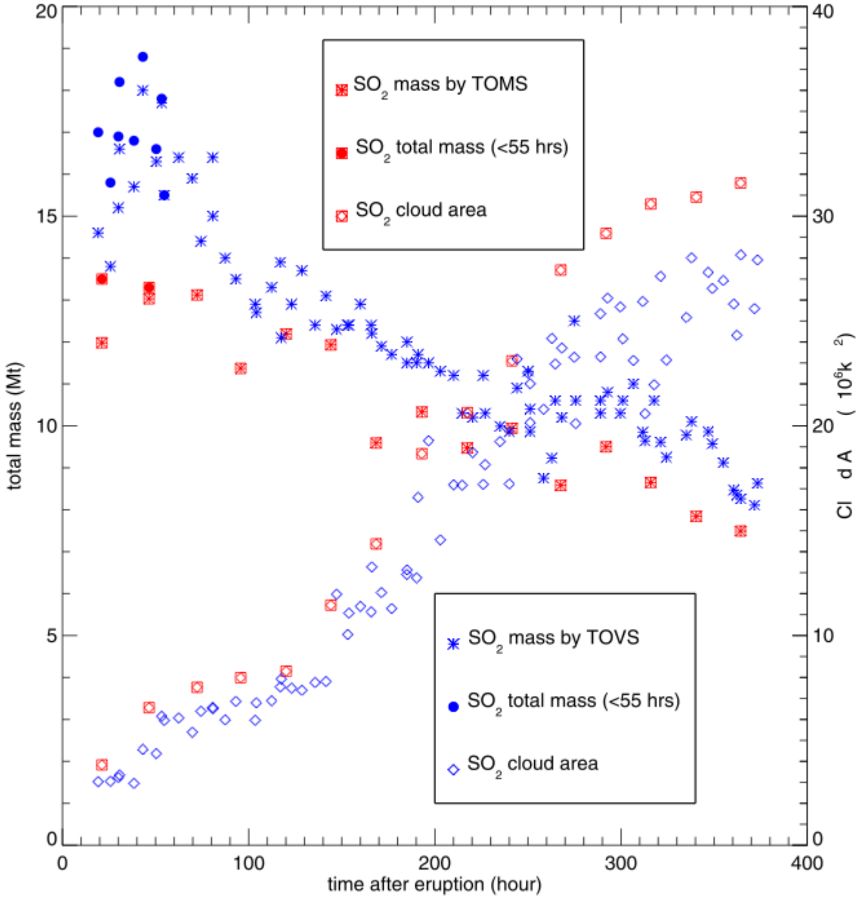

1991 Pinatubo SO_2 mass evolution from TOMS and TOVS (*Guo et al.*, 2004)

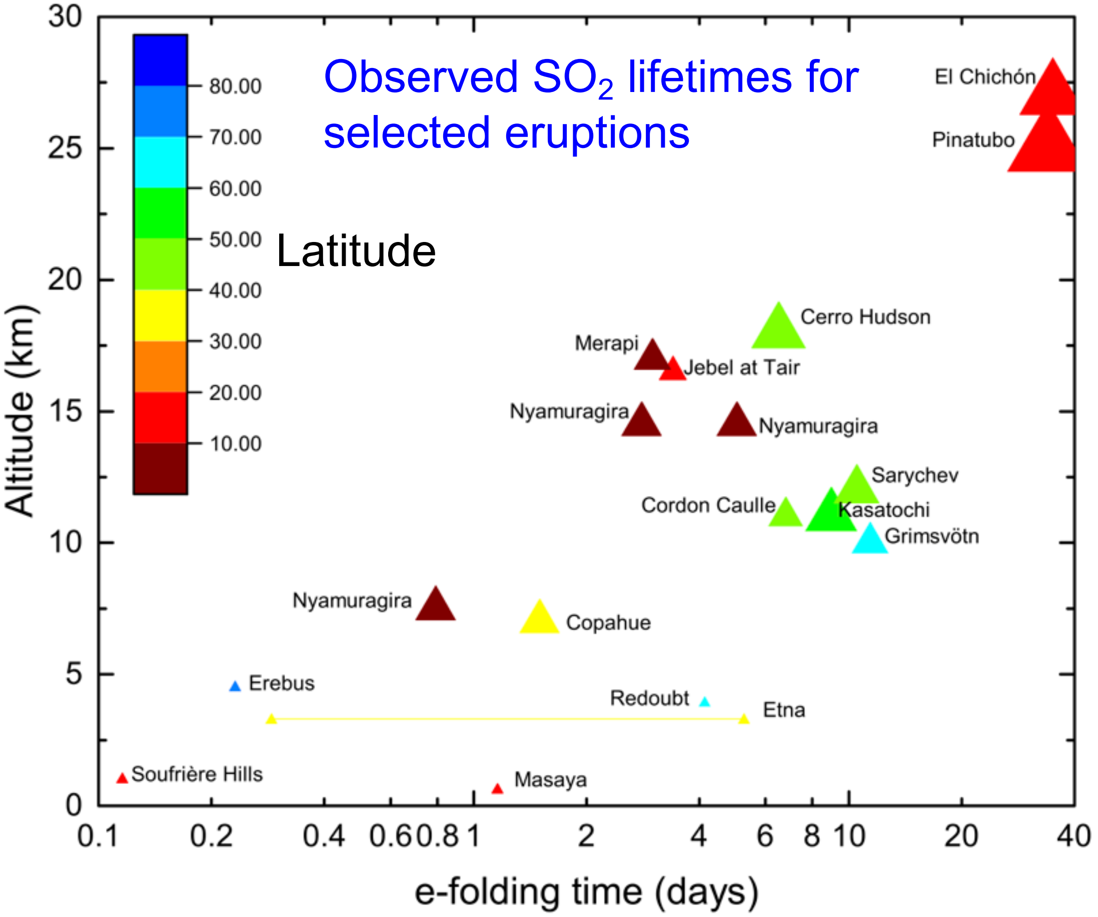

Carn et al. (2016)

- A ‘2^{nd} day’ SO_2 mass peak is sometimes observed; possible reasons include:
  - Oxidation of co-erupted H_2S to SO_2 (*Bluth et al.*, 1995)
  - Optically thick fresh plume partially masks detection of SO_2 (*Bluth et al.*, 1995)
  - Release of gas-phase SO_2 from SO_2 - ice - ash mixtures (*Textor et al.*, 2003)
- e-folding time of volcanic SO_2 used to test chemical schemes in climate models

Eruptive volcanic SO_2 emissions (1978-2018)

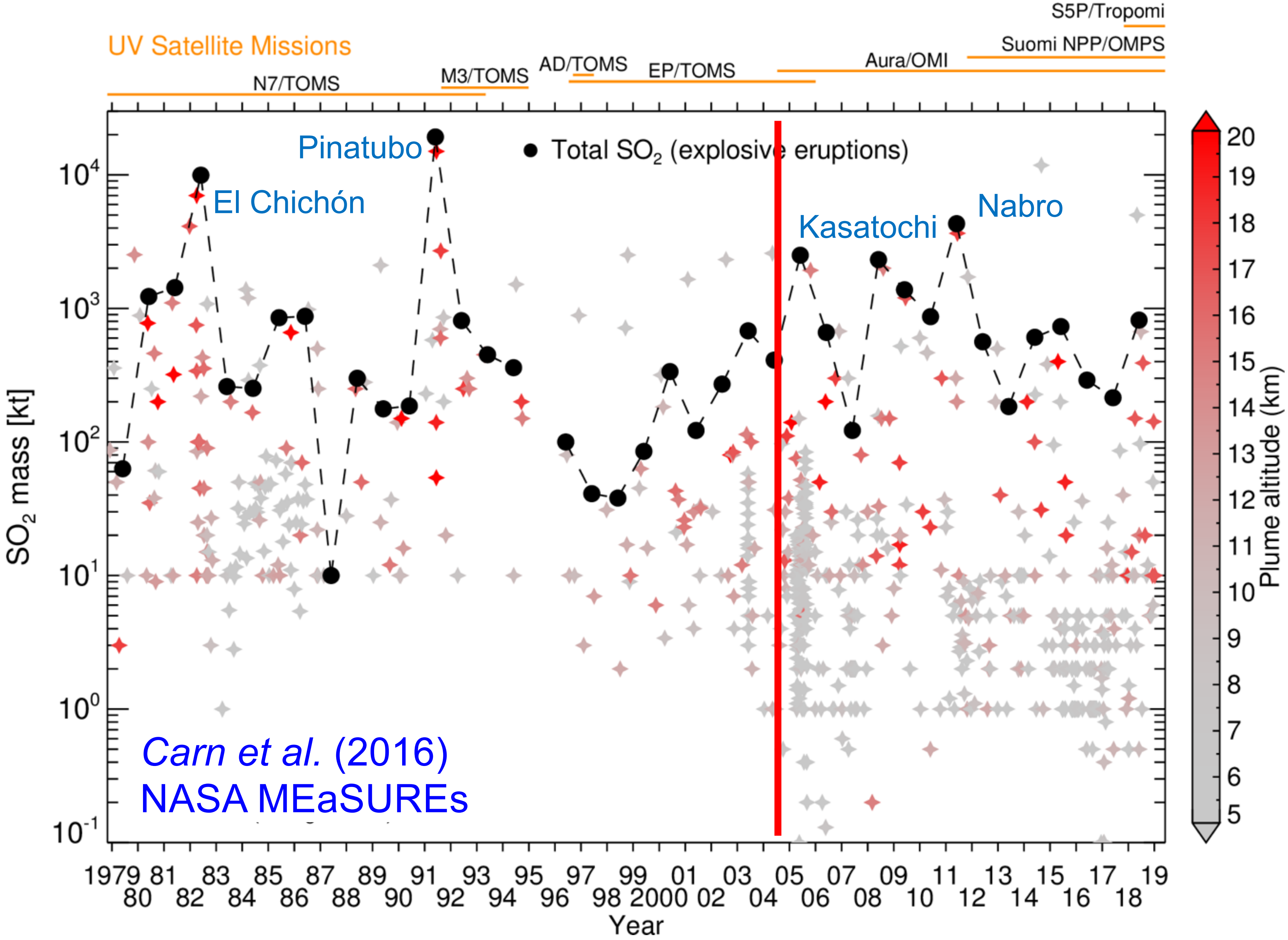

Carn et al. (2016)

NASA MEaSUREs

Excess sulfur in volcanic eruptions

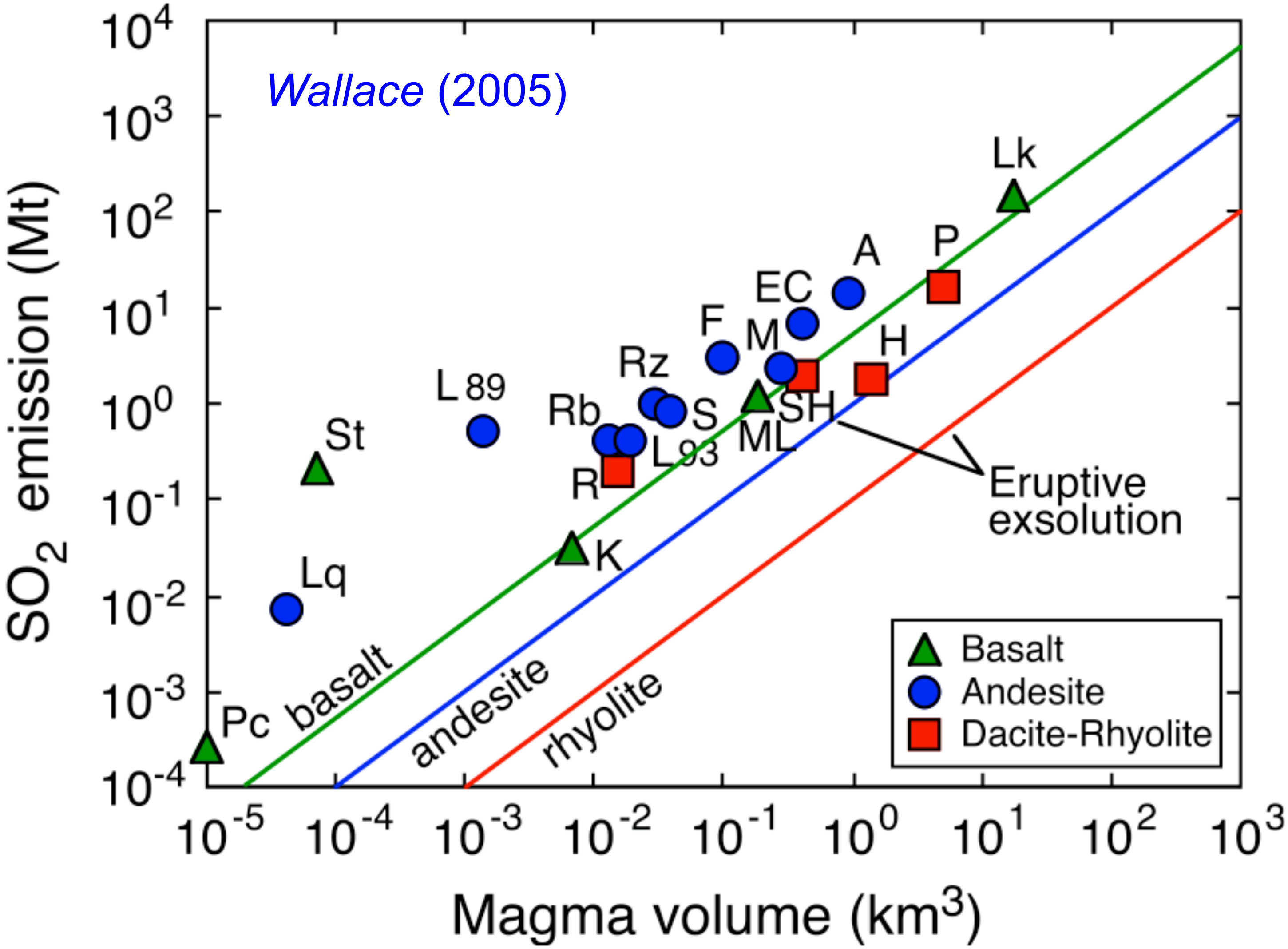

- Satellite data revealed disconnect with the ‘petrological method’
- Now widely attributed to existence of pre-eruptive vapor phase in magmas
- Distribution of this vapor phase impacts eruption sulfur yield

SO_2 emissions vs. Volcanic Explosivity Index (VEI)

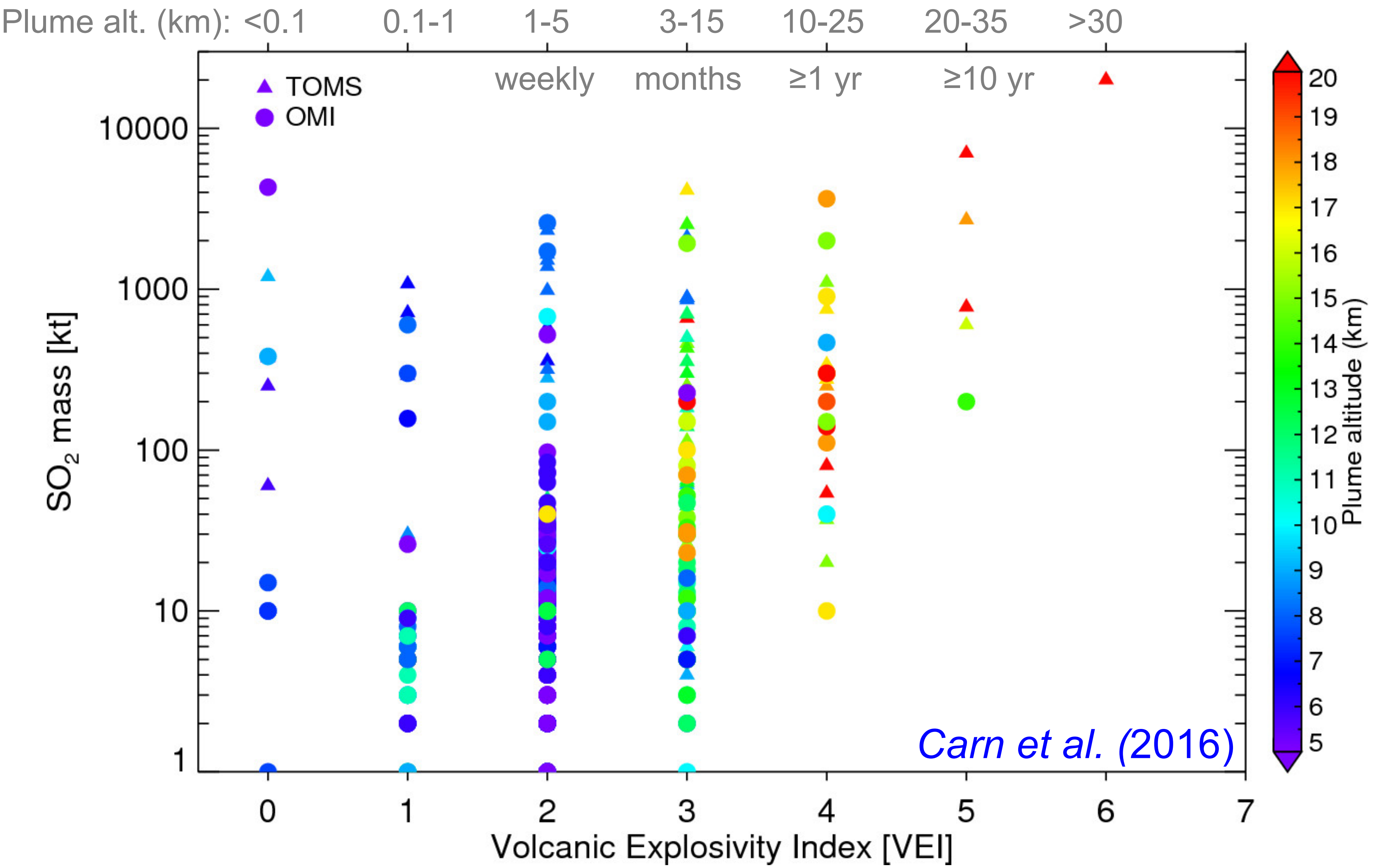

Carn et al. (2016)

- Eruption VEIs from Smithsonian Global Volcanism Program database (VOTW 4.0)
- SO_2 data from TOMS, OMI, OMPS, AIRS, HIRS satellite measurements

SO_2 emissions vs. VEI (explosive eruptions)

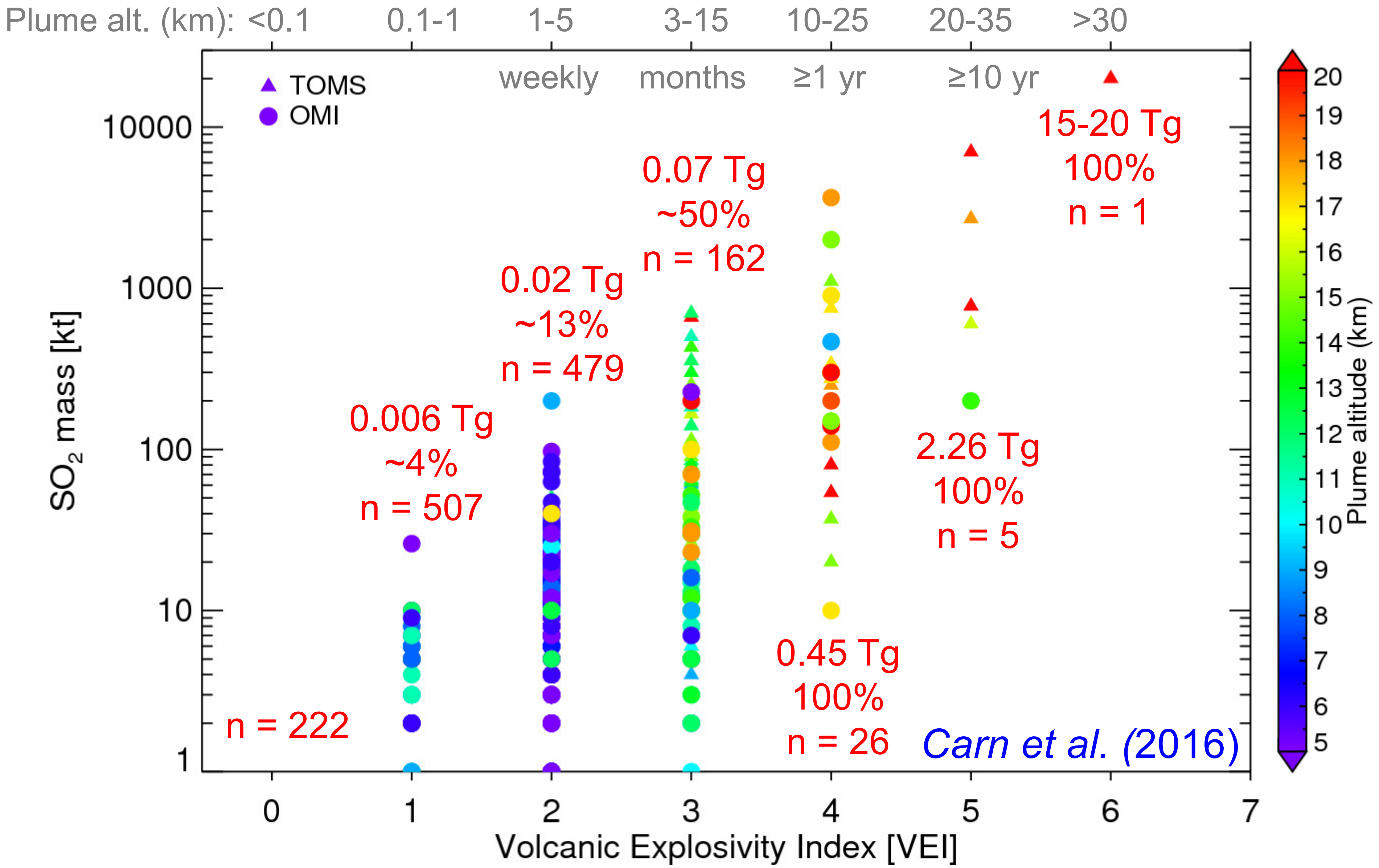

Carn et al. (2016)

- Broad correlation between explosive SO_2 emissions and VEI, but large scatter
- May reflect release of variable amounts of pre-eruptive vapor during eruptions

Impact of magma compressibility on deformation

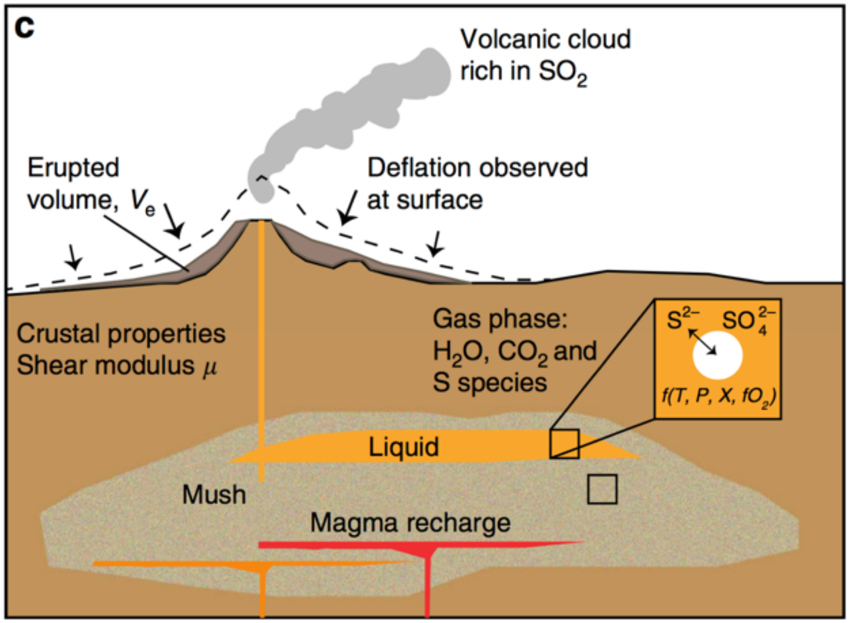

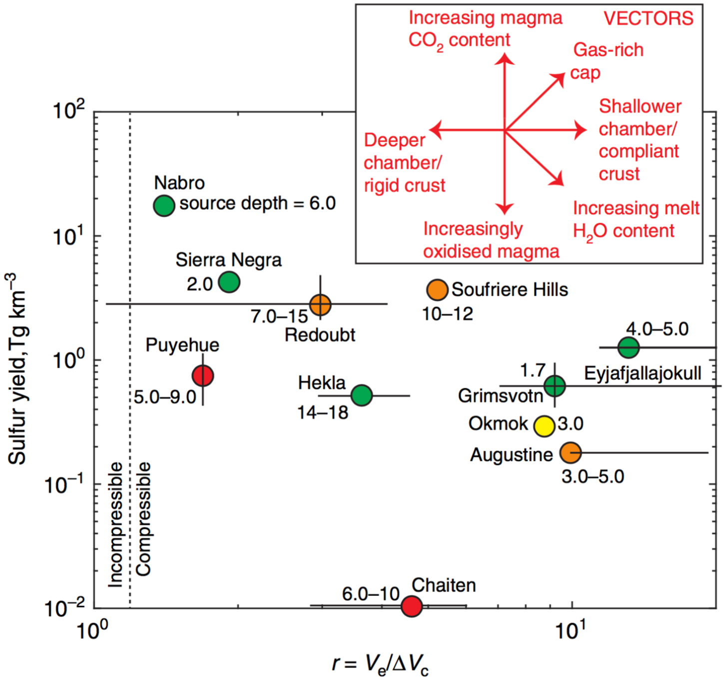

Jay et al. (2014)

McCormick-Kilbride et al. (2016)

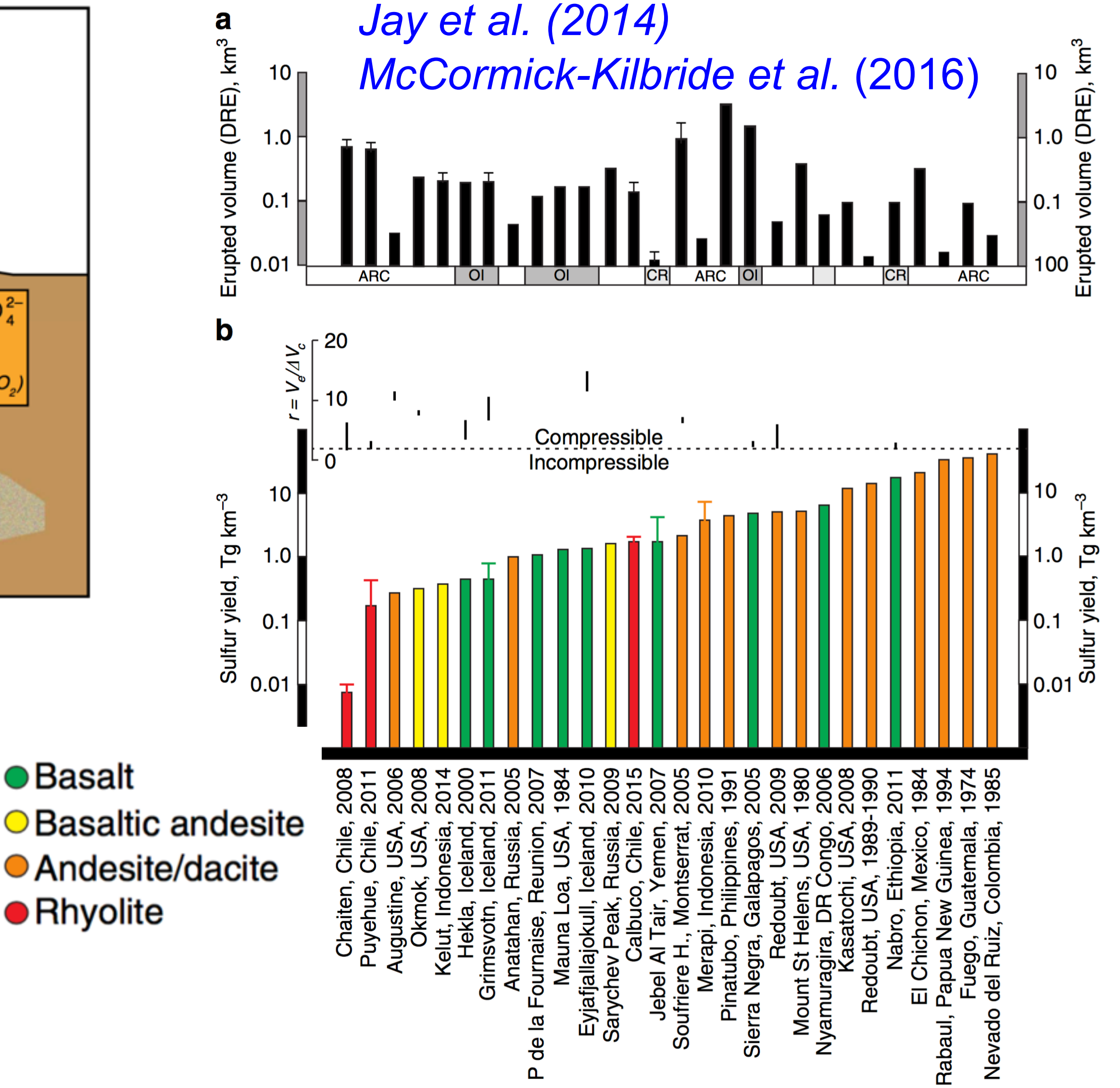

- r = erupted volume / obs. deformation
- Not only SO_2 contributing to compressibility
- Precursors to major SO_2-producing eruptions?

Passive volcanic degassing

Nyiragongo (DR Congo)

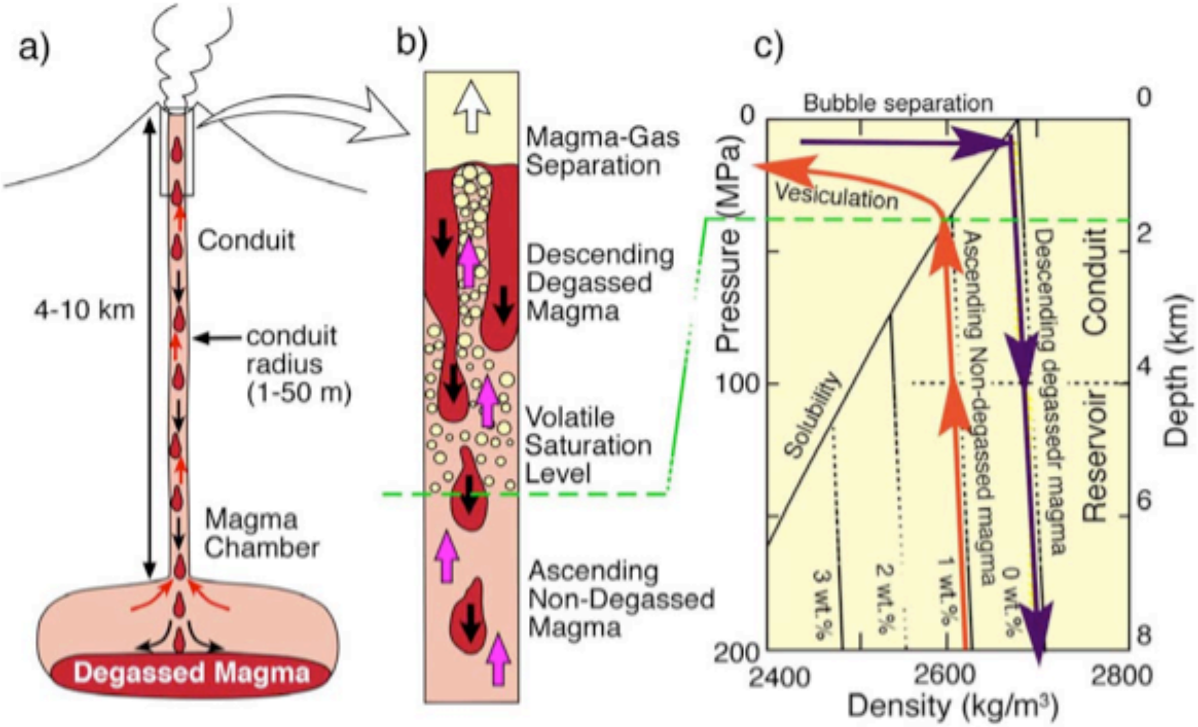

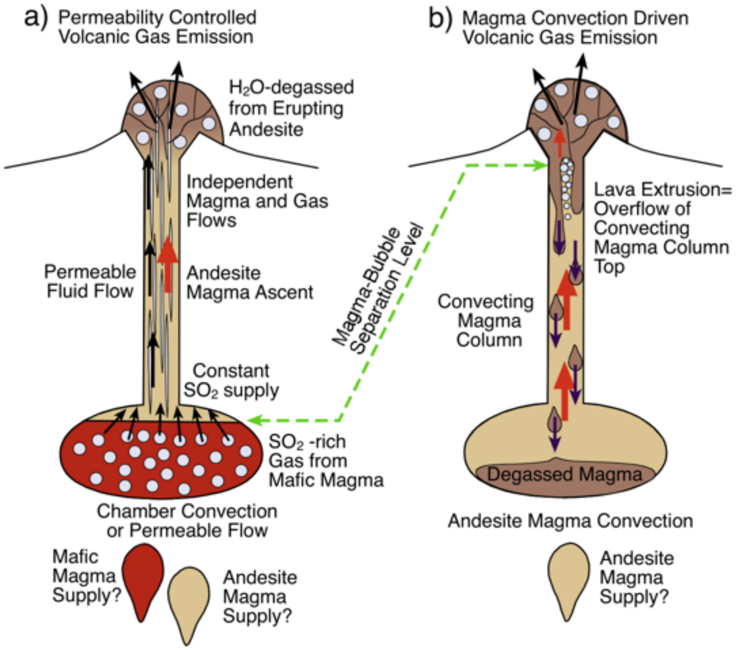

- On average, ~80-90% of volcanic SO_2 emissions emitted by passive (non-eruptive) degassing
- Significant environmental and health impacts
- Conduit convection or permeable conduit models usually invoked to explain high gas fluxes
- Only consistently detectable from space relatively recently (post-2004; Ozone Monitoring Instrument)

Kazahaya et al (1994); *Shinohara* (2008)

Global volcanic SO_2 emissions inventories

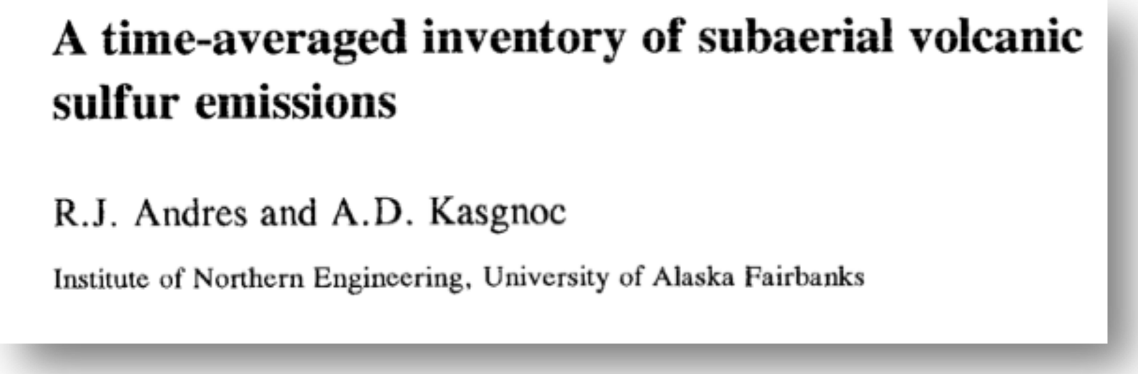

A time-averaged inventory of subaerial volcanic sulfur emissions

R.J. Andres and A.D. Kasgnoc

Institute of Northern Engineering, University of Alaska Fairbanks

- Volcanic degassing ‘source term’ in atmospheric chemistry and climate models
- Climate impact of tropospheric volcanic emissions (sulfate aerosol)
- Estimation of global fluxes of other volcanic gases (e.g., CO_2) and trace metals (e.g., Hg)
- Identifying potential field sites for volcanic gas studies

SCIENTIFIC REPORTS

OPEN

A decade of global volcanic SO_2 emissions measured from space

S. A. Carn[1], V. E. Fioletov[2], C. A. McLinden[2], C. Li[3,4] & N. A. Krotkov[4]

Sulfur emissions (~100 Tg/yr)

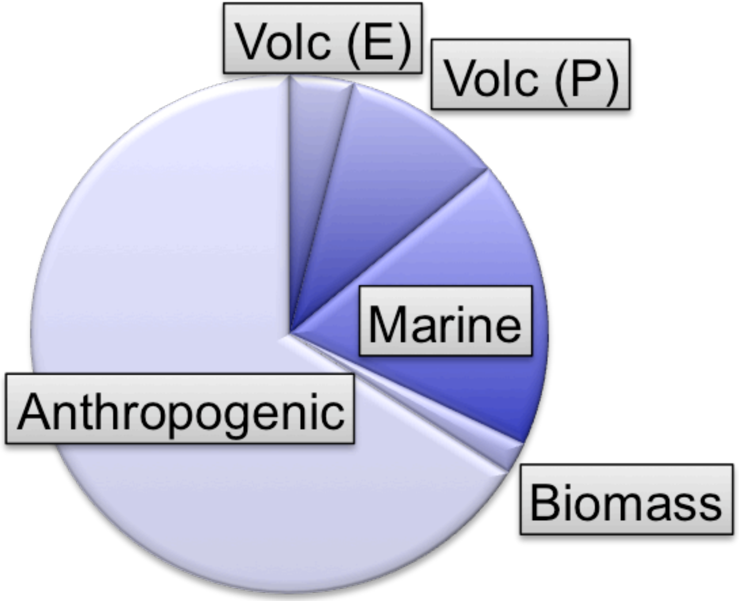

Sulfate burden

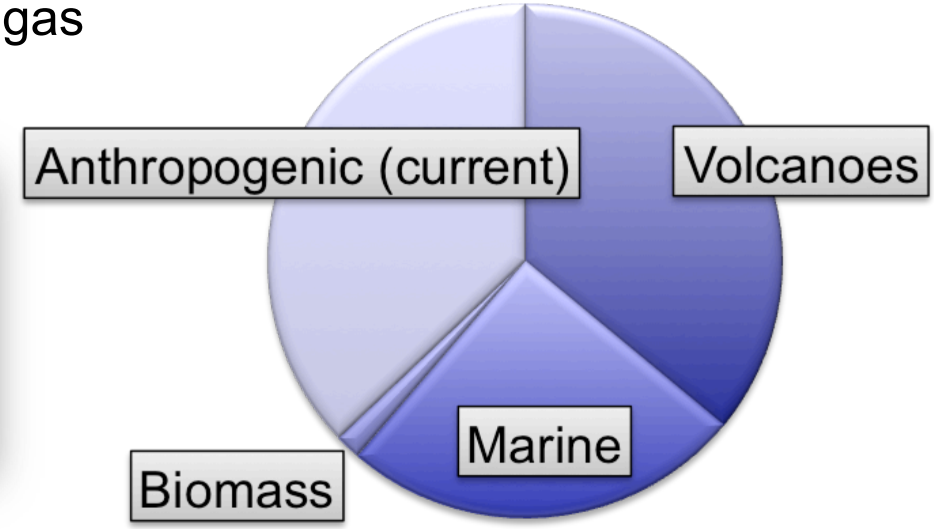

Graf et al. (1997); *Andres & Kasgnoc* (1998); *Shinohara* (2013); *Fioletov et al*. (2016); *Carn et al.* (2017)

Passive volcanic degassing from space

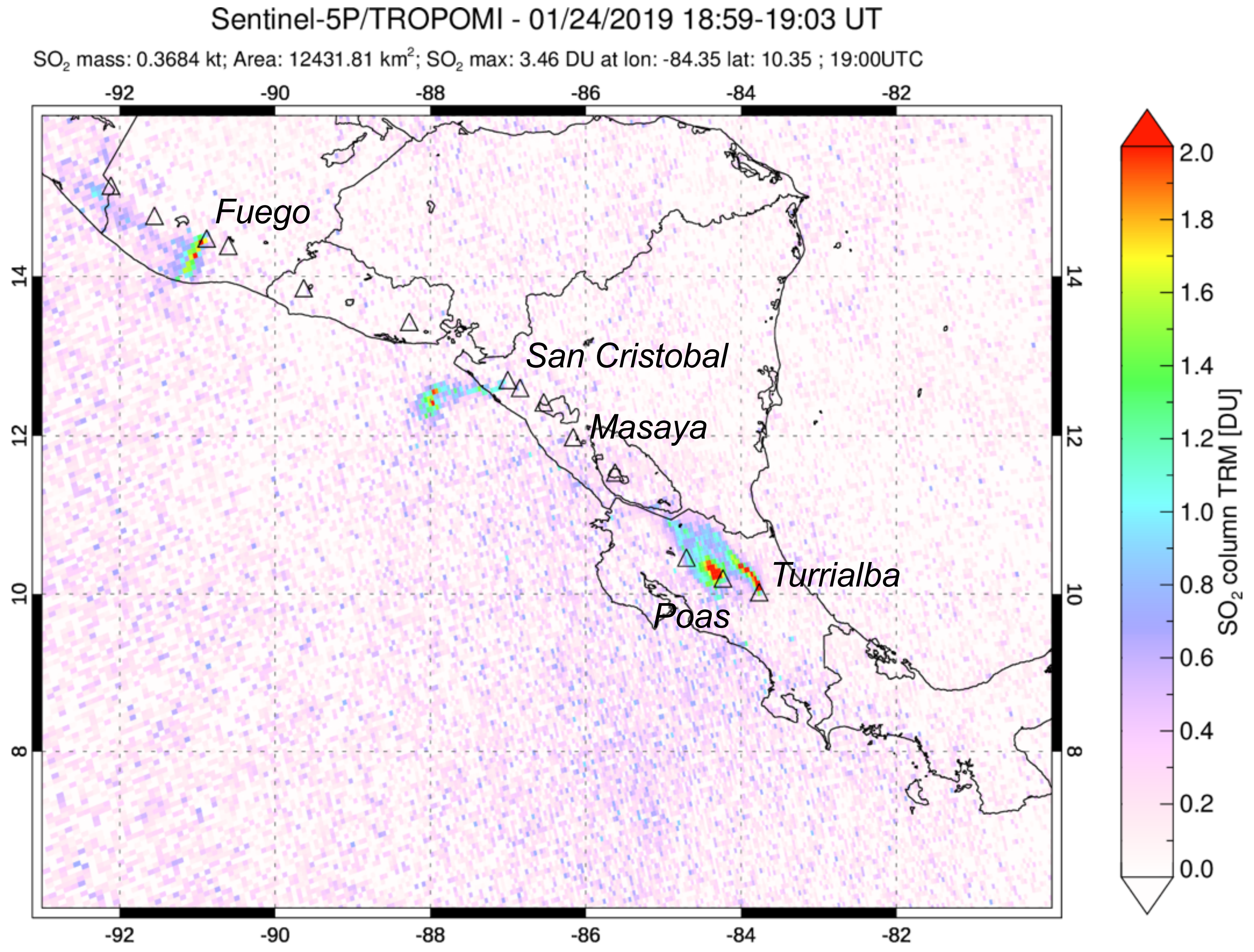

Sentinel-5P/TROPOMI - 01/24/2019 18:59-19:03 UT

SO_2 mass: 0.3684 kt; Area: 12431.81 km^2; SO_2 max: 3.46 DU at lon: -84.35 lat: 10.35 ; 19:00UTC

Data: BIRA-IASB/DLR/ESA/EU

- Plumes from strong SO_2 emitters (100s-1000s tons/day) visible on a daily basis in satellite data
- Detection of weaker degassing sources requires time-averaging – but simple data ‘stacking’ less effective if wind direction is variable

SO_2 source ID and emission estimation

- 3-year averages (e.g., 2005-2007) of global NASA Ozone Monitoring Instrument (OMI) SO_2 data

- Spatial smoothing and wind rotation techniques (upwind – downwind difference) used to identify SO_2 sources (volcanic and anthropogenic)

- Exponentially-modified Gaussian fit to average SO_2 plume to estimate annual mean SO_2 flux for each source

- Detection limit of ~16-30 tons/day SO_2

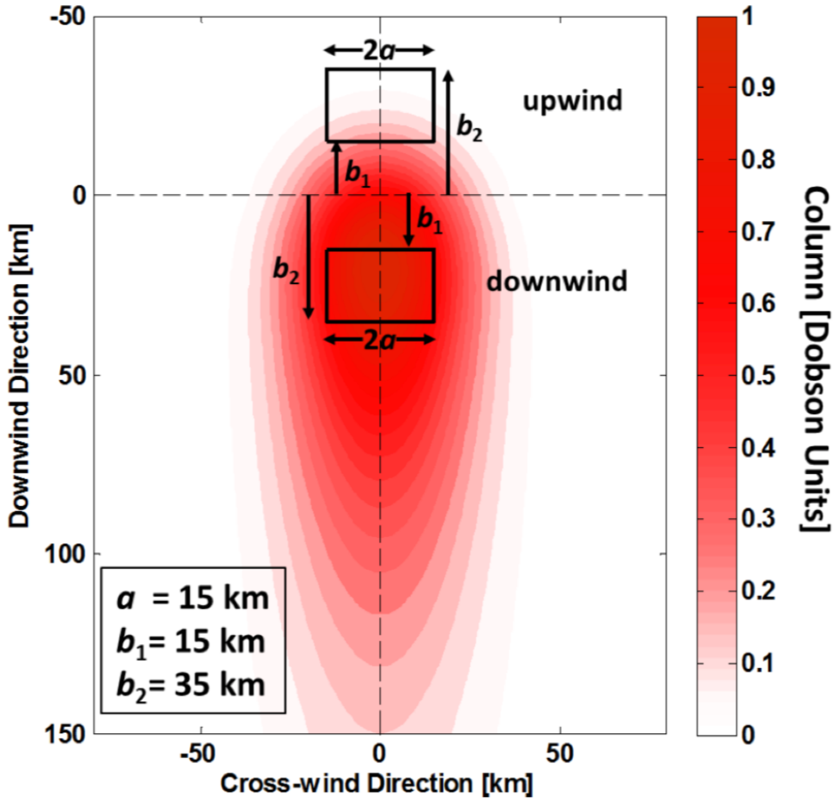

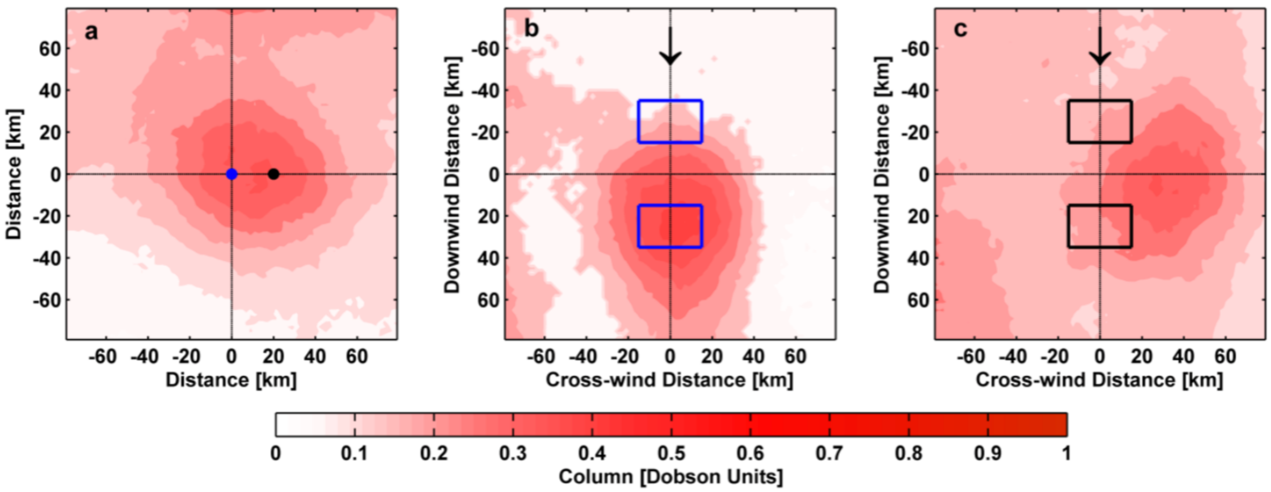

Fioletov et al. (2011, 2015, 2016)
McLinden et al. (2016)

New global volcanic SO_2 emission inventory

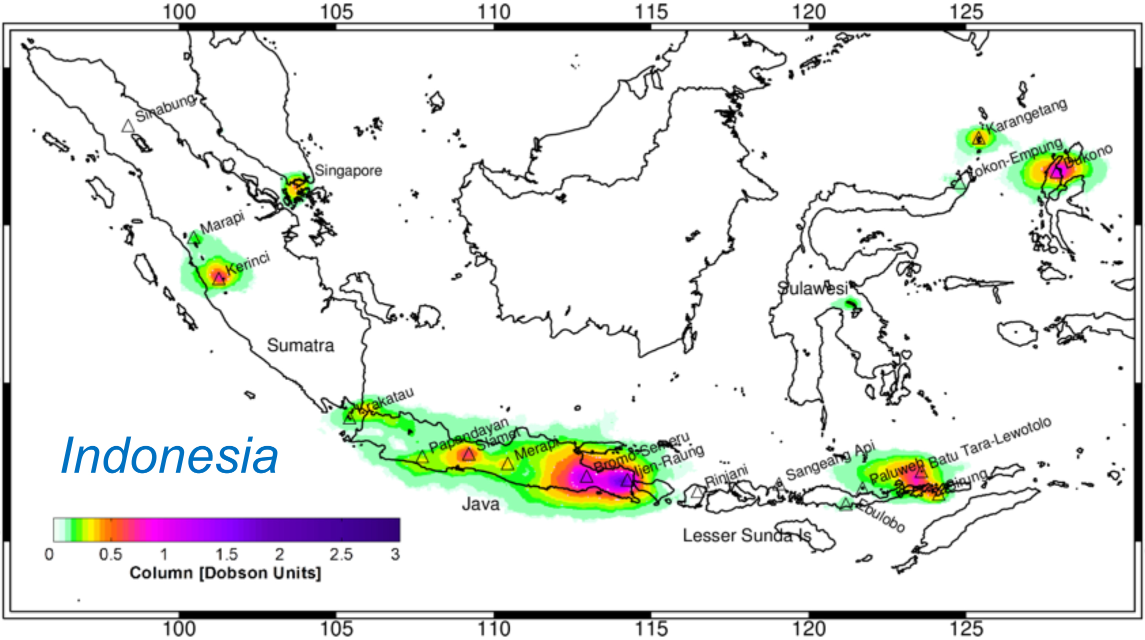

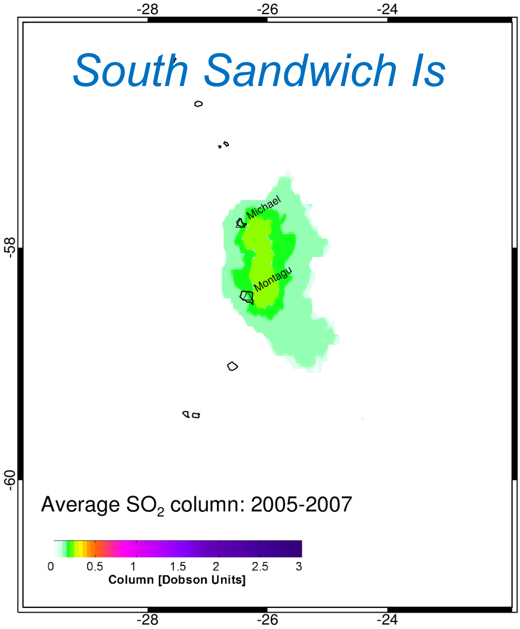

- Globally, 90-100 volcanic SO_2 sources quantified (10-20% ‘new’)

- Total SO_2 flux of 23+/-2 Tg/yr (~63 kt/day); ~80-90% of total SO_2 flux from passive + eruptive degassing

- Lowest flux: ~32 t/d; could be extended to weaker sources with new Sentinel-5P/TROPOMI data

Carn et al. (2017)

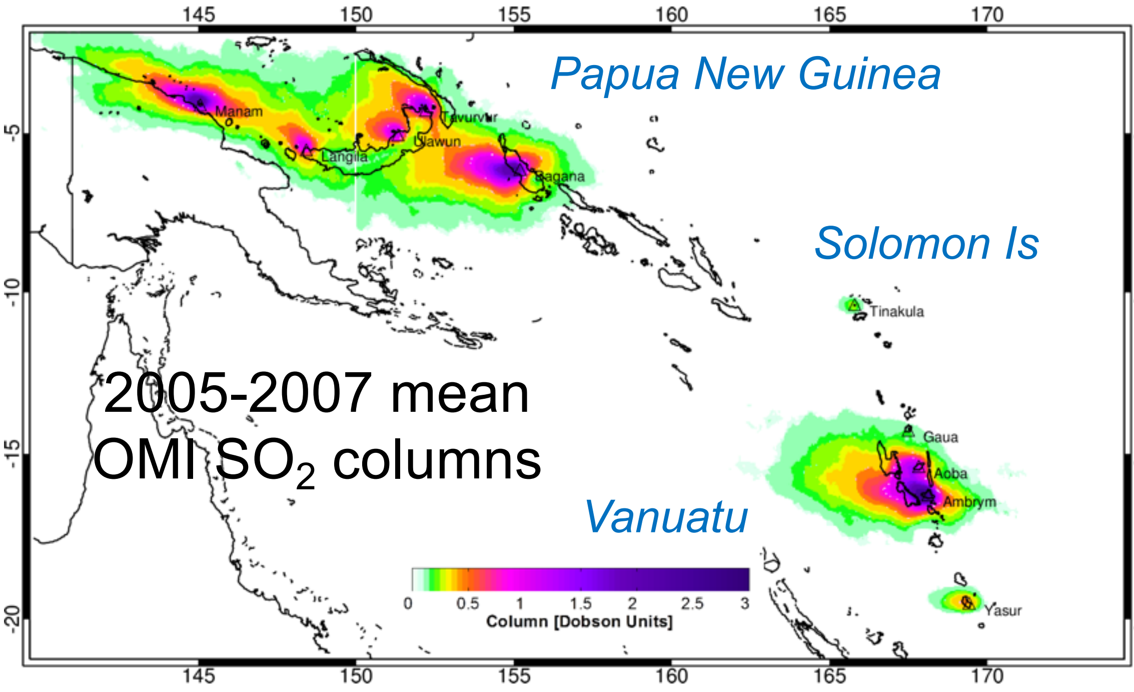

2005-2007 mean OMI SO_2 columns

Trends in tropospheric volcanic SO_2 emissions

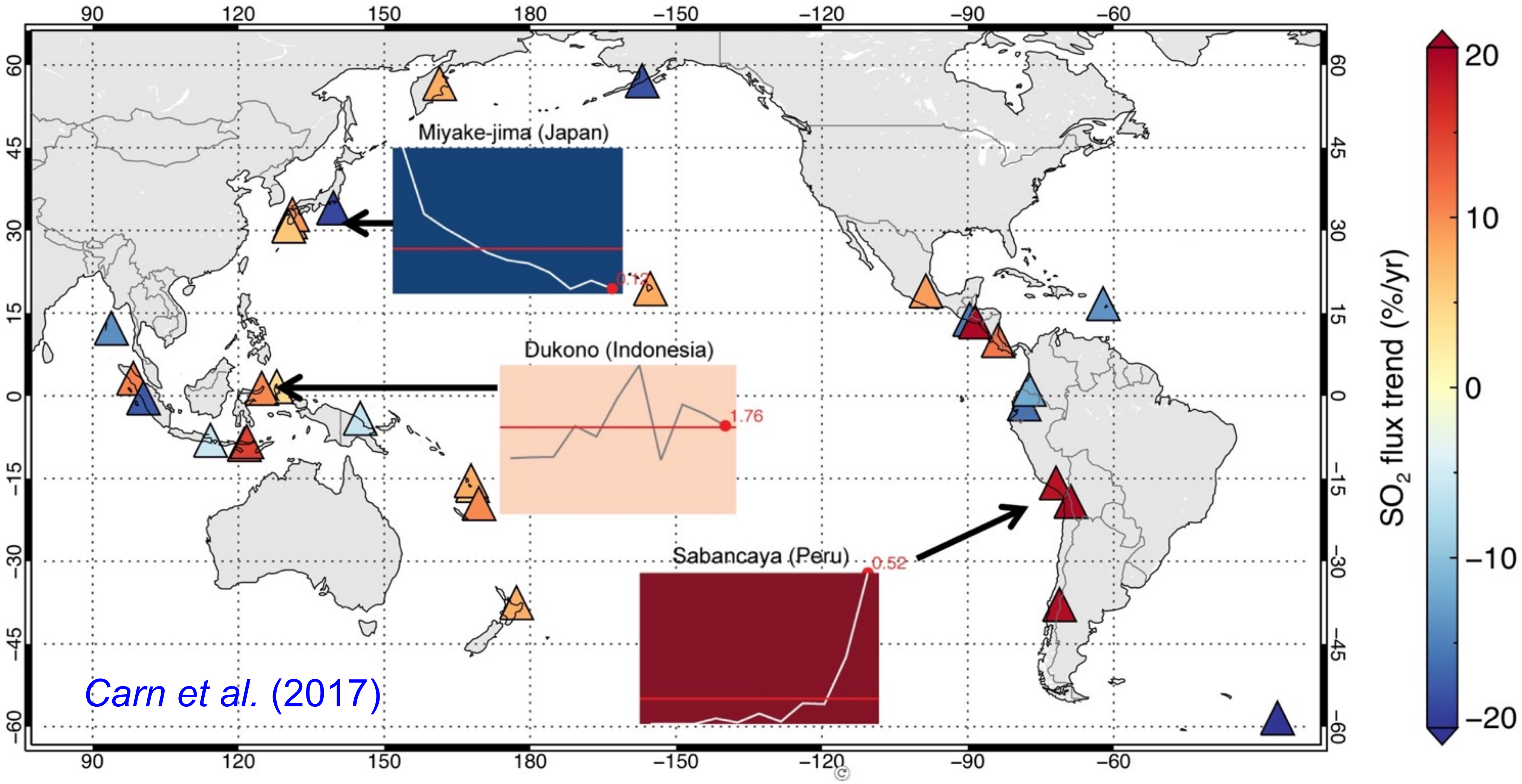

Carn et al. (2017)

- ~30% of volcanic SO_2 sources show significant +/- decadal trends in emissions
- ~80% of sources also erupted during the decade (eruption VEIs below 4)
- New insight into volcanic life cycles?

Multi-parameter perspective on volcanic unrest

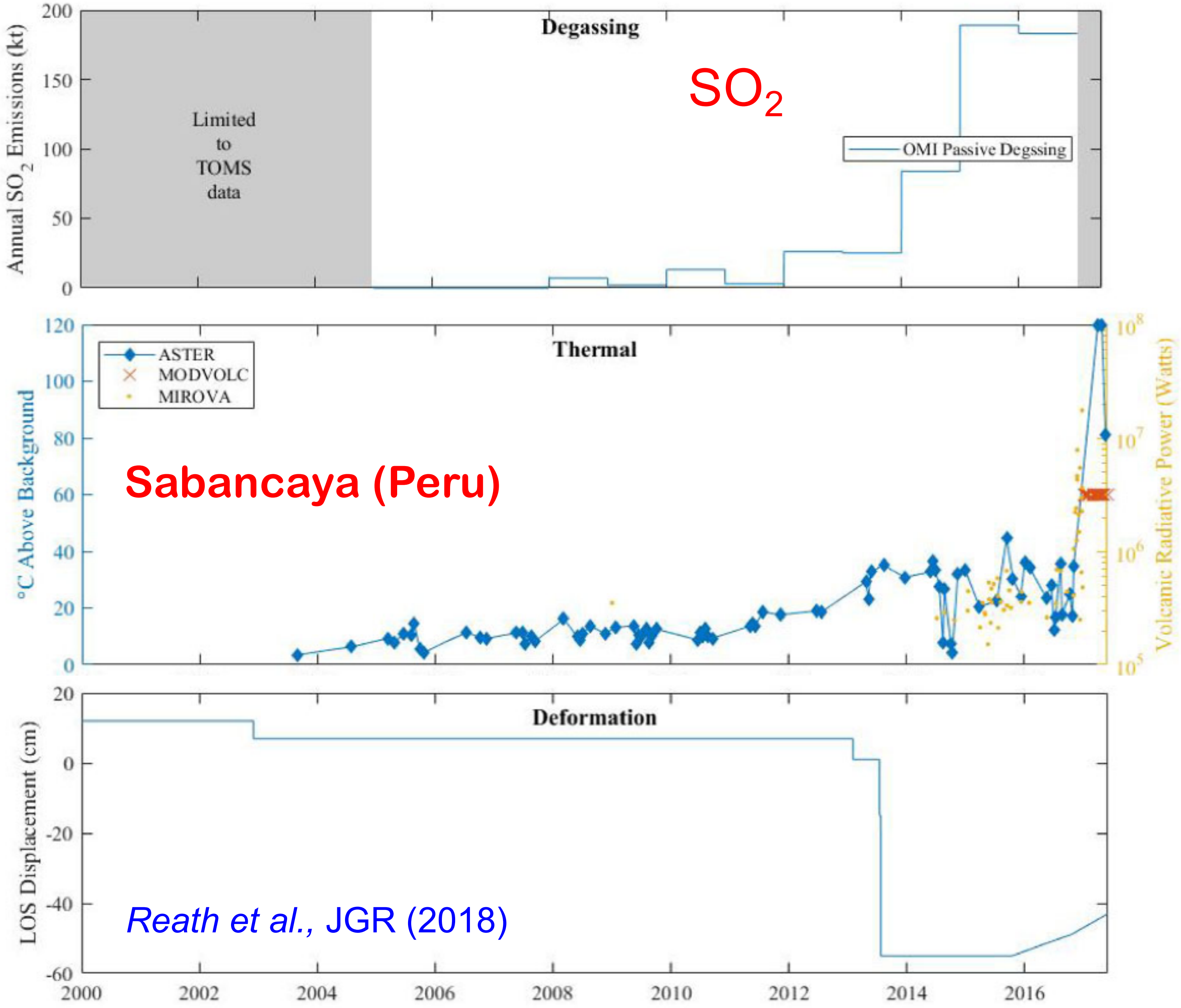

SO_2

Sabancaya (Peru)

Reath et al., JGR (2018)

Improved estimates of volcanic CO_2 emissions

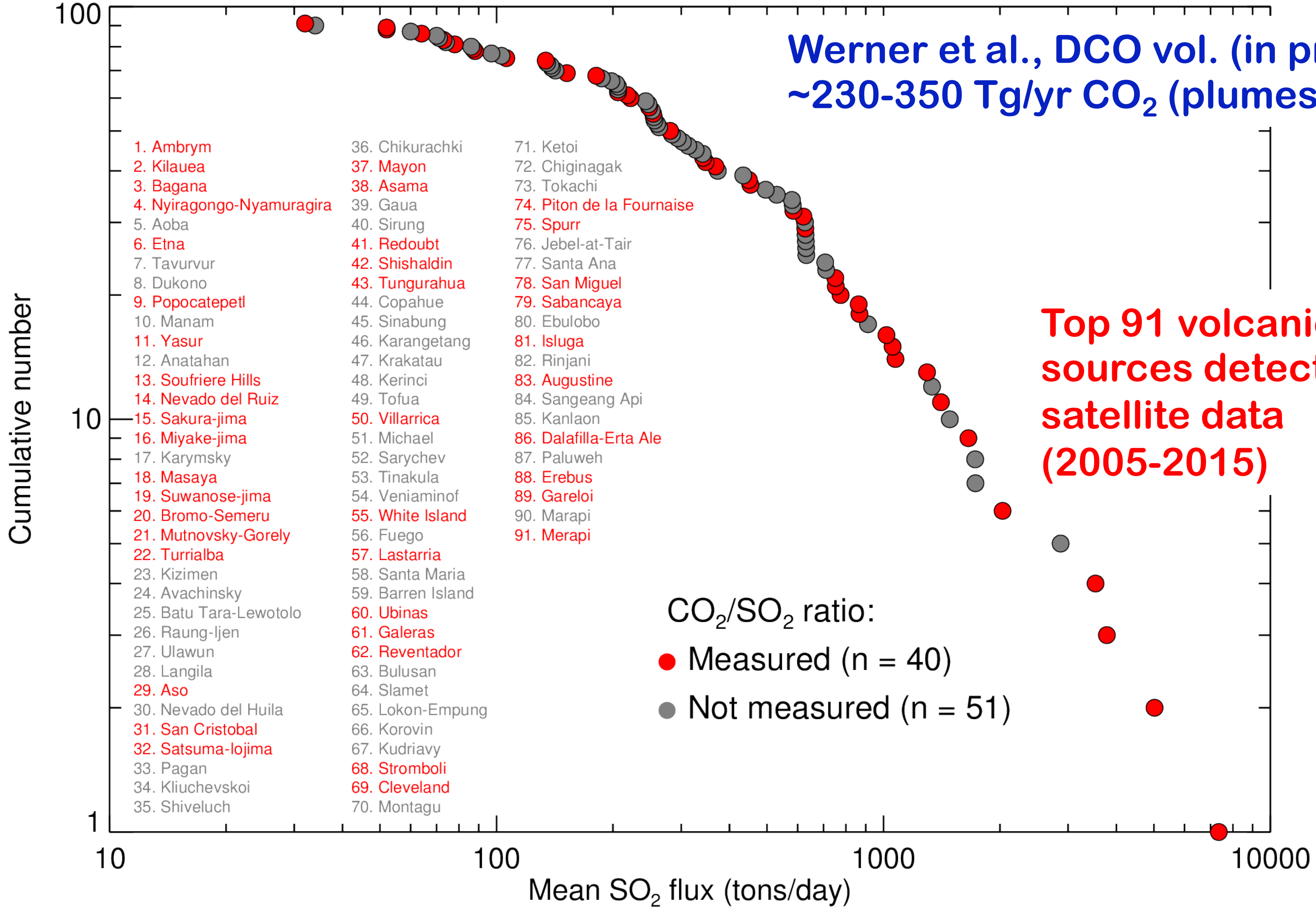

Werner et al., DCO vol. (in prep.)
~230-350 Tg/yr CO_2 (plumes only)

Top 91 volcanic SO_2 sources detected in satellite data (2005-2015)

- CO_2/SO_2 ratios measured at many of the strongest SO_2 sources
- ~50% of SO_2 sources still lack CO_2 data (see *Aiuppa et al.*, ESR, 2017)

Detection of passive volcanic CO_2 emissions

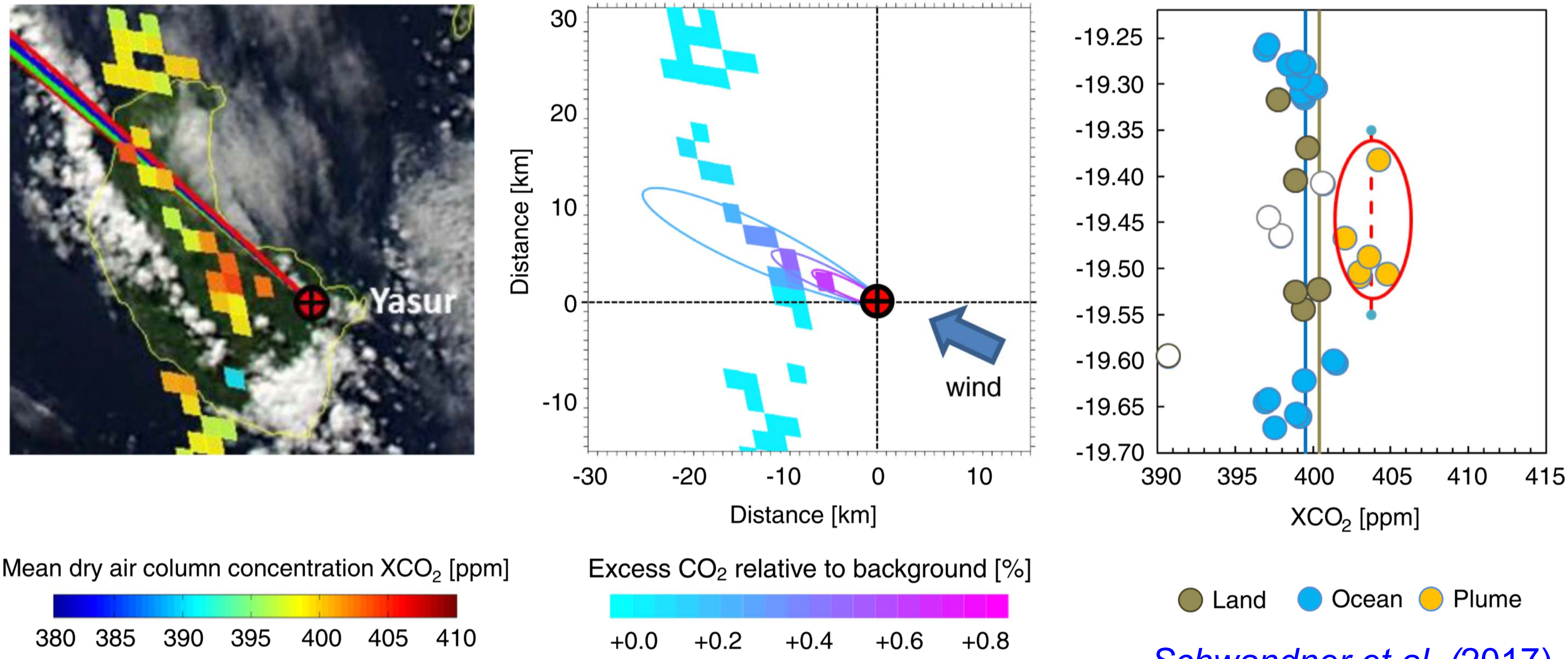

Schwandner et al. (2017)

- Due to its lower solubility in magmas, CO_2 is likely a more reliable volcanic eruption 'precursor' than SO_2, but much more difficult to detect from space
- CO_2 sensing satellites include the NASA Orbiting Carbon Observatory-2 (OCO-2) and the Japanese Greenhouse Gases Observing Satellite (GOSAT)
- Spatial coverage is poor and measurement precision is a few ppm CO_2
- One (known) successful detection of volcanic CO_2 emissions at Yasur (Vanuatu)

Detection of passive volcanic CO_2 emissions

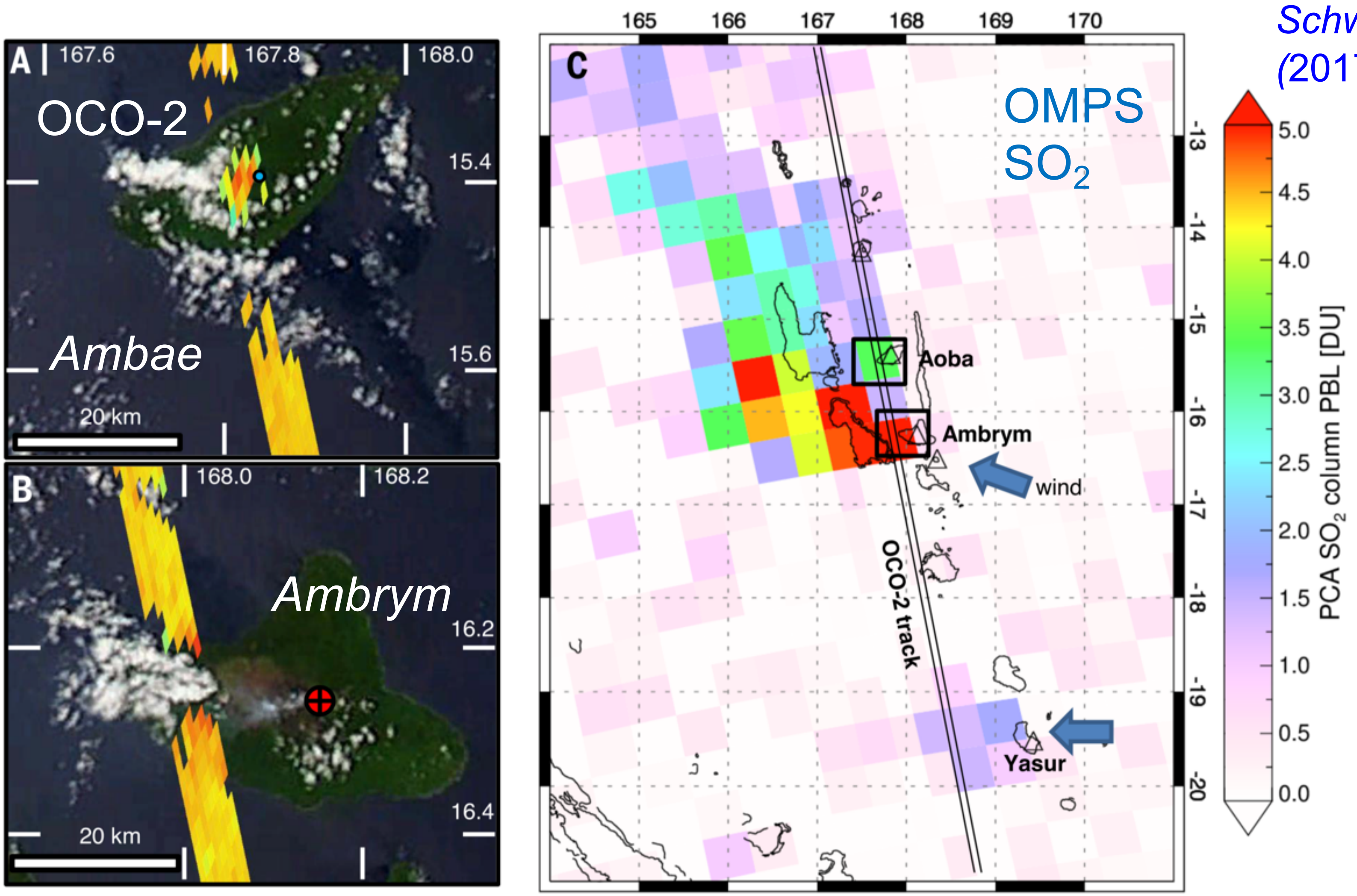

Schwandner et al. (2017)

- Orbiting Carbon Observatory-3 (OCO-3) was deployed on the International Space Station in May 2019. Can be pointed at targets ('stare mode') such as volcanoes.
- Proxy methods for CO_2 (e.g., based on vegetation impacts) may be a useful alternative to direct measurement

Do ‘pre-eruptive’ volcanic SO_2 emissions actually happen?

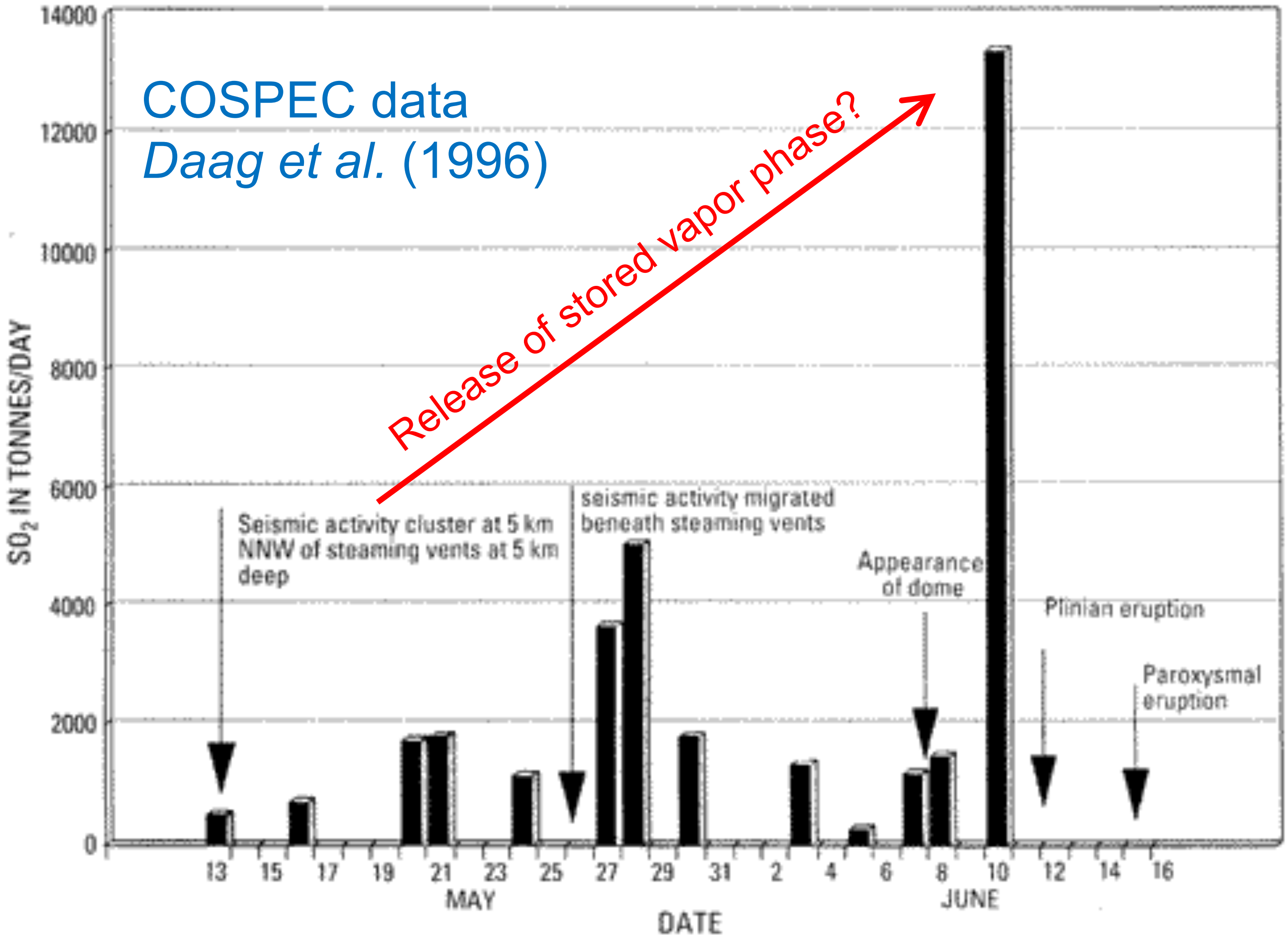
COSPEC data
Daag et al. (1996)

Release of stored vapor phase?


Pinatubo 1991

- Gas data generally subordinate to seismicity and deformation as a volcanic unrest indicator, due to perceived lack of data (note also that CO_2 more useful than SO_2)
- Deformation is the indicator of pre-eruptive unrest that on average provides the longest lead-time prior to an eruption (*Philipson et al*., 2013; *Furtney et al*., 2018)

How does volcanic degassing respond to external triggers?

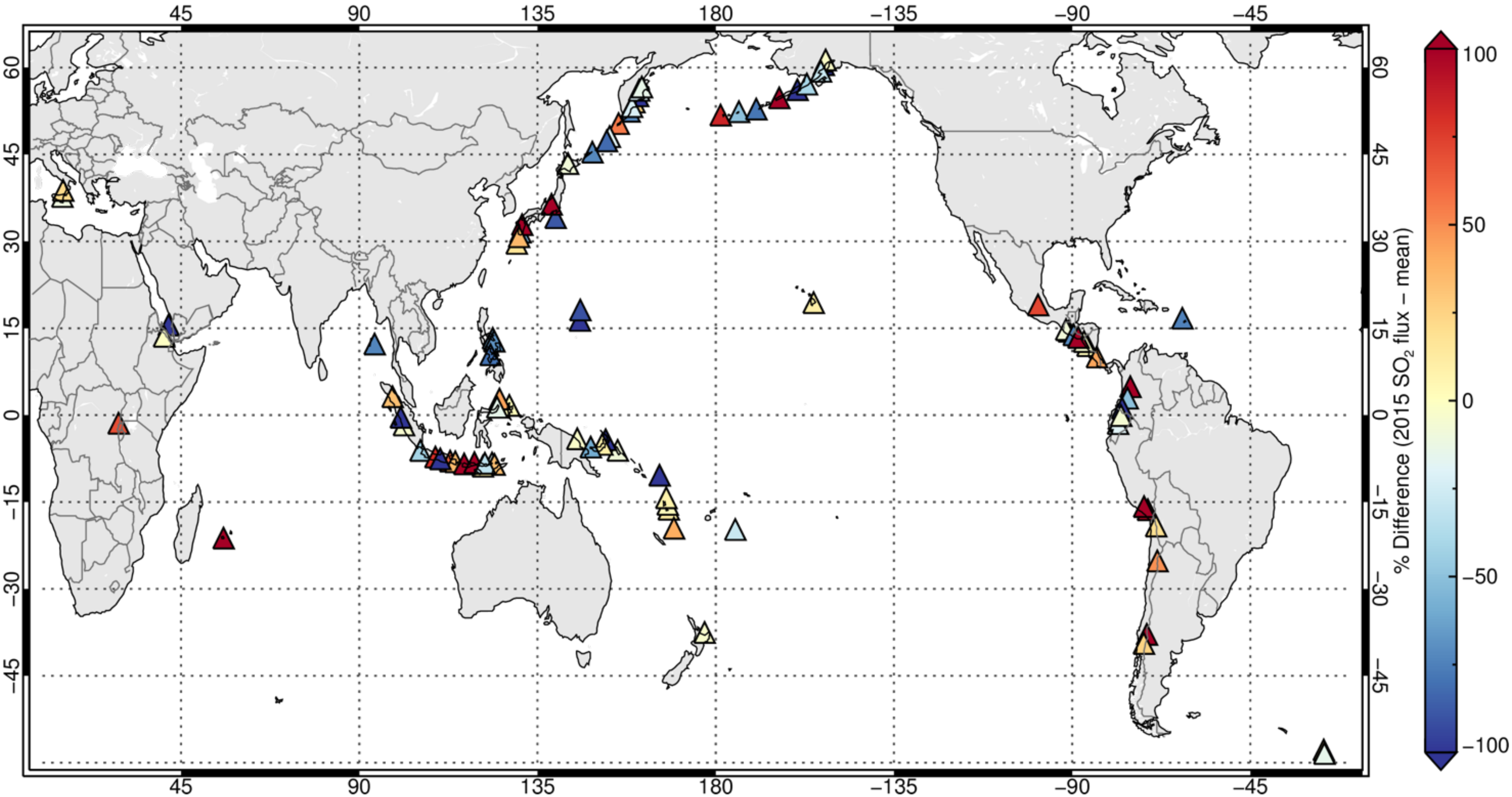

Distribution of volcanoes with satellite-detected passive SO$_2$ emissions

Earthquake triggering of volcanic degassing

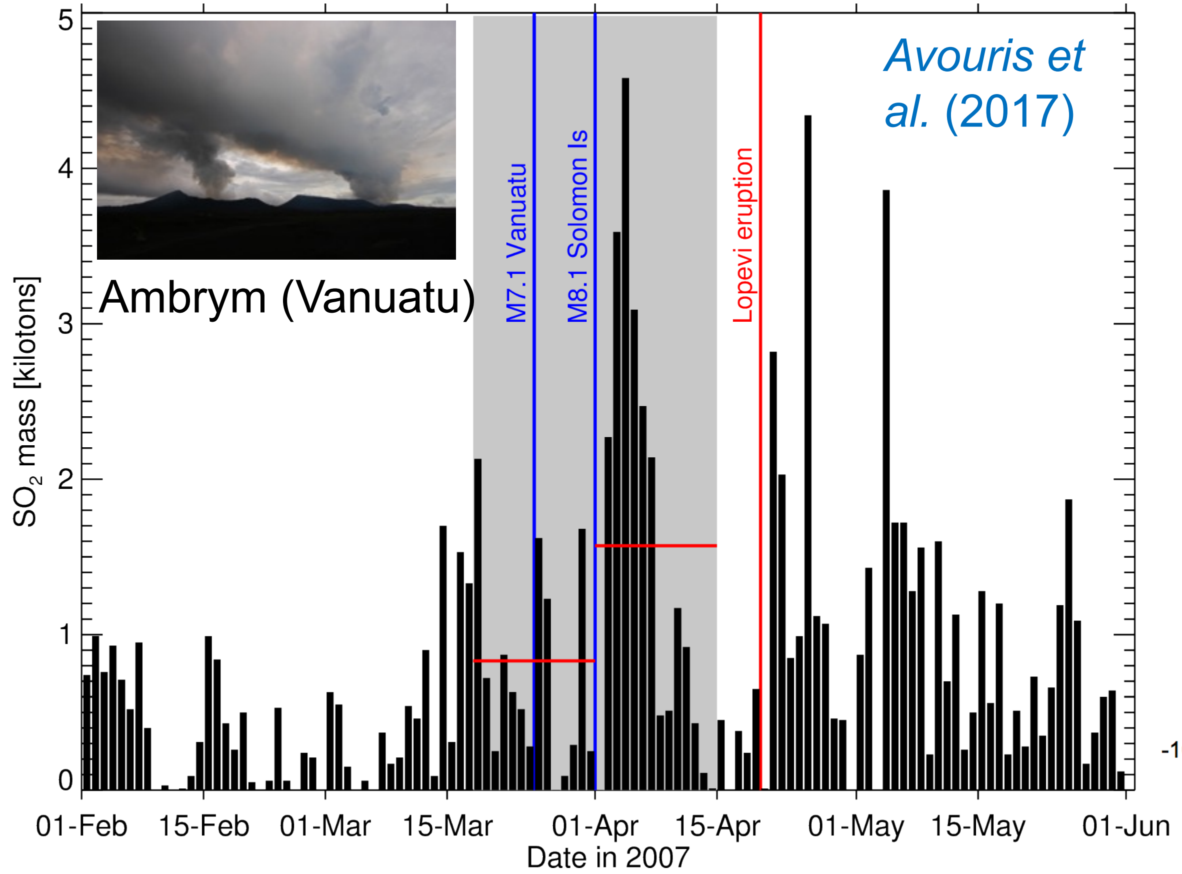

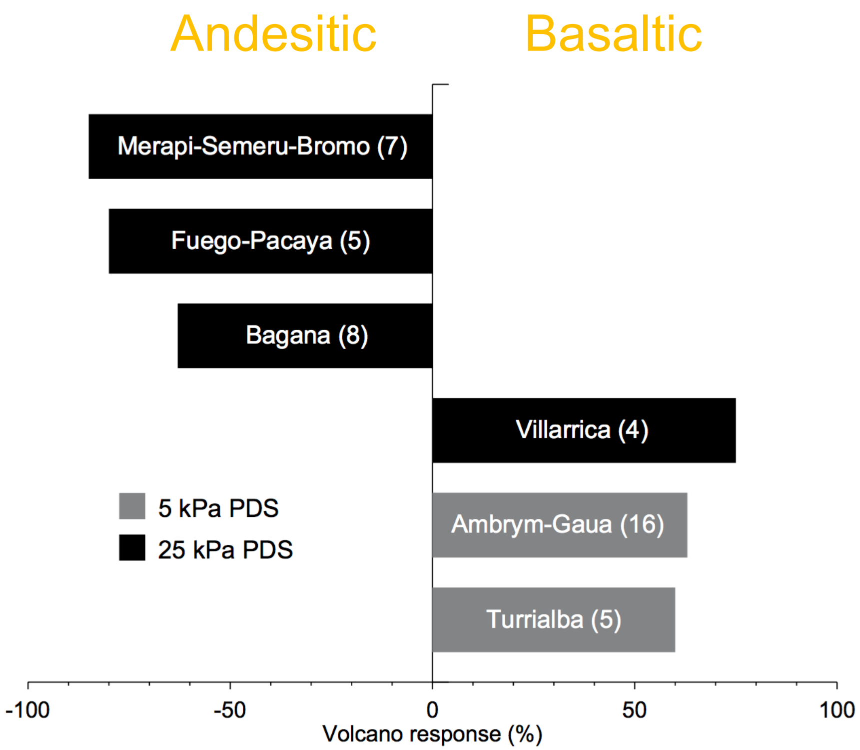

- Long-term interest in the interactions between earthquakes and volcanoes
- Global, consistent SO$_2$ measurements by satellites allow monitoring of volcanic response to earthquakes more often and on larger scales
- *Avouris et al.* (2017) modeled peak dynamic stress (PDS) generated by shallow $M_w \geq 7$ earthquakes at 12 degassing volcanoes; basaltic and andesitic volcanoes showed positive (↑SO$_2$) and negative (↓SO$_2$) response to PDS, respectively
- Stimulated new analog modeling studies of magma sloshing, resonance etc.

Brodsky and Manga (2006); *Namiki et al.* (2016); *Namiki et al*. (2018)

The (near) future

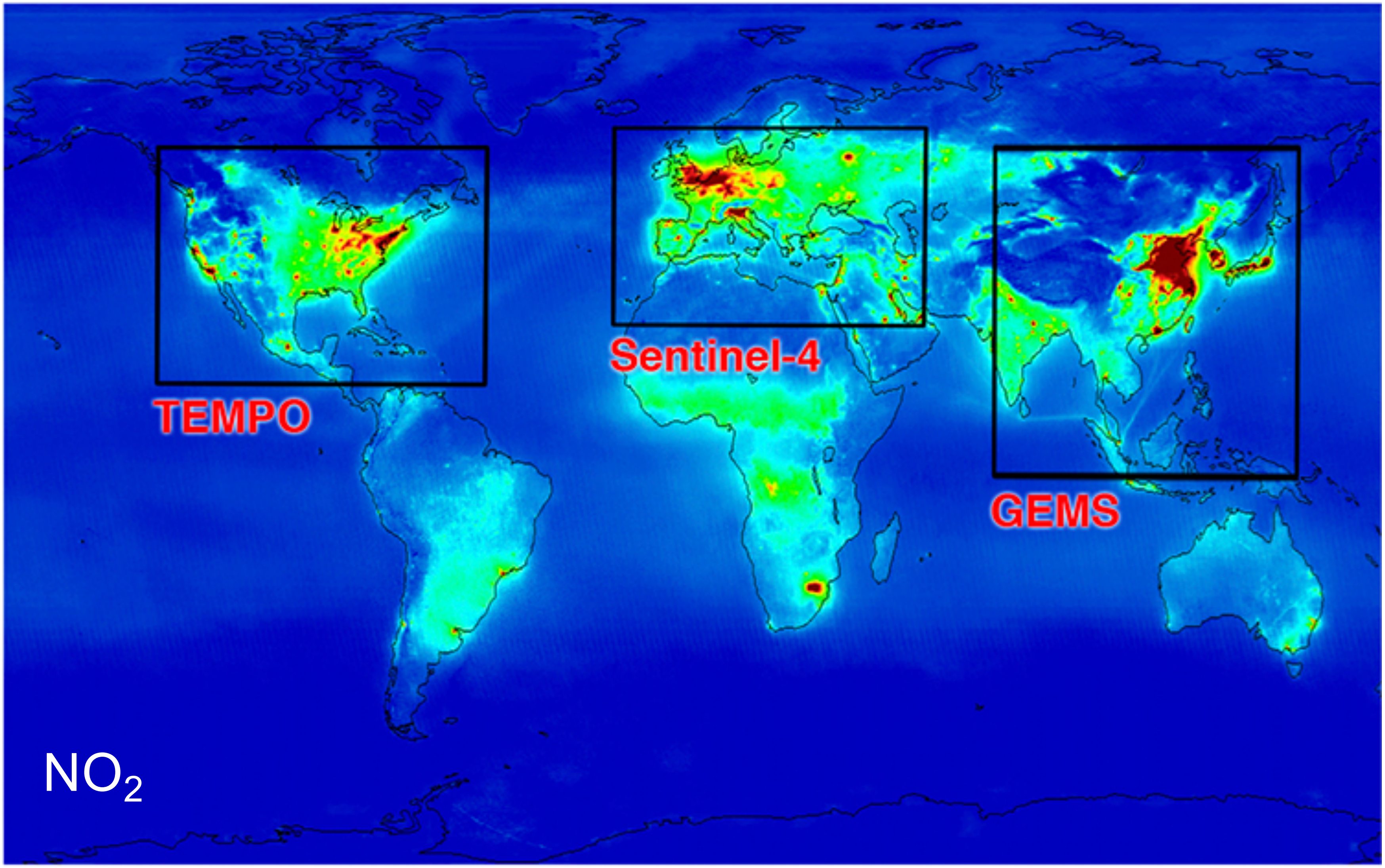

- Geostationary UV measurements (driven by air quality)
  - Some volcanic regions covered
- Cubesat constellations (e.g., Planet Labs)

Some research questions

- Given the measurement bias towards SO_2, what is the total volatile inventory (H_2O, CO_2, SO_2, …) of active volcanism?
- What proportion of sulfur gases are scavenged in eruption columns and what processes control this? Climate vs. environmental impact.
- What would be the precursors to the next major, SO_2-rich eruption? NASA has a major interest in preparing observational assets.
- What is the mass flux of volcanic ash from active volcanism?
- How many volcanoes are passively degassing vs. erupting?
- How can we combine satellite measurements of degassing, deformation and heat flux to better understand volcanic unrest, volcanic cycles, and eruption precursors (2017-19 USGS Powell Center project)?
- What are the implications for models of magma migration in trans-crustal magmatic systems for observable trends in degassing?
- To what extent do earthquakes cause variations in degassing?

Satellite SO$_2$ sensor constellation

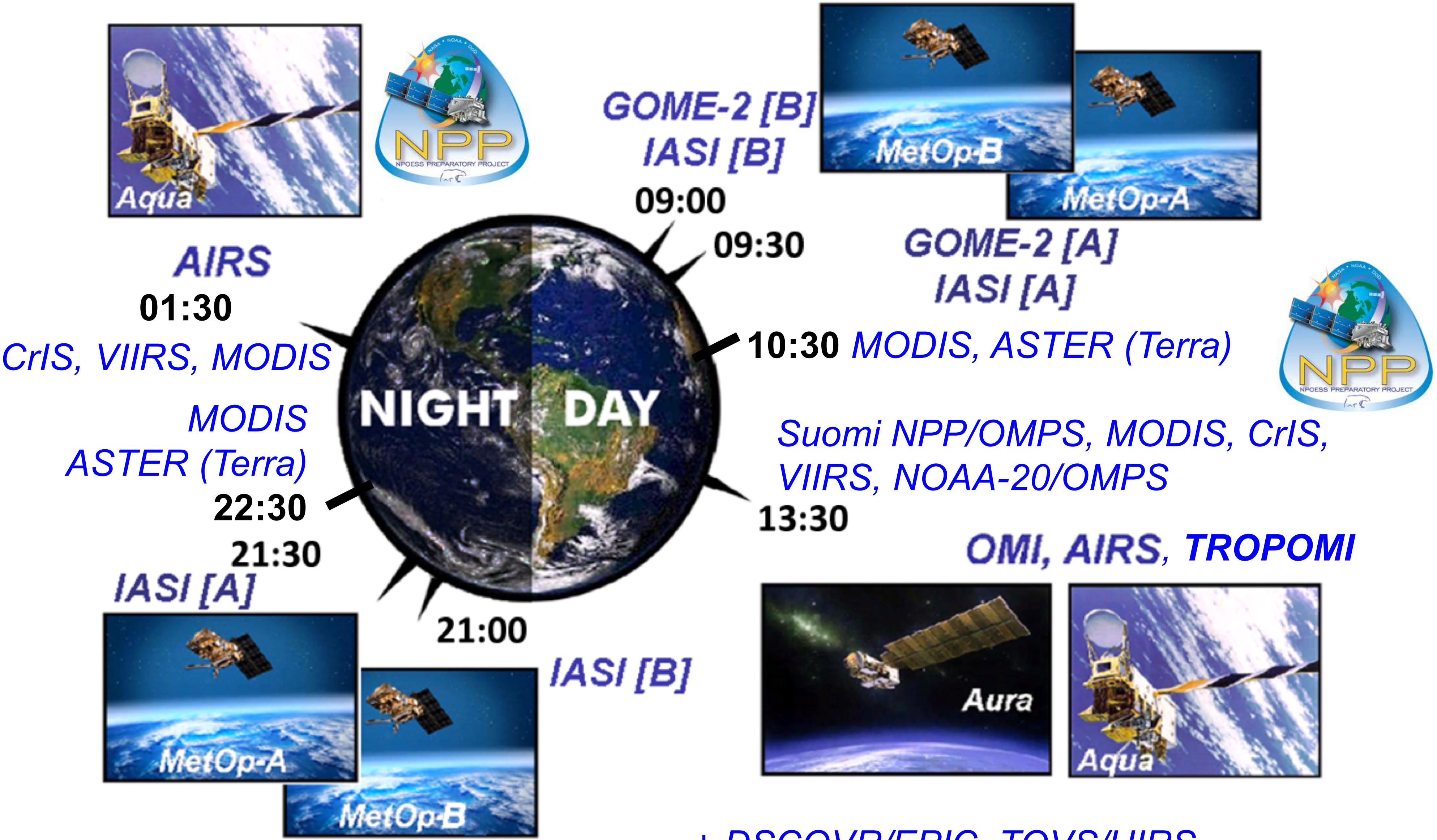

GOME-2 [B]
IASI [B]
09:00

09:30
GOME-2 [A]
IASI [A]

AIRS
01:30
CrIS, VIIRS, MODIS

10:30 MODIS, ASTER (Terra)

MODIS
ASTER (Terra)
22:30

Suomi NPP/OMPS, MODIS, CrIS, VIIRS, NOAA-20/OMPS
13:30

21:30
IASI [A]

OMI, AIRS, **TROPOMI**

21:00
IASI [B]

+ DSCOVR/EPIC, TOVS/HIRS, MSG/SEVIRI, GOES/ABI, Himawari-8/AHI

Adapted from *Brenot et al. (2014)*